Cracow Colloquium on f- electron systems

Cracow, 24th- 27th June 2015

Program and abstracts

Cracow Colloquium on f-electron systems (CCFES2015) takes place at the Pedagogical University of Cracow, Poland, on 24th-27th June, 2015.

CCFES2015 is organized by the Faculty of Mathematics, Physics and Technical Science, Pedagogical University of Cracow (PUC), in cooperation with Faculty of Mathematics and Physics, Charles University in Prague (CUNI) and Faculty of Applied Physics and Mathematics, Gdansk University of Technology (PG).

CCFES2015 is organized within the scope of Poland-Czech cooperation in the framework of Polish-Czech project ID(CZ) 7AMB14PLO36 (ID(PL) 9004/R14/R15) in 2014-2015, which was approved by Polish Ministry of Science and Higher Education and Czech Ministry of Education, Youth and Sports.

CCFES2015 is initiated by "Prague Colloquium on f-electron systems" (PCFES) organized every two years (since 1992, most recently in 2014).

CCFES2015 is also an activity included to "Calendar of the Jubilee" for celebration of 70 years of Pedagogical University of Cracow. Pedagogical University of Cracow is the earliest Pedagogical University in postwar Poland founded on 11th May, 1946.

„Cracow Colloquium on f-electron systems" (CCFES2015) obywa się w dn. 24-27 czerwca 2015r. w Uniwersytecie Pedagogicznym im. Komisji Edukacji Narodowej w Krakowie.

Konferencja CCFES2015 jest zorganizowana przez Wydział Matematyczno-Fizyczno-Techniczny Uniwersytetu Pedagogicznego w Krakowie (PUC) we współpracy z Wydziałem Matematyki i Fizyki Uniwersytetu Karola w Pradze (CUNI) oraz z Wydziałem Fizyki Technicznej i Matematyki Stosowanej Politechniki Gdańskiej (PG).

CCFES2015 jest zorganizowana w ramach współpracy pomiędzy Polską i Czechami w ramach realizacji projektu polsko-czeskiego ID(CZ) 7AMB14PLO36 (ID(PL) 9004/R14/R15). Projekt ten został zaakceptowany do realizacji na lata 2014-2015 przez Ministerstwo Nauki i Szkolnictwa Wyższego we współpracy z Czeskim Ministerstwem Edukacji, Młodzieży i Sportu.

Konferencja CCFES2015 jest inicjowana przez "Prague Colloquium on f-electron systems" (PCFES) organizowaną co dwa lata (odbywa się od 1992, a ostatnio w 2014).

CCFES2015 jest również aktywnością, która jest uwzględniona w „Kalendarium obchodów jubileuszowych" 70 lat naszej Uczelni. Uniwersytet Pedagogiczny w Krakowie jest pierwszym Uniwersytetem Pedagogicznym w powojennej Polsce, założonym 11 maja 1946.

Dear Friends and Colleagues,

We are glad to welcome you in Cracow at Cracow Colloquium on f-electron systems (CCFES2015) held on 24th – 27th June, 2015 at the Pedagogical University of Cracow.

CCFES2015 is a forum for informal discussion encompassing diverse aspects of the chemistry, physics and materials science of the Rare Earths and Actinides and related materials. It will bring together researchers from all the fields involved, emphasizing interdisciplinary interactions, lively discussions on current issues in rare earths and actinides science.

CCFES2015 will be attended by 82 participants from 16 countries, which we feel as a success, since it takes place for the first time in Cracow. We are especially happy that nearly 43% of participants are Ph.D. students.

CCFES2015 is also an activity of the Faculty of Mathematics, Physics and Technical Science included to "Calendar of the Jubilee" for celebration of 70 years of our University. Pedagogical University of Cracow is the earliest Pedagogical University in postwar Poland founded on 11th May, 1946.

We wish you a fruitful and enjoyable time at the colloquium and in Cracow.

Nhu-Tarnawska Hoa Kim Ngan
On behalf of Organizing Committee
of CCFES2015

Władysław Błasiak
Dean of Faculty of Mathematics,
Physics and Technical Science,
Pedagogical University of Cracow.

ORGANIZING COMMITTEE

Co-chairmen:
Nhu-Tarnawska Hoa Kim Ngan (PUC)
Ladislav Havela (CUNI)
Tomasz Klimczuk (PG)

Members:
Artur Błachowski
Ryszard Radwański
Krzysztof Ruebenbauer
Štěpán Sechovský
Jan Suchanicz
Zbigniew Tarnawski
Magdalena Krupska
Sylwia Sowa
Kamila Komędera
Agnieszka Kozub

INVITED SPEAKERS

Ernest Bauer (Wien)
Henryk Figiel (Cracow)
Krzystof Gofryk (Idaho)
António Pereira Gonçalves (Sacavém)
Itzhak Halevy (Beer-Sheva)
Dariusz Kaczorowski (Wrocław)
Peter Riseborough (Philadelphia)
Józef Spałek (Cracow)
Andrzej Ślebarski (Katowice)
Klára Uhlířová (Prague)

VENUE

Pedagogical University of Cracow, Podchorążych 2, 30 084 Kraków.
Lecture hall **110N**
in the new building of PUC, the main entrance at Chmiela street,
behind the main building of PUC.

CONTACT

Faculty of Mathematics, Physics and Technical Science, Pedagogical University of Cracow
ul. Podchorążych 2, 30 084 Kraków.
Phone: +48 12 662 7801
Fax: +48 12 635 8858
Email: ccfes2015@up.krakow.pl
Website: http://www.ccfes2015.up.krakow.pl

COLLOQUIUM NAME BADGES

All participants are kindly asked to wear their name badges during the colloquium. The name badge also serves as an admission to lunches and dinner.

WELCOM RECEPTION

Welcome reception will be on Wednesday (24 June, 2015), from 18.00, close to the lecture hall 110N on the first floor in the new building of PUC.

MEALS AND REFRESHMENT

Morning and afternoon tea and coffee and other drinks for participants will be served during the breaks between the scientific sessions.

The Polish-style lunch with warm food will be provided for all registered participants during the lunch time, in the restaurant Eden, at the street Bydgoska 19A, 5 min. walk from the conference site. (See the map included at the end of the abstract book.)

Refreshment will be served during the poster session.

COLLOQUIUM DINNER

The conference dinner will be on Friday, (26 June, 2015), from 19.00, in the restaurant CK Browar at the street Podwale 6/7. (See the map included in the end of the abstract book.)

ABSTRACT BOOK EDITORS

Nhu-Tarnawska Hoa Kim Ngan
Štěpán Sechovský

PROGRAM

Wednesday, 24 June 2015		
9.00-18.00	**Registration** Pedagogical University of Cracow (PUC), in the new building of PUC, the main entrance at Chmiela street (behind the main building of PUC), close to the **lecture hall 110N** on the first floor.	
18.00-20.00	**Welcome Reception** Pedagogical University of Cracow (PUC), in the new building of PUC, the main entrance at Chmiela street ((behind the main building of PUC), close to the **lecture hall 110N** on the first floor.	
Thursday, 25 June 2015		
9.00-17.00	**Registration** Pedagogical University of Cracow (PUC), in the new building of PUC, the main entrance at Chmiela street (behind the main building of PUC), close to the **lecture hall 110N** on the first floor.	
	Opening session	**Chair: Nhu-Tarnawska Hoa Kim Ngan, Ladislav Havela, Tomasz Klimczuk**
9.00 - 9.20	**Welcome address** Honorary guests of CCFES2015: Kazimierz Karolczak - Vice-Rector of the Pedagogical University of Cracow (PUC) Władysław Błasiak - Dean of Faculty of Mathematics, Physics and Technical Science (WMFT)-PUC Bartłomiej Pokrzywka - Director of Institute of Physics (IF)-PUC	
	Session 1: Exotic f-electron systems	**Chair: Vladimír Sechovský**
9.20-10.00 **I-01**	Dariusz Kaczorowski	Superconductivity in weakly-correlated non-centrosymmetric compounds
10.00-10.40 **I-02**	Ernst Bauer	Substitution and pressure driven magnetic instabilities of non-Fermi liquid $Ce_3Pd_4Si_4$
10.40-11.10	*Coffee/tea break*	
	Session 2: Actinides	**Chair: Tomasz Klimczuk**
11.10-11.40 **I-03**	Antonio Gonçalves	The beauty and complexity in the U-Fe-Ge system
11.40-12.00 **O-01**	Itzhak Halevy	Structural, electronic, and magnetic characteristics of Np_2Co_{17} under ambient and high pressure
12.00-12.20 **O-02**	Marcin Wysokiński	Classical and quantum criticalities in the itinerant ferromagnet UGe_2: A microscopic interpretation
12.20-14.00	*Lunch break*	
	Session 3: Rare earths	**Chair: Krzysztof Ruebenbauer**
14.00-14.30 **I-04**	Andrzej Ślebarski	Study of skutterudite-related $Ce_3M_4Sn_{13}$ and $La_3M_4Sn_{13}$ (M = Co, Ru, Rh); A pathway from f- and d-electron correlations to superconductivity
14.30-15.00 **I-05**	Henryk Figiel	Hydrogen in RMn_2 Laves Phases
15.00-15.20 **O-03**	Michał Falkowski	Ce_2Rh_3Ge: an extraordinary example of the sensitive balance between magnetic order, single-ion Kondo and mixed-valence behavior
15.20-15.40 **O-04**	Silvie Mašková	Magnetic properties and crystal structure of RE_2T_2Mg and their hydrides
15.40-16.00	*Coffee/tea break*	
	Session 4: Theory I	**Chair: Peter Riseborough**
16.00-16.30 **I-06**	Józef Spałek	Correlation-induced d-wave superconductivity within the Anderson-Kondo lattice model: A fully microscopic approach
16.30-16.50 **O-05**	Marcin Abram	Microscopic model of full magnetic phase-diagram of itinerant ferromagnet UGe_2
16.50-17.10 **O-06**	José-Luiz Fereira	Kondo alloys: from local to coherent Fermi liquids
17.10-19.30	***Poster session** (see list of posters in the end of the program) and refreshment*	

I -invited talk; O-oral talk; O-y oral talk in the session for young scientists; P-posters

Friday, 26 June 2015		
	Session 5: Novel materials and techniques **Chair: Krzysztof Gofryk**	
9.00-9.30 **I-07**	Klára Uhlířová	Implementation of a microfabrication technique in research of novel heavy fermion compounds
9.30-9.50 **O-07**	Lan Maria Tran	Influence of Eu^{2+} magnetic moment order on superconductivity in $Eu_{0.73}Ca_{0.27}(Fe_{0.87}Co_{0.13})_2As_2$ and $Eu(Fe_{0.81}Co_{0.19})_2As_2$
09.50-10.10 **O-08**	Cornelia Hintze	Magnetization measurements on $La_{1-x}Sr_xMnO_3$ nanoparticles
10.10-10.30 **O-09**	Ilya Taydakov	New highly luminescent lanthanide complexes based on pyrazole substituted 1.3-diketones – synthesis and photophysical properties.
10.30-11.00	*Coffee/tea break*	
	Session 6: Theory II **Chair: Ryszard Radwański**	
11.00-11.30 **I-08**	Peter Riseborough	Incomplete Protection of the Surface Weyl Cones of the Kondo Insulator SmB_6: Spin Exciton Scattering
11.30-11.50 **O-10**	Alexander Shick	Racah materials: role of atomic multiplets in intermediate valence systems
11.50-12.10 **O-11**	Urszula Wdowik	Influence of defects on the dynamical properties of d- and f-electron systems
12.10-12.30 **O-12**	Vardan Apinyan	Excitonic insulator state and condensation in the intermediate valent semiconductor $TmSe_{0.45}Te_{0.55}$
12.30-14.00	*Lunch break*	
	Session 7: Actinides and rare earths **Chair: Ladislav Havela**	
14.00-14.30 **I-09**	Krzysztof Gofryk	Spin-Phonon Interactions in Uranium Dioxide
14.30-14.50 **O-13**	Paweł Starowicz	Momentum dependence of a Kondo resonance in $Ce_2Co_{0.8}Si_{3.2}$
14.50-15.10 **O-14**	Khrystyna Miliyanchuk	Unique hydrogenation properties of R_2Ni_2M compounds with the W_2CoB_2-type structure
15.10-15.30 **O-15**	Michał Winiarski	Exploring the diversity of $CeCr_2Al_{20}$-type ternary cage aluminides
15.30-16.00	*Coffee/tea break*	
	Session 8: Session for young scientists **Chair: Artur Blachowski**	
16.00-16.15 **O-y1**	Sylwia Sowa	Structure and superconducting transition in U-Pt and U-Pd alloys prepared by splat cooling technique
16.15-16.30 **O-y2**	George Beridze	Efficient calculations of f-materials relevant for nuclear waste management using DFT+U
16.30-16.45 **O-y3**	Magdalena Krupska	Interdiffusion and ion beam mixing effect in bi-layer magnetite-on-Fe films prepared by the MBE technique on MgO(001) substrate
16.45-17.00 **O-y4**	Judyta Strychalska	La_3Co – superconductivity on the edge of ferromagnetism
17.00-17.15 **O-y5**	Urszula Lewczuk	Influence of Ba doping of $Na_{0.5}Bi_{0.5}TiO_3$ ceramics on their structural, dielectric and ferroelectric properties
17.15-17.30 **O-y6**	Renata Bujakewicz-Korońska	Properties of barium titanate modified by Co doping
19.00-22.00	***Conference dinner***	

I -invited talk; O-oral talk; O-y oral talk in the session for young scientists; P-posters

Saturday, 27 June 2015

	Session 9: Uranium alloys and their hydrides **Chair: N.-T.H. Kim-Ngan** ***Session devoted to Polish-Czech bilateral project***	
9.00-9.30 **I-10**	Ladislav Havela	Different routes of UH_3 alloying and impact onto the 5f magnetism
9.30-9.50 **O-16**	Daria Drozdenko	Preparation of U alloys for EBSD mapping
9.50-10.10 **O-17**	Mychaylo Paukov	Magnetic properties of double doped UH_3-based hydrides
9.50-10.10	Kim Nhu-Tarnawska	*Krakow and Prague - the formal and informal cooperation*
10.30-11.00	*Coffee/tea break*	
	Session 10: High-pressure effects **Chair: Zbigniew Tarnawski**	
11.00-11.30 **I-11**	Itzhak Halevy	The effect of high-pressure and high-temperature on the crystal structure of sesquioxide: Y_2O_3, Er_2O_3 and Sc_2O_3
11.30-11.50 **O-18**	Tomasz Klimczuk	Chemical pressure effect in $SmNiC_2$
11.50-12.10 **O-19**	Fabrice Wilhelm	XMCD study of ferromagnetism in $YbCu_2Si_2$ under pressure
12.10-12.30	**Summary** (Ladia Havela) **Awards for two best posters** (Tomasz Klimczuk) **Closing** (Nhu-Tarnawska Hoa Kim Ngan)	
12.30-14.00	*Lunch break*	
from 14.00	Free time in Krakow	

I -invited talk; O-oral talk; O-y oral talk in the session for young scientists; P-posters

LIST OF POSTERS

No.	Presenting author	Title
P-01	Alexander V. Andreev	High-field study of a $TbFe_5Al_7$ single crystal
P-02	Ozkendir Osman Murat	Influence of Er-substitution on the Crystal and Magnetic Properties of Ferric Borate Sample
P-03	Agnieszka Kozub	Screening of magnetic moment at Co impurity in Cu host
P-04	José-Luiz Ferreira	Valence fluctuations and magnetism in lanthanide systems
P-05	Rafał Kurleto	Electronic properties of $CeNi_9In_2$ compound
P-06	Aleksandra K. Jasek	Magnetic spiral order in iron pnictides FeAs and FeSb
P-07	N.-T.H. Kim-Ngan	The use of ultrafast cooling for phase stabilization and phase modification in f-electron alloys
P-08	Tomasz Toliński	Thermopower, electrical resistivity and thermal conductivity of the $CeNi_2(Si_{1-y}Ge_y)_2$ alloys
P-09	Jakub Šebesta	Magnetic studies of $TmCo_2$ singlecrystal
P-10	Zuzanna Piotrowska	Synthesis and magnetic properties of the GaN nanoceramics doped with transition metals
P-11	Jaroslav Valenta	Magnetism and its suppression in $CeCo_{0.715}Si_{2.285}$
P-12	Mane Sahakyan	Electronic band structure calculation and physical properties of the non-centrosymmetric superconductor Th_7Co_3
P-13	Kamila Komędera	^{57}Fe and ^{151}Eu Mössbauer spectroscopy of $(Eu_{0.72}Ca_{0.28})(Fe_{1.64}Co_{0.36})As_2$ iron-based superconductor
P-14	Andrzej Kozłowski	Mössbauer effect studies of first and second order magnetite single crystals
P-15	Andrzej Kruk	Electrochemical properties of cathode-electrolyte gradient system for use in proton-conducting fuel cells PCFC
P-16	Karol Synoradzki	Reentrant spin-glass state and magnetocaloric effect in the $Ce(Cu_{0.675}Ni_{0.375})_4Mn$ alloy
P-17	Margarida Henriques	New quaternary iron-rich compounds U-Fe-Ge-Sn
P-18	Zbigniew Tarnawski	Study of Ti, V and their oxides-based thin films in the search for hydrogen storage materials
P-19	Dawid M. Nalęcz	Magnetic phase transition in antiferromagnetic $SrMnO_3$ and K_2CoF_4 perovskites
P-20	Ryszard Radwański	Really first principles calculations - Quantum Atomistic Solid State Theory (QUASST) for UPd_2Al_3, UGa_2 and UO_2
P-21	Magdalena Mędala	Ab initio phonon dynamics in the layered ternary diselenide KNi_2Se_2
P-22	E. El Moussafir	Characterization of lead titanate thin films prepared by sol gel process
P-23	Artur Maksymov	The resonance transition in spin-crossover molecular nanomagnets
P-24	Pablo Hernández-Gómez	Magnetic disaccommodation in La-Co substituted strontium M-type hexaferrites
P-25	Łukasz Jarosiński	Dielectric properties of graphene based composites
P-26	Paweł Kazubowski	Studies of visual attention and emotion in physics problem solving
P-27	Monika Szklarska-Łukasik	Crystal structure, electron band structure and magnetostriction of the $Tb_{0.27}Dy_{0.73}(Fe_{0.7-x}Ni_xCo_{0.3})_2$ intermetallics (x=0, 0.1, 0.2)
P-28	Barbara Winiarska	Crystal structure and electrical properties of the $Tb_{0.27}Dy_{0.73}(Fe_{1-x}Al_x)_2$ compounds
P-29	Barbara Winiarska	Electron band structure and magnetostriction of the $Tb_{0.27}Dy_{0.73}(Fe_{1-x}Co_x)_2$ series
P-30	Dorota Sitko	Effects of Eu substitution on the physical properties of $BaTiO_3$ ceramics
P-31	Monika Karpierz	Effects of $PbTiO_3$ doping on dielectric, thermal and ferroelectric properties of $Na_{0.5}Bi_{0.5}TiO_3$ ceramics

I -invited talk; O-oral talk; O-y oral talk in the session for young scientists; P-posters

Abstracts

Superconductivity in weakly-correlated non-centrosymmetric compounds

Dariusz Kaczorowski
Institute of Low Temperature and Structure Research, Polish Academy of Sciences,
P.O. Box 1410, 50-950 Wrocław, Poland

Superconductivity in materials lacking an inversion center, like $CePt_3Si$, $CeRhSi_3$ or UIr, exhibits an unconventional character that can be attributed to lifting the spin degeneracy of conduction bands due to the Rashba-type anti-symmetric spin-orbit coupling. This may lead to mixed singlet-triplet parity of the superconducting state with line nodes in the energy gap and helical vortex phases. However, all these unconventional superconductors simultaneously show strong electronic correlations, which strongly influence their superconducting characteristics. In order to discriminate between the roles played by the lack of inversion center and the strong correlations among electrons on the appearance of triplet pairing, complementary studies of various weakly-correlated non-centrosymmetric systems are indispensable. Here, we present our results recently obtained for a few Th-based ternaries, eg., ThIrSi, $ThIrSi_3$ and $ThIr_2Si_2$, which crystallize with different non-centrosymmetric structures. Each compound was characterized as a moderately- or strongly-coupled type II BCS-like superconductor, with the upper critical field being close to the Pauli-Clogston limit. Though no unconventional features were detected in the superconducting characteristics, some hints at substantial contribution of spin fluctuations into to the thermodynamic properties were found in both normal and superconducting states.

This research was supported by the National Science Centre (Poland) under grant no. 2014/13/B/ST3/04544.

Email of presenting author: D.Kaczorowski@int.pan.wroc.pl

Substitution and pressure driven magnetic instabilities of non-Fermi liquid $Ce_3Pd_4Si_4$

N. Robisch[1], K. Sirhan[1], I. Messner[1], R. Kurinjimala[1], B. Raab[1], F. Kneidinger[1], H. Michor[1], J. Sereni[2], A. Gribanov[3], P. Rogl[4], E. Bauer[1]
[1]Institute of Solid State Physics, Vienna University of Technology, A-1040 Wien, Austria
[2]CAB Bariloche, San Carlos de Bariloche, Argentina
[3]Department of Chemistry, Moscow State University, GSP-1, 119991 Moscow, Russia
[4]Institute of Physical Chemistry, University of Vienna, A-1090 Wien, Austria

An experimental investigation of ternary $Ce_3Pd_4Si_4$ evidenced non-Fermi liquid properties due to the proximity of this paramagnetic compound to a quantum critical point. The ground state observed for this Ce system appears to be a result of mutual interactions of the crystalline electric field, of the Kondo effect and of RKKY interactions. A subtle change of the balance of these interactions e.g., by pressure or by substitutions is expected to trigger some instability, presumably of magnetic origin. The aim of the present investigation is to reveal the response of the system when certain atoms in $Ce_3Pd_4Si_4$ are exchanged by different other appropriate elements. Here we will show, how long range magnetic order in the substituted materials develops on a substitution of Ce/La, of Pd/Ni and of Si/Ge from a study of temperature, pressure and magnetic field dependent transport properties, of magnetization and of specific heat.

Work supported by the Austrian FWF, P22295.

Email of the presenting author: bauer@ifp.tuwien.ac.at

The beauty and complexity in the U-Fe-Ge system

A.P. Gonçalves[1], M.S. Henriques[1,2], L. Havela[3]
[1]C2TN, Instituto Superior Técnico, Universidade de Lisboa, Campus Tecnológico e Nuclear, Estrada Nacional 10, 2695-066 Bobadela LRS, Portugal
[2] Institute of Physics, AVCR, Na Slovance 2, 182 21 Prague, Czech Republic
[3]Faculty of Mathematics and Physics, Charles University, Ke Karlovu 5, 12116 Prague, Czech Republic

U-M-X (M = transition metal, X = p element) systems have been extensively studied due to their importance for basic science, reflected in the discovery of some of the most exotic ground states of matter, and significance for nuclear technologies. However, investigations in the full compostion ranges are still lacking in many of them.

Following our previous works on U-Fe-T (T = p-element) systems, we decided to explore the complete U-Fe-Ge system and characterize the existing compounds. This system was observed to be very rich, with fourteen ternary stable phases present in the isothermal section at 900ºC (four homogeneity ranges and ten intermetallic compounds), nine of them discovered for the first time. Moreover, three original structure types, $U_{34}Fe_{4-x}Ge_{33}$, $U_9Fe_7Ge_{24}$ (both tetragonal, space group I4/mmm) and $U_6Fe_{22}Ge_{13}$ (orthorhombic, space group Pbam) were identified, and unusual physical properties were observed. Therefore, the structure and physical properties of selected ternary compounds were also studied in detail and relations between both were established.

Email of the presenting author: apg@ctn.ist.utl.pt

Study of skutterudite-related $Ce_3M_4Sn_{13}$ and $La_3M_4Sn_{13}$ (M = Co, Ru, Rh); A pathway from *f*- and *d*-electron correlations to superconductivity

Andrzej Ślebarski
Institute of Physics, University of Silesia, 40-007 Katowice, Poland

Strongly correlated *f*- and *d*-electron systems are presently among the most intriguing and versatile materials. A wide variety of interesting phenomena can be attributed to electronic correlations, among them metal-insulator transitions, heavy fermion and non-Fermi liquid behaviors, quantum criticality, and unconventional superconductivity.

A key parameter in the strongly correlated electron systems (SCES) is the exchange between local magnetic moments of the *f*-electron states and the conduction carriers, J_{sf}. As J_{sf} is changed, the system can be tuned from a magnetically ordered metal to a heavy Fermi liquid under change in temperature, alloy composition, magnetic field, or pressure. Recently [1,2], it was shown that the skutterudite-related $Ce_3M_4Sn_{13}$ (M = Co, Ru, Rh) heavy fermions exhibit a behavior characteristic of the Ce-based systems with comparable Kondo and magnetic energy scales, and can be near a magnetic QCP. Within the system of $Ce_3M_4Sn_{13}$, $Ce_3Rh_4Sn_{13}$ has also generated much interest due to positive magnetoresistivity (MR) effect, which can be suggested as a result of possible strong correlations originating from *d*-electrons. Moreover, the superconductivity in $La_3M_4Sn_{13}$ has attracted considerable attention and provided an avenue by which to better understand the relationship between superconductivity and magnetism in the presence of strong electron correlations. The main goal of this review is to compare the physical low-temperature properties of selected $Ce_3M_4Sn_{13}$ and $La_3M_4Sn_{13}$ compounds. In order to study the quantum criticality, we investigated the low-temperature thermodynamic and electric transport properties. We show evidence of nanoscale inhomogeneity as a bulk property of $La_3Rh_4Sn_{13}$ and $La_3Ru_4Sn_{13}$ in the sense that the samples exhibit electronic disorder over length scale similar to the coherence length which cannot be removed by any standard annealing procedure. Such a substantial nanoscale electronic inhomogeneity is characteristic of the bulk $Bi_2Sr_2CaCu_2O_{8+x}$ high-Tc materials and some heavy fermions with unconventional superconductivity.

References
[1] A. L. Cornelius, et al., Physica B **378-380**, 113 (2006).
[2] A. Ślebarski et al., Intermetallics, **54**, 199 (2014).

Email of the presenting author: andrzej.slebarski@us.edu.pl

Hydrogen in RMn_2 Laves Phases

Henryk Figiel[1], Andrzej Budziak[2]
[1]*Faculty of Physics and Applied Computer Science, AGH University of Science and Technology, al. Mickiewicza 30, 30-059 Kraków, Poland,*
[2] *Institute of Nuclear Physics PAN, ul Radzikowskiego 152, 31 -342 Kraków, Poland*

Hydrogen is seen as one of the important energy carriers of this century and is indicated as a fuel of future. Research problem of physical properties of metal hydrides is strongly connected with very actual topical issues of the hydrogen storage. Especially interesting and promising are hydrides of intermetallic compounds. Among widely studied RT_2H_x systems (*R* a rare earth or alkaline metal, *T* – transition metal like Fe, Co, Ni and Mn), the hydrides RMn_2H_x present very interesting physical properties. It comes from the fact that already alone RT_2 compounds exhibit a complex interaction of two sublattices: the *R*- and 3d-metal sublattice. The first one can be described with the localized 4f magnetic moments, while the other is regarded as essentially an itinerant electron system.

The RMn_2 compounds can absorb very easily large amount of hydrogen, which locates inside of characteristic tetrahedrons build of *R* and Mn atoms. The systematic investigation (XRD, ND, NMR and magnetic measurements) of the RMn_2H_x hydrides with R = Y, Nd, Sm, Gd, Tb, Dy, Ho and Er allowed to observe the role of rare earth metal in hydrogen induced structural and magnetic transformations. Hydrogen absorption in RMn_2 compounds leads to magnetic and structural changes: an increase of the magnetic ordering temperature - from below 100 K up to (200 - 400) K depending on the hydrogen concentration, structure transformations and an increase of the cell volume (even up to 30 %).

The role of the host structures (Laves phases of the *C*14 and *C*15 type) in formation of hydrides and their magnetic properties is presented – on the base of obtained results the universal structural phase diagram model of RMn_2H_x is proposed. The influence of f-electron elements on the physical properties of RMn_2H_x hydrides is presented and discussed. It is shown that all the RMn_2H_x hydrides in magnetic ordering state are ferrimagnetic, and their total magnetization strongly depends on hydrogen concentration. A modified model describing the changes of unit-cell volume as a function of the hydrogen concentration is proposed as well.

Email of the presenting author: figiel@agh.edu.pl

Correlation-induced *d*-wave superconductivity within the Anderson-Kondo lattice model: A fully microscopic approach

Józef Spałek[1,2] and Olga Howczak[1]
[1]*Marian Smoluchowski Institute of Physics, Jagiellonian University, ulica Łojasiewicza 11, PL 30-348 Kraków, Poland*
[2]*Academic Centre for Materials and Nanotechnology, AGH University of Science and Technology, Aleja Mickiewicza 30, PL 30-059 Kraków, Poland*

We discuss the appearance of the *d*-wave superconductivity and its coexistence with magnetism within a fully microscopic Anderson-Kondo lattice model derived from Periodic Anderson model [1]. The pairing originates from a competition between the Kondo interaction and the *f-f* superexchange. We use the so-called statistically consistent Gutzwiller approximation [2]. The coexistence regimes of antiferromagnetism with superconductivity are determined and appear in the vicinity of the Kondo-insulating quantum critical point. We compare our results with those obtained in the Kondo-lattice limit, where the startling *f*-electrons are localized [3], as well as discuss the valence change [4] accompanying the onset of superconductivity.

The work was partly supported by Grant TEAM from the Foundation for Polish Science (FNP) and by Grant MAESTRO, No. DEC-2012/04/A/ST3/00342 from the National Science Centre (NCN).

References

[1] O. Howczak and J. Spałek, J. Phys.: Condens. Matter **24**, 205602 (2012) pp. 1-14; O. Howczak, J. Kaczmarczyk and J. Spałek, in Special Issue: *Quantum Criticality and Novel Phases*, Phys. Stat. Sol. B **250**, 609-614 (2013).
[2] M. M. Wysokiński, M. Abram, and J. Spałek, Phys. Rev. B **90**, 081114(R) (2014); ibid. 91, 081108(R) (2015).
[3] O. Bodensiek, R. Žitko, M. Vojta, M. Jarrell, and T. Pruschke, Phys. Rev. Lett. **110**, 146406 (2013).
[4] S. Watanabe, A. Tsuruta, K. Miyake, and J. Flouquet, Phys. Rev. Lett. **100**, 236401 (2008).

Email of the presenting author: ufspalek@if.uj.edu.pl

Implementation of a microfabrication technique in research of novel heavy fermion compounds

Klára Uhlířová, Jan Prokleška, Barbora Vondráčková, Marie Kratochvílová, Michal Dušek, Jeroen Custers, Vladimír Sechovský
[1] *Department of Condensed matter Physics, Faculty of Mathematics and Physics, Charles University, Ke Karlovu 5, 12116 Prague, Czech Republic*
[2] *Department of Structure Analysis, Institute of Physics ASCR, v.v.i., Na Slovance 2, 182 21 Prague, Czech Republic*

The family of $Ce_nT_mIn_{3n+2m}$ (n = 1, 2; m = 1; T = transition metal) heavy fermion compounds has been intensively studied owing to variety of magnetic ordering and superconductivity. They crystallize in tetragonal type structure with $CeIn_3$- and TIn_2- layers alternating along the *c*-axis. Besides the well-known $CeTIn_5$ and Ce_2TIn_8 (T = Co, Rh, Ir) compounds, new materials $CePt_2In_7$, Ce_2PtIn_8, Ce_3PtIn_{11}, Ce_2PdIn_8, $Ce_5Pd_2In_{19}$ and Ce_3PdIn_{11} have been discovered recently [1-3].

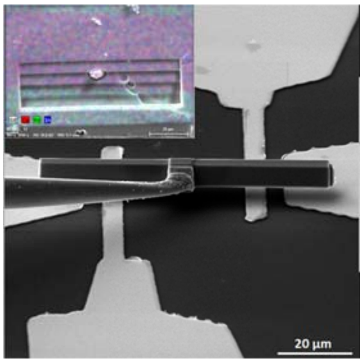

Our investigations revealed that the series of $Ce_nPd_mIn_{3n+2m}$ compounds covers the widest known composition range. The existence of a system of compounds with various layer-stacking opens a possibility to study a scenario of evolution of magnetism and superconductivity with the dimensionality of the Fermi surface. Ce_2PdIn_8 shows no magnetic ordering but becomes superconducting below T_c = 0.7 K. In Ce_3PdIn_{11}, we have observed magnetic order below T_N = 1.7 K and subsequent transition to superconducting state below T_c = 0.4 K. A specific feature of the $Ce_nPd_mIn_{3n+2m}$ compounds is the lattice parameter *a* of their tetragonal structure being almost identical with the lattice parameter of the cubic $CeIn_3$. This may play an important role in the stability of various compounds with different combinations of $CeIn_3$- and $PdIn_2$- layer stacking; however, it also seems to result in difficulties with sample preparation. Multilayer inclusions of neighboring phases are hardly avoidable in growing single crystals from metallic flux. While tuning the growth conditions of Ce_3PdIn_{11} and Ce_2PdIn_8, thin layers of $CePdIn_5$ have been found in several samples. Further attempts to obtained larger samples of $CePdIn_5$ were not successful.

In order to isolate the $CePdIn_5$ single crystals and verify the results obtained on Ce_3PdIn_{11} and Ce_2PdIn_8 single crystals, microfabrication of samples by focused ion beam (FIB) microscope has been developed. By this method, few tens of micrometers long bars can be cut from desired area of sample (inspected by elemental mapping) and transferred on a substrate as shown in the Figure. In combination with electron beam lithography, the sample can be subject to electric transport measurement, microcalorimetry etc. Our current progress in sample preparation for electrical measurements as well as a recently published high magnetic field study of $CeRhIn_5$ [4] have shown the power of the focused ion beam microscopy technique in the studies of heavy fermion compounds.

References
[1] Z. M. Kurenbaeva et al., Intermetallics 16 (2008) 979
[2] A. Tursina et al., J. Sol. State Chem. 200 (2013) 7
[3] M. Kratochvílová et., al. J. Cryst. Growth 397 (2014) 47
[4] P. Moll et al., Nature Communications 6 (2015) 6663

Email of the presenting author: klara@mag.mff.cuni.cz

Incomplete Protection of the Surface Weyl Cones of the Kondo Insulator SmB_6: Spin Exciton Scattering

Peter S Riseborough[1], G.A. Kapilevich[1], A.X. Gray[1], Miklos Gulacsi[2],
Tomasz Durakiewicz[3], J.L. Smith[3]
[1]*Temple University, Philadelphia. Pa 19122 USA*
[2]*Max Planck Institute for Complex Systsems, Dresden, Germany*
[3]*Los Alamos National laboratory, Los Alamos, New Mexico 87545, USA*

The compound SmB_6 is a Kondo Insulator, where the lowest-energy bulk electronic excitations are spin-excitons. It also has surface states that are subjected to strong spin-orbit coupling. It has been suggested that SmB_6 is also a topological insulator. Here we show that, despite the absence of time-reversal symmetry breaking and the presence of strong spin-orbit coupling, the chiral spin texture of the Weyl cone is not completely protected. In particular, we show that the spin-exciton mediated scattering produces features in the surface electronic spectrum at energies separated from the surface Fermi energy by the spin-exciton energy. Despite the features being far removed from the surface Fermi energy, they are extremely temperature dependent. The temperature variation occurs over a characteristic scale determined by the dispersion of the spin-exciton. The structures may be observed by electron spectroscopy at low temperatures.

Email of the presenting author: prisebor@temple.edu

Spin-Phonon Interactions in Uranium Dioxide

K. Gofryk[1], J.C. Lashley[2], M. Jaime[2], C.R. Stanek[2], D.A. Andersson[2],
T. Durakiewicz[2], J.L. Smith[2]
[1]*Idaho National Laboratory, USA*
[2]*Los Alamos National Laboratory, USA*

Despite more than sixty years of intense research of uranium dioxide, a thorough understanding is lacking for the microscopic processes that control its transport and thermodynamic properties. It is by far the most studied actinide material as it is a primary fuel used in light water nuclear reactors.

Although UO_2 is best known as an engineering material, its properties indicate rare interactions between charge, spin and lattice, reminiscent of emergent phenomena. Despite large experimental and theoretical efforts it is unclear how different degrees of freedom and quasiparticle excitations interact and what is the relationship to the thermal behavior. Here we report our new experimental and theoretical studies on oriented and well-characterized uranium dioxide single crystals.

Our preliminary results on thermal behavior of uranium dioxide revealed a few important aspects of its collective quasiparticle couplings and interactions. We found that the overall shape and magnitude of the thermal conductivity of UO_2 is atypical for insulating crystals (see Fig. 1a). The thermal conductivity exhibits a pronounced double-peak structure with maxima occurring at ~10 and ~220 K and a minimum at the Neel temperature. Typically, as exemplified in $\kappa(T)$ of ThO_2 (see Fig. 1a), the phonon thermal conductivity rises quickly and reaches its maximum well below 100 K, after which phonon–phonon scattering leads to rapid decrease. Our extensive magnetostriction and thermal transport studies indicate that strong spin-lattice coupling and resonant scattering are important for understanding the general thermal behavior in this material. The unusual behavior of $\kappa(T)$ in UO_2 is due to resonant scattering of phonons through excitations of the spins (in the paramagnetic phase) and absence of this scattering mechanism below $T_N = 30.8$ K due to spin ordering. Our initial thermal conductivity analysis gives ~3.5 meV for the resonance energy (see Figure 1b).

Interestingly, inelastic neutron scattering studies have identified a dynamic Jahn–Teller distortion in <100> lattice directions that splits the ground state into three singlets with dispersive peaks of magnetic character between 3 and 10 meV [1].

During the talk I will discuss implications of these results.

References
[1] R. Caciuffo, et al., Phys. Rev. B 59, 13892 (1999)
[2] M. Mann et al., Cryst. Growth Des. 10, 2146 (2010)
[3] K. Gofryk et al., Nature Comm. 5, 4551 (2014)

Email of the presenting author: krzysztof.gofryk@inl.gov

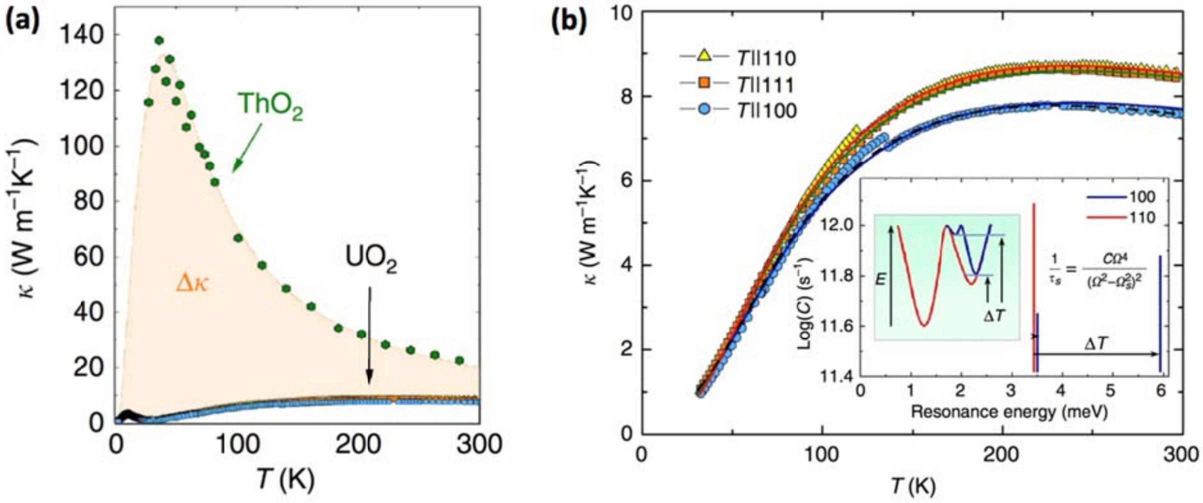

Figure 1 (a) Thermal conductivity of uranium dioxide single crystals compared with reference data for ThO_2 (data for ThO_2 is taken from [2]). (b) Measured UO_2 thermal conductivity fitted to the extended Callaway model that takes into account a resonant spin-phonon scattering. The difference in resonance scattering parameters for the <110> and <100> crystallographic directions is illustrated in the inset. Figures taken from [3].

Different routes of UH_3 alloying and impact onto the 5*f* magnetism

L. Havela[1], M. Paukov[1], I. Tkach[1], Z. Matěj[1], D. Kriegner[1], I. Turek[1], M. Diviš[1],
M. Cieslar[1], D. Drozdenko[1], N.-T. H. Kim-Ngan[2], A.V. Andreev[3]
[1]*Charles University, Faculty of Mathematics and Physics, Ke Karlovu 5,*
12116 Prague 2, Czech Republic
[2]*Institute of Physics, Pedagogical University, Podchorazych 2, 30 084 Cracow, Poland*
[3]*Institute of Physics, Academy of Sciences of the Czech Republic, Prague, Czech Republic*

UH_3 belongs to the first known 5*f* materials with magnetic ordering [1]. However, we cannot conclude that we understand it well. One of persisting issues are the properties of α-UH_3, which remains, besides the stable β-UH_3 phase, as a metastable species never existing in a pure form. The other issue is (in)adequacy of description by conventional *ab-initio* calculations (see e.g. [2]), which does not seem to reproduce well e.g. photoelectron spectra [3].

Tuning of properties by alloying is one of common probes into a system investigated. In fact several routes of preparation of alloyed U trihydrides, UH_3, were discovered. Starting from the U_6T compounds, hydrogenation leads to T atoms embedded in the β-UH_3 structure, with transition-metal atoms T occupying one of the U sites. The most thoroughly investigated is the hydride, obtained from U_6Fe, denoted as U_6FeH_{17} [4]. ^{57}Fe Mössbauer spectroscopy indicated Fe occupying the U^{II} positions in the β-UH_3 structure. Analogous process leads to U_6CoH_{18} [5] from U_6Co. U_6Mn and U_6Ni are likely to provide the same type of hydride [6].

We have been hydrogenating γ-U alloys, using various transition metals helping (together with ultrafast cooling) to retain the *bcc* U structure down to low temperatures. As such alloys are essentially weak Pauli paramagnets and conventional superconductors [7]. We found that they are much more resistant to hydrogen attack, and high pressures of H_2 gas had to be applied [8,9]. The H absorption corresponds to approx. 3H/atoms per 1 U atom. In none of the cases the alloying metals segregate and two different structures were obtained. The hydrides $(UH_3)_{1-x}Zr_x$ form the α-UH_3 structure, i.e. the *bcc* structure expands and fills by H [9]. Hence basic electronic properties of α-UH_3 could be established. Starting from $U_{1-x}Mo_x$, we obtained $(UH_3)_{1-x}Mo_x$, which tends to be β-UH_3 like, but has the grain size of 1 nm only, i.e. is practically amorphous. This amorphous phase also easily accepts additional dopants, as Zr, Fe, Ti, V..., however magnetic properties remain only weakly affected. It is quite remarkable that all such materials are ferromagnets with the Curie temperature in the range 160-205 K, even if the active U sublattice is diluted by more than 30% of other metals. Fig.1 demonstrates that even the T_C variation with the concentration of alloying element is similar despite different structure. In this respect the hydrides are different than conventional band ferromagnets, sensitive to inter-atomic spacings and alloying. Albeit all are metallic, the U-H interaction, which can have partly ionic character, plays clearly important role. Electronic structure calculations (performed for the α-UH_3 structure and in ferromagnetic or Disordered Local Moment state, with possible random Zr occupancy [9]) suggest a transfer of U-6*d* and 7*s* electrons into H-1*s* states, reducing the hybridization of 5*f* and non-*f* states, supporting thus magnetism even if the U-U spacing is below the Hill limit. Using the LDA+U technique, the ionicity should come out even more pronounced [2]

Speciation of the hydrides into three different groups does not mean we understand all structure details, namely the sites occupied by alloying atoms and arrangement of H atoms around. The weak dependence of properties on structure and composition hints to importance of U-H interaction, leaving the traditional major tuning parameter, U-U spacing, as secondary. The type of alloying metal has also almost no effect on the lattice parameters, which could be understood in case of Zr (atomic radius 160 pm, i.e. slightly higher than U, 156 pm), but not for Fe (126 pm) or Mo (140 pm). We cannot, for example, exclude that Mo is effectively wrapping nanograins of UH_3…but can such nanograins have even higher T_C than UH_3 in bulk? To get better insight into the structure, HR-TEM and PDF (pair distribution function) experiments are planned.

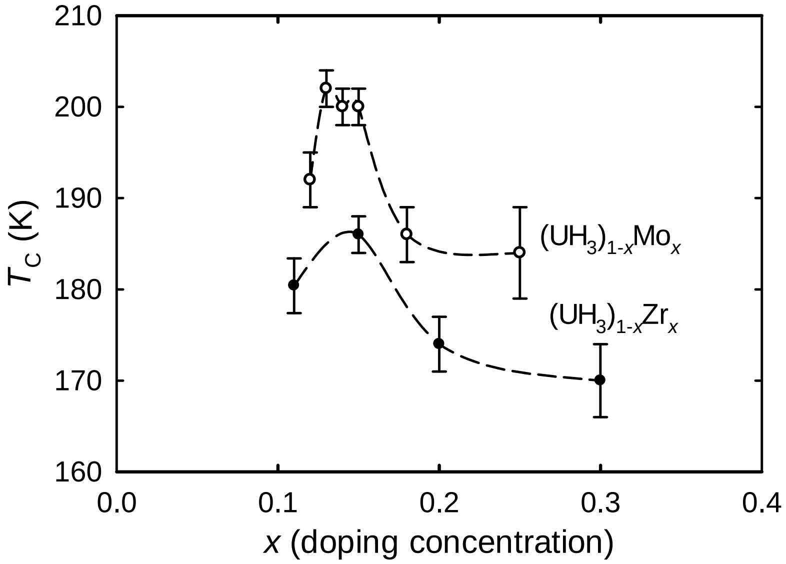

Figure 1. Concentration dependence of the Curie temperatures for the hydrides $(UH_3)_{1-x}Mo_x$ and $(UH_3)_{1-x}Zr_x$.

Acknowledgments

This work was supported by the Czech Science Foundation under the Grant No 15–01100S. M. Paukov was supported by the Grant Agency of the Charles University under the project No. 1332314. Experiments were partly performed at MLTL (http://mltl.eu), which is supported within the program of Czech Research Infrastructures (project No. LM2011025). Participation of N.-T.H.K-N. was supported by the program MOBILITY 7AMB14PL036 (Czech-Polish bilateral cooperation ID(PL) 9004/R14/R15).

References

[1] R. Troc and W. Suski, J. Alloys Comp. **219** (1995) 1.
[2] Y. Zhang et al., J. Nucl. Mater. **430** (2012) 137.
[3] T. Gouder et al., Mater.Res.Soc.Symp.Proc. **986** (2007) 17.
[4] H. Drulis et al. Phys. Rev. B **52** (1995) 9500.
[5] A. V. Andreev et al., Phys. Stat. Sol. A **98**, (1986) K47.
[6] H. Ito et al., J. Alloys Comp. **271** (1998) 629.
[7] I. Tkach et al., Physica C **498** (2014) 14.
[8] I. Tkach et al., Phys. Rev. B **88** (2013) 060407(R).
[9] I. Tkach et al. Phys.Rev. B **91** (2015) 115116.

Email of the presenting author: Havela@mag.mff.cuni.cz

The effect of high-pressure and high-temperature on the crystal structure of sesquioxide: Y_2O_3, Er_2O_3 and Sc_2O_3

I. Halevy[1,2], S. Barzilai[1], O. Yeheskel[1], E. Tiferet[1], R. Carmon[2], S. Ghose[3], J. Hu[3]
[1]Nuclear Research Center - Negev, Physics Department, P.O. Box 9001,
Beer-Sheva, ISRAEL
[2]Department of Nuclear Engineering, Ben-Gurion University,
84105 Beer-Sheva, ISRAEL
[3]Brookhaven National Laboratory, NSLS, Upton, NY 11973, USA

A sesquioxide is an oxide containing three atoms of oxygen with two atoms (or radicals) of another element. For example, aluminium oxide (Al_2O_3) is a sesquioxide. Many sesquioxides contain the metal in the +3 oxidation state and the oxide ion, e.g., Al_2O_3, La_2O_3. The alkali metal sesquioxides are exceptions and contain both peroxide, (O_2^{-2}) and superoxide, (O^{-2}) ions, e.g. Rb_2O_3 is formulated $[(Rb^+)_2(O_2^{-2})(O^{-2})_2]$. Sesquioxides of iron and aluminium are found in soil. The crystal chemistry of the rare earth sesquioxides was first studied in 1964 but it is still under debate to this day. In the rare-earth sesquioxides there is a known sequence of phase transitions, from cubic to monoclinic and finally to hexagonal, as the pressure is increasing. While decreasing the pressure irreversibility occurs in the symmetry, going from hexagonal to monoclinic only. This sequence can occur as function of temperature or pressure. Y_2O_3 is a rare-earth sesquioxide which has been widely used in coating materials and as red-emitting phosphor.

In this study, crystal structure of sesquioxides Y_2O_3, Sc_2O_3 and Er_2O_3 was studied under high-pressure and high-temperature. In the case of Y_2O_3 a nanometric powder was heated to 1450 ºC to obtain the cubic phase.

The pressure was applied via a Merrill-Bassett type diamond anvil cell (DAC) and a "Tel-Aviv" type DAC [1] (Fig. 1). The experiments were conducted using a polychromatic X-ray beam, and the pressure was measured utilizing the fluorescence of Ruby technique. (NSLS- X17C)

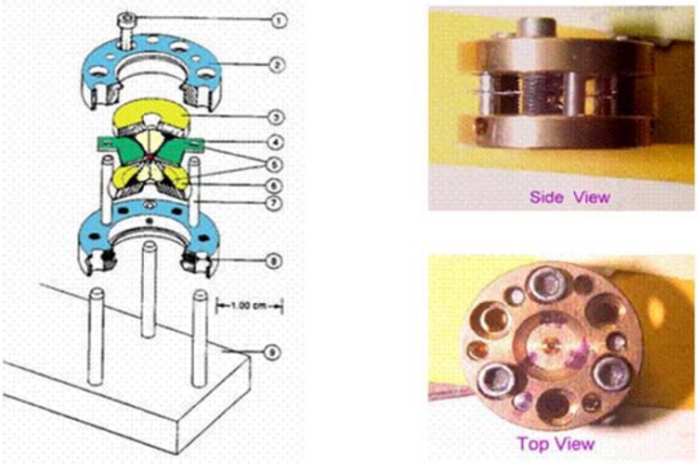

Figure 1."Tel-Aviv" diamond-anvil cell, scheme and photo [1].

While Sc_2O_3 [2] keeps its cubic phase up to 30.5 GPa (Fig. 2a), Er_2O_3 (Fig. 2b) and Y_2O_3 [3] (Fig. 2c) undergo two phase transformations under high-pressure in the pressure range used in the experiment. The volume reduction as function of pressure indicating the phase transformation is shown in Fig. 2d.

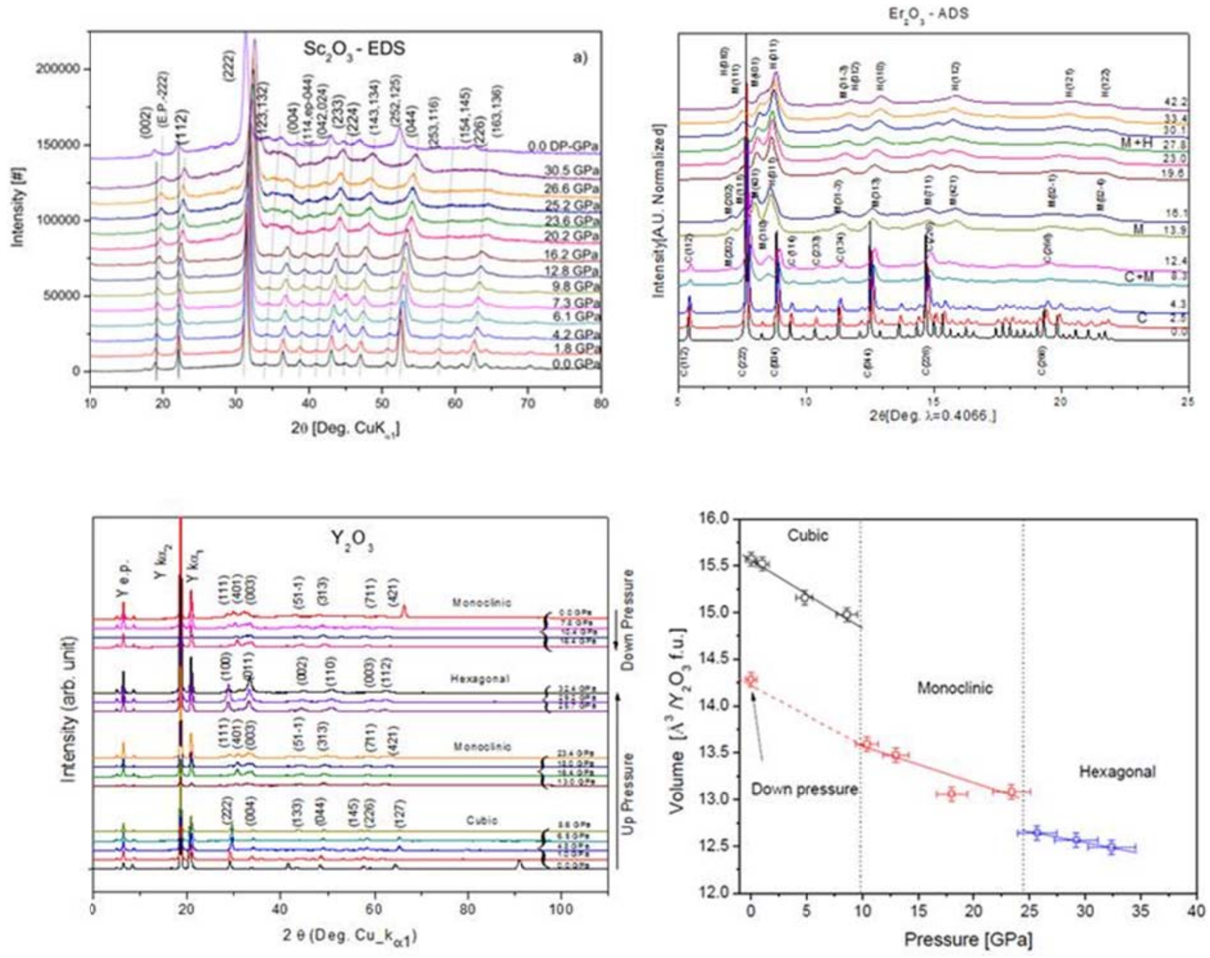

Figure 2. The X-Ray diffraction of Sc_2O_3 (a), Er_2O_3 (b) and Y_2O_3 (c) as function of pressure. The volume reduction as function of pressure for Y_2O_3 indicating the phase transformation is shown in (d).

Ab-initio calculations were carried out in the framework of DFT using the full potential method with Augmented Plane Waves + local orbitals (APW+lo) formalism, as implemented in the WIEN 2k code [4].

B_0 is the isothermal bulk modulus at room temperature and ambient pressure, and B_0' is the partial derivative of the isothermal bulk modulus against pressure under the same conditions. The data were fitted with the Vinet equation.

$$P(V) = 3B_0\left(\frac{V}{V_0}\right)^{-\frac{2}{3}}\left(1-\left(\frac{V}{V_0}\right)^{\frac{1}{3}}\right)\exp\left(\frac{3}{2}\left(B_0'-1\right)\left(1-\left(\frac{V}{V_0}\right)^{\frac{1}{3}}\right)\right)$$

The similarities and differences between sesquioxides Y_2O_3, Sc_2O_3 and Er_2O_3 will be discussed.

References
[1] E. Sterer, M.P. Pasternak, R.D. Taylor, *Rev Sci Instr* 61 (1990) 1117.
[2] S. Barzilai, I. Halevy, O. Yeheskel, *Journal of Applied Physics*, 110 (2011) 043532.
[3] I. Halevy, R. Carmon, M.L. Winterrose, O. Yeheskel, E. Tiferet, and S. Ghose, *Journal of Physics: Conference Series* 215 (2010) 012003.
[4] K. Schwarz, P. Blaha, G.K.H. Madsen, *Comp. Phys. Comm.*, 147 (2002) 17-76.

Email of the presenting author: halevy.itzhak.dr@gmail.com

Structural, electronic, and magnetic characteristics of Np_2Co_{17} under ambient and high pressure

I. Halevy[1,2], A. Hen[2,3], S. Heathman[3], I. Orion[2], E. Colineau[3], R. Eloirdi[3], J.-C. Griveau[3],
F. Wilhelm[4], A. Rogalev[4], J.-P. Sanchez[5], N. Magnani[3,6], A. B. Shick[3,7],
P. M. Oppeneer[8], R. Caciuffo[3]
[1]*Physics Department, Nuclear Research Center Negev, Beer-Sheva, Israel*
[2]*Nuclear Engineering Department, Ben Gurion University, IL84105 Beer-Sheva, Israel*
[3]*European Commission, Joint Research Centre, ITU, Karlsruhe, Germany*
[4]*European Synchrotron Radiation Facility (ESRF), Grenoble, France*
[5]*SPSMS, UMR-E CEA/UJF-Grenoble 1, INAC, FR-38054 Grenoble, France*
[6]*Lawrence Berkeley National Laboratory, Berkeley, California 94720, USA*
[7]*Institute of Physics, Academy of Sciences, Prague, Czech Republic*
[8]*Department of Physics and Astronomy Uppsala University, Uppsala, Sweden*

A previously unknown neptunium-transition-metal binary compound Np_2Co_{17} has been synthesized and characterized by means of powder X-ray diffraction, ^{237}Np Mossbauer spectroscopy, SQUID magnetometry, and X-ray magnetic circular dichroism (XMCD). The compound crystallizes in a Th_2Ni_{17}-type hexagonal structure with room-temperature lattice parameters a = 8.3107(1) Å and c = 8.1058(1) Å (Fig. 1). Refined structural parameters for Np_2Co_{17} at room temperature are shown in Table I.

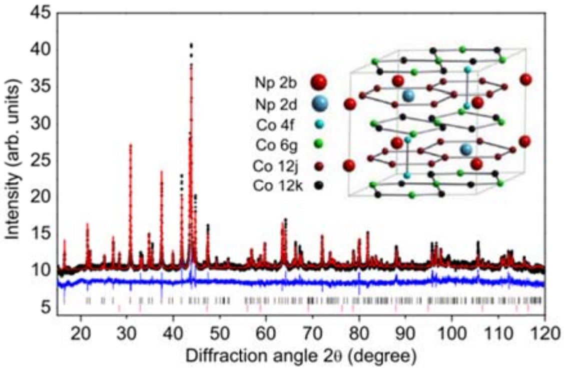

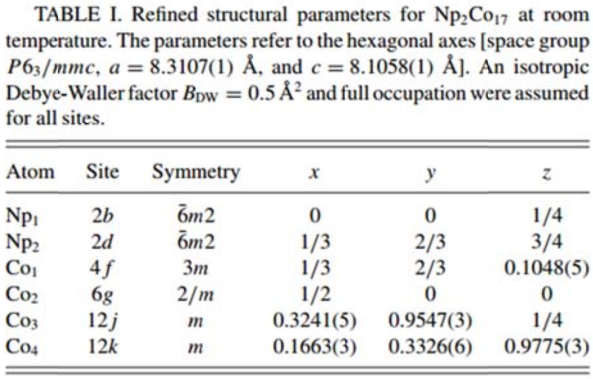

TABLE I. Refined structural parameters for Np_2Co_{17} at room temperature. The parameters refer to the hexagonal axes [space group $P6_3/mmc$, $a = 8.3107(1)$ Å, and $c = 8.1058(1)$ Å]. An isotropic Debye-Waller factor $B_{DW} = 0.5$ Å^2 and full occupation were assumed for all sites.

Atom	Site	Symmetry	x	y	z
Np_1	2*b*	$\bar{6}m2$	0	0	1/4
Np_2	2*d*	$\bar{6}m2$	1/3	2/3	3/4
Co_1	4*f*	3*m*	1/3	2/3	0.1048(5)
Co_2	6*g*	2/*m*	1/2	0	0
Co_3	12*j*	*m*	0.3241(5)	0.9547(3)	1/4
Co_4	12*k*	*m*	0.1663(3)	0.3326(6)	0.9775(3)

Magnetization curves indicate the occurrence of ferromagnetic order below $T_C > 350$ K. Mössbauer spectra suggest a Np^{3+} oxidation state and give an ordered moment of $\mu_{Np} = 1.57(4)\ \mu_B$ and $\mu_{Np} = 1.63(4)\ \mu_B$ for the Np atoms (Fig. 2). Combining these values with a sum-rule analysis of the XMCD spectra (Fig. 3) measured at the neptunium $M_{4,5}$ absorption edges, one obtains the spin and orbital contributions to the site-averaged Np moment ($\mu_S = -1.88(9)\ \mu_B$, $\mu_L = 3.48(9)\ \mu_B$). The structural behavior of Np_2Co_{17} is investigated by means of high-pressure diamond-anvil compression measurements and is compared with that of the isostructural compounds Lu_2Co_{17} and Lu_2Ni_{17}. The Th_2Ni_{17}-type hexagonal crystal structure is preserved with no measurable discontinuous volume collapses up to the highest achieved pressure, p = 43 GPa for Np_2Co_{17} (Fig. 4).

The Np_2Co_{17} High-Pressure data fits to the Birch-Murnaghan and Vinet equations of state give values of the isothermal bulk modulus and its pressure derivative of $B_0 = 286$ GPa and $B_0 = 3$, revealing that this Np compound is a highly incompressible solid with stiffness comparable to that of superhard covalently bonded materials. For the Lu_2T_{17} (T = Co, Ni) compounds, the measured bulk modulus changes from B_0 = 137 GPa for T = Co to B_0 = 257 GPa for T = Ni (Fig. 5).

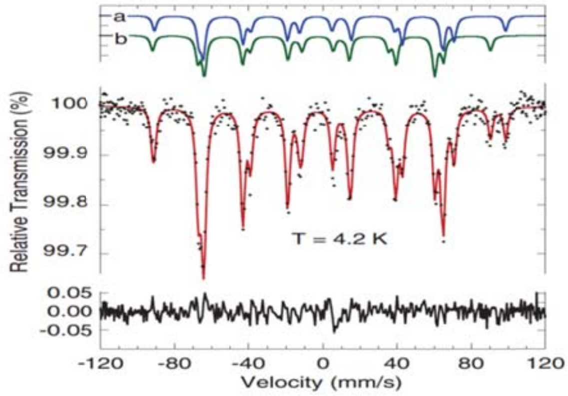

Figure 2. ^{237}Np Mössbauer spectrum of Np_2Co_{17} taken at 4.2 K in the ferromagnetic state.

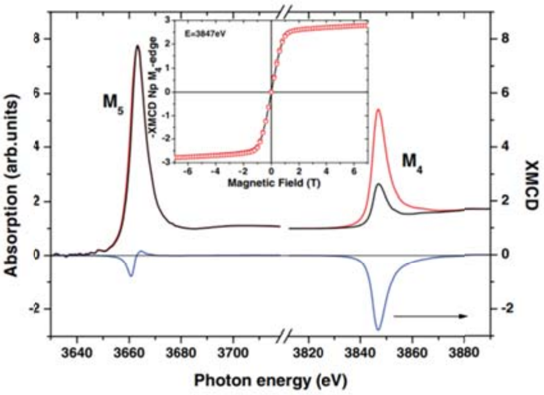

Figure 3. X-ray-absorption spectra $\mu^{+,-}$ measured at 50 K at the $M_{4,5}$ Np absorption edges in Np_2Co_{17}.

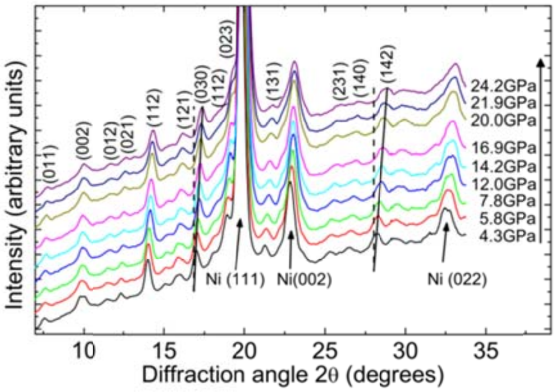

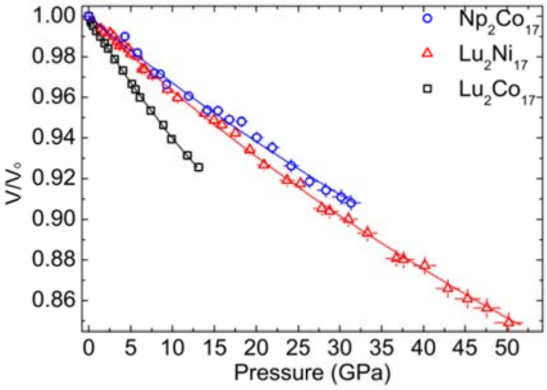

Figure 4. Diffraction patterns of Np_2Co_{17} for selected.

equation
Lu_2Ni_{17}.

The isothermal equation of state for the studied compounds are in excellent agreement with the results of ab initio fully relativistic, full-potential local spin-density functional calculations. Theoretical estimates of the bulk modulus are given also for Np_2Ni_{17}, for which B_0 is predicted to assume values intermediate between those measured for Lu_2Ni_{17} and Np_2Co_{17}.

References
[1] I Halevy et al., Phys. Rev. B 85, 014434 (2012)
[2] A. Hen et al., Phys. Rev. B 90, 054107 (2014)

Email of the presenting author: halevy.itzhak.dr@gmail.com

Classical and quantum criticalities in the itinerant ferromagnet UGe_2: A microscopic interpretation

Marcin M. Wysokiński, Marcin Abram, Józef Spałek
Marian Smoluchowski Institute of Physics, Jagiellonian University, Łojasiewicza 11,
PL-30-348 Kraków, Poland

We present [1,2] a microscopic interpretation of the complete magnetic phase diagram of the ferromagnetic superconductor UGe_2 as a function of applied magnetic field, pressure, and temperature, including its classical and quantum critical points. Our predictions are based on the Anderson Lattice Model tackled by the modified Gutzwiller approximation (SGA [3]). Appearance of two distinct ferromagnetic phases in our approach is associated with change of Fermi surface topology. Our predictions at temperature $T=0$ of magnetic and electronic properties compare favourably with the experimental findings of UGe_2 as seen in the neutron scattering, the magnetization data, and in the de Haas - van Alphen oscillations. For $T>0$, we provide a quantitative description of the all critical points observed in this compound [4], namely the critical ending point, the tricritical point, and the quantum critical ending point. Moreover, we propose that a new quantum critical point appears in close vicinity to the spin-triplet superconducting dome. We characterize it as a Lifshitz quantum critical point and suggest that it can be related to the appearance of quantum critical fluctuations near the Fermi-surface-topology instability, and hence is related to the onset of the spin-triplet superconductivity.

Support of the National Science Centre (NCN), Grant MAESTRO, No. DEC-2012/04/A/ST3/00342 and of the foundation for Polish Science (FNP), grant TEAM is acknowledged.

References
[1] M. M. Wysokiński, M. Abram, J. Spałek, Phys. Rev. B 90, 081114(R) (2014)
[2] M. M. Wysokiński, M. Abram, J. Spałek, Phys. Rev. B 91, 081108(R) (2014)
[3] M. M. Wysokiński, J. Spałek, J. Phys.: Condens. Matter 26, 055601 (2014)
[4] V. Taufour, D. Aoki, G. Knebel, J. Flouquet, Phys. Rev. Lett. 89, 147005 (2010)

Email of the presenting author: marcin.wysokinski@uj.edu.pl

Ce_2Rh_3Ge: an extraordinary example of the sensitive balance between magnetic order, single-ion Kondo and mixed-valence behaviour

M. Falkowski[1], A.M. Strydom[2,3]
[1]*Institute of Molecular Physics, Polish Academy of Sciences, Smoluchowskiego 17,*
60–179 Poznań, Poland
[2]*Highly Correlated Matter Research Group, Physics Department, University of Johannesburg*
PO Box 524, Auckland Park 2006, South Africa
[3]*Institute of Solid State Physics, Vienna University of Technology, Wiedner Hauptstr. 8–10*
Vienna, Austria

Among the large variety of Ce-compounds containing cerium ions in a mixed-valent $Ce^{3+/4+}$ state, only very few cases have been reported in which the unstable valence ions actually condense into robust and long-range magnetic order at low temperature. This is an enigmatic ground state because the higher-temperature mixed-valent state is known to wash local moment magnetism away into the highly degenerate conduction electron sea of a metal [1–3]. Our physical investigations are placing Ce_2Rh_3Ge sensitively balanced between single-ion Kondo and mixed-valence behaviour, combined with the surprising onset of long-range magnetic order at low temperature. The compound Ce_2Rh_3Ge possesses only a single site for the Ce ions, and crystallizes in the rhombohedral, ternary, ordered variant of the cubic Laves $MgCu_2$-type of structure with space group $R\bar{3}m$ and lattice parameters $a = 5.5816(6)$ Å; $c = 11.9392(9)$ Å. The experimental results from $\chi(T)$, $M(B)$, $C_p(T,B)$ and $\rho(T,B)$ confirm magnetic ordering below $T_C = 4$ K, most probably of ferromagnetic origin. The $\chi^{-1}(T)$ data show the existence of a broad high-temperature minimum at 450 K as is frequently observed for cerium compounds suffering from an instable 4*f* shell and mixed or intermediate valent $Ce^{3+/4+}$. To facilitate a study of the mixed-valent behaviour in Ce_2Rh_3Ge the $\chi^{-1}(T)$ data were analyzed in the frame of the inter-configurational fluctuation (ICF) model, confirming the valence fluctuation of Ce ions. The high-field moment of magnetization $M(B)$ per Ce ion obtained at $T = 2$ K is strongly reduced in comparison to the theoretical value expected for the free Ce^{+3} ion which is consistent with a presence a strong hybridization between localized 4*f* electron and conduction electrons, which produces an intermediate valence on the Ce ion. Estimated from $C_p(T)$ data, the Sommerfeld coefficient $\gamma = 10.8$ mJ/Ce-mol·K^2 reflects only a very weakly enhanced effective mass. The 4*f* electron resistivity at low temperatures contracts into a local minimum followed by an increase in logarithmic manner $\rho_{4f}(T) \propto -\ln T$ towards T_C. In combination with the negative magnetic field dependence of the electrical resistivity in the paramagnetic phase, this confirm the Kondo interaction in Ce_2Rh_3Ge. Moreover, we have found a good scaling of A/γ^2 ratio of Ce_2Rh_3Ge with the theoretical value of the Kadowaki–Woods scheme, which firmly classifies Ce_2Rh_3Ge as a mixed-valence compound. The estimated value of Wilson ratio $\chi(T\rightarrow 0)/\gamma$ is close to the value expected for Fermi liquid systems.

References
[1] A.M. Strydom, Physica B 404 (2009) 2981
[2] D.D. Khalyavin et al., Phys. Rev. B 89 (2014) 064422
[3] D. Kaczorowski et al., J. Alloys Compd. 557 (2013) 23

Email of the presenting author: falkowski@ifmpan.poznan.pl

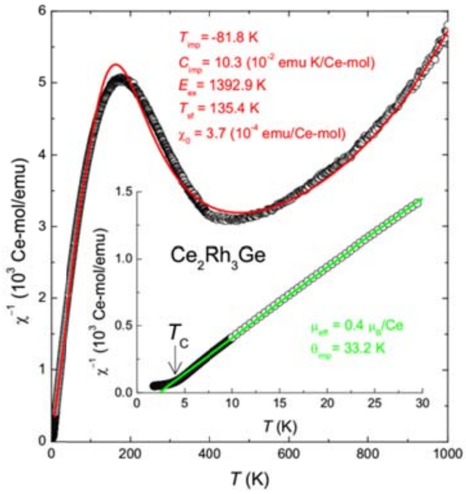

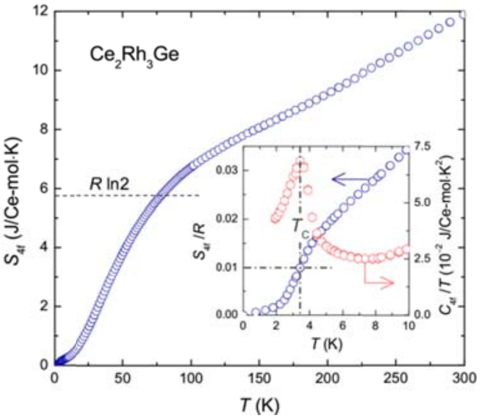

(T)
the
ght-
on
nce

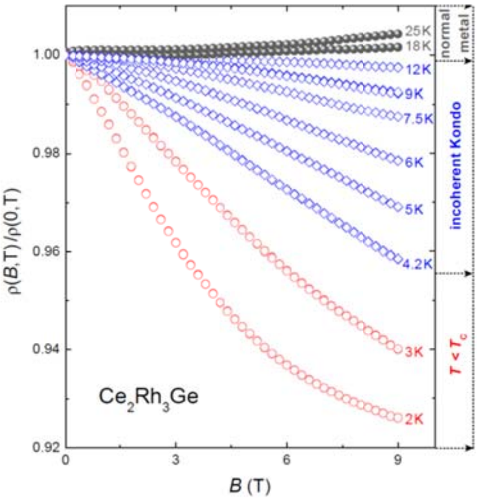

Figure 5. The magnetic field dependence of magnetoresistivity isotherms of Ce$_2$Rh$_3$Ge at selected temperatures, below T_C, in paramagnetic incoherent Kondo scattering region, and for paramagnetic region where Fermi liquid state is dominating.

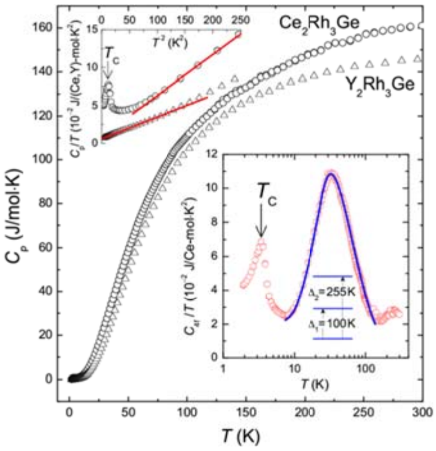

at $C_p(T)$ of
s C_p/T vs. T^2
icient γ are
specific heat
ted by arrow
ne represent
s of energies

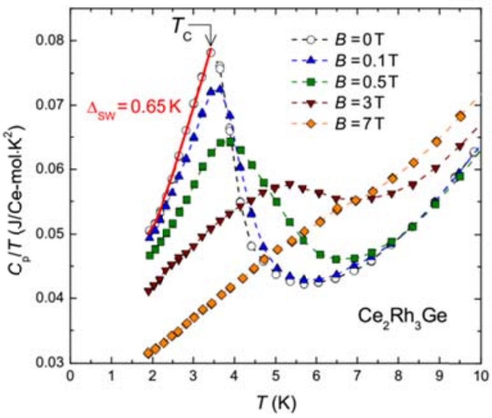

Ce$_2$Rh$_3$Ge in
gnetic fields.
n against the

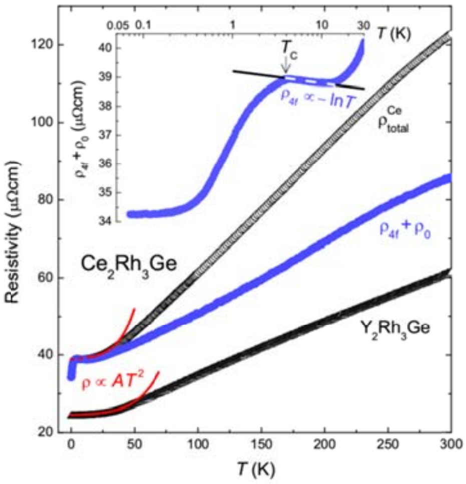

d electrical
e 4f electron
Rh$_3$Ge. Inset
emperatures
temperature
white dashed
ln$T$.

Magnetic properties and crystal structure of RE_2T_2Mg and their hydrides

S. Maskova[1], R.V. Denys[2], I. Halevy[3], K. Miliyanchuk[4], L. Akselrud[4], V. Yartys[2], M. Giovannini[5], L. Havela[1]
[1] *Charles University, Prague, Czech Republic*
[2] *Institute for Energy Technology, Kjeller, Norway*
[3] *Nuclear Research Center Negev, Beer-Sheva, Israel*
[4] *Ivan Franko National University of Lviv, Lviv, Ukraine*
[5] *University of Genova, Genova, Italy*

We have been studying several RE_2T_2Mg (RE = rare-earth, T = transition metal) compounds crystallizing in tetragonal Mo_2FeB_2 structure ($P4/mbm$). In this structure, RE atoms form a triangular motif bringing magnetic frustration into the system. As a consequence the magnetization typically shows several metamagnetic transitions. Figs. 1a and 1b show field dependence of magnetization obtained at $T = 2$ K for Tb_2Ni_2Mg and Tb_2Pd_2Mg, respectively. Both compounds reveal similar magnetic behavior. They are antiferromagnets with $T_N \approx$ 35 K and 60 K, respectively (Figs. 3a and 3b). Both compounds show 2 metamagnetic transitions in the fields up to 60 T. The transitions for Pd-sample are shifted to higher fields.

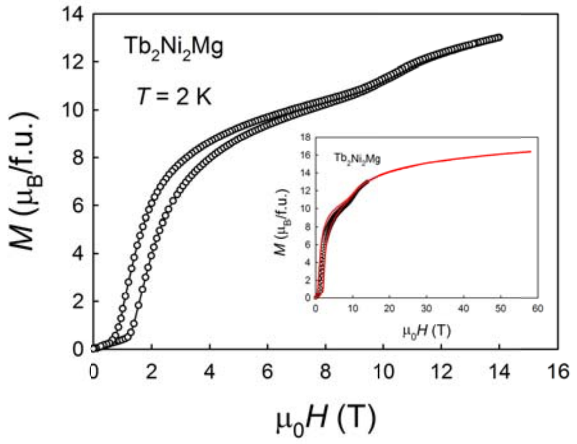

Figure 1a. The field dependence of magnetization obtained at $T = 2$ K for Tb_2Ni_2Mg. The inset shows measured curve obtained using pulsed magnetic field.

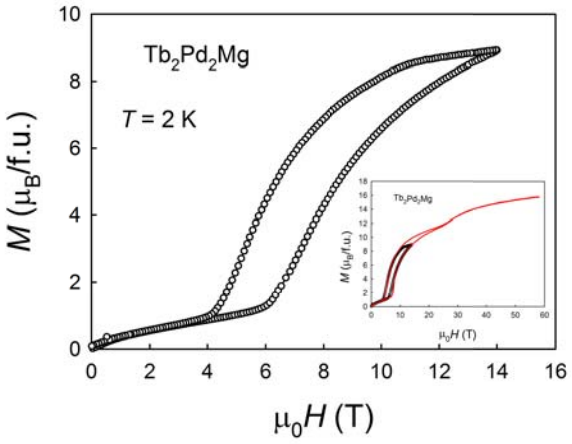

Figure 1b. The field dependence of magnetization obtained at $T = 2$ K for Tb_2Pd_2Mg. The inset shows measured curve obtained using pulsed magnetic field.

Magnetic properties are highly dependent on the exchange interactions between nearest (N) and next-nearest (NN) neighbors. Considering the role of the balance between the N- and NN-exchange we have decided to use the hydrogenation (room temperature, $p \approx 12$ bar) as the tool for weakening their absolute and relative strengths. It was found that Ni-compounds tend to absorb up to 8 H/f.u (Fig. 2a). The crystal structure is changed to monoclinic structure (space group $P21/c$) [1,2]. On the other hand, we have found that the hydrogen absorption in Pd-compounds is lower, not reaching more than 7 H/f.u. (Fig. 2b) and the crystal structure is modified in different way. The Tb_2Pd_2Mg-hydride crystallizes in a new orthorhombic structure type ($Fmmm$).

So as to test the stability of the hydrides we have performed the controlled temperature-induced desorption experiment in closed volume. The desorption occurs in several steps pointing to several different hydrogen positions in the structure (first 7 hours in the Figs. 2a and 2b). During the subsequent cooling with the same rate some of the hydrogen is reabsorbed. X-ray diffraction of the fully desorbed samples, when we did not let the reabsorption happen (hydrogen pumped out from the system at high *T*), showed that in the case of Mg-compounds, the hydrogen absorption in not reversible. Upon desorption of H the initial crystal structure is not restored.

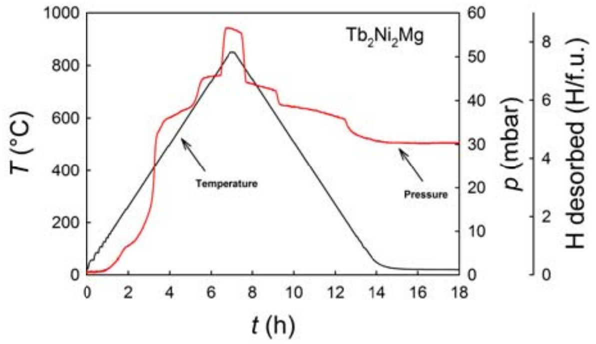

Figure 2a. The record of development of temperature and pressure during the desorption experiment performed on $Tb_2Ni_2MgH_x$.

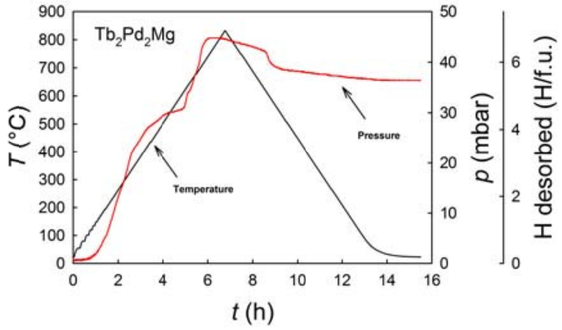

Figure 2b. The record of development of temperature and pressure during the desorption experiment performed on $Tb_2Pd_2MgH_x$.

The magnetic ordering temperatures of all RE-compounds studied are dramatically reduced by the hydrogenation (Figs 3a and 3b). Such general dramatic weakening of the RKKY exchange interaction should have a strong reason – most likely the impact of hydrogenation on the system of conduction electrons.

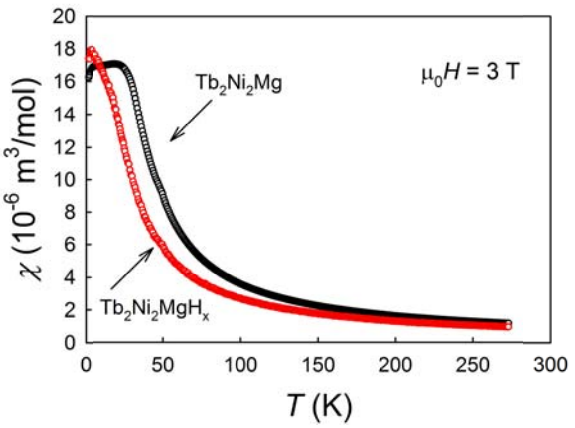

Figure 3a. The temperature dependence of magnetic susceptibility measured in $\mu_0H = 3$ T for Tb_2Ni_2Mg compared with its hydride.

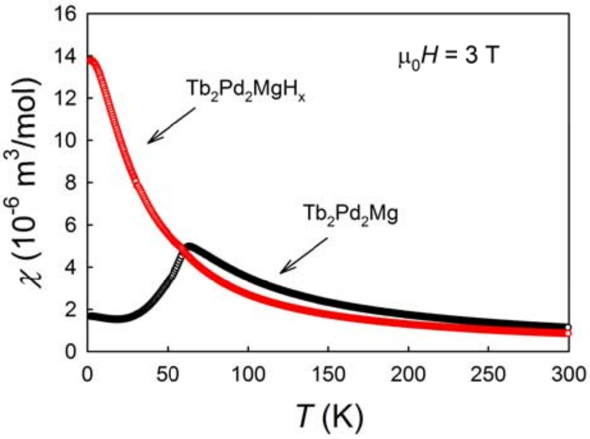

Figure 3b. The temperature dependence of magnetic susceptibility measured in $\mu_0H = 3$ T for Tb_2Pd_2Mg compared with its hydride.

References
[1] Bernard Chevalier, Aleksandra A. Krolak, Jean-Louis Bobet, Etienne Gaudin, Francois Weill, Wilfried Hermes, and Rainer Pottgen, *Inorg. Chem.* 2008, *47*, 10419-10424.
[2] Jean-Noel Chotard, Yaroslav Filinchuk, Bernard Revaz, and Klaus Yvon, *Angew. Chem. Int. Ed.* 2006, 45, 7770 –7773

Email of the presenting author: maskova@mag.mff.cuni.cz

Microscopic model of full magnetic phase-diagram of itinerant ferromagnet UGe_2

Marcin Abram[1], Marcin M. Wysokiński[1], Józef Spałek[2]
[1]Marian Smoluchowski Institute of Physics, Jagiellonian University, ulica Łojasiewicza 11, PL 30-348 Kraków, Poland
[2]Academic Centre for Materials and Nanotechnology, AGH University of Science and Technology, Aleja Mickiewicza 30, PL 30-059 Kraków, Poland

We provide [1,2] the microscopic model which provides a fairly complete description of the electronic and magnetic properties of UGe_2. It is based on the Anderson-lattice model treated in the modified Gutzwiller approximation (SGA) [3]. We explain the appearance of the experimentally observed magnetic phases, namely strong-ferromagnetism, weak-ferromagnetism, as well as the transition to paramagnetism. We show that the sequence and evolution of those phases in the applied magnetic field can be explained in a natural manner as an effect of the competition between the Coulomb repulsion of the uranium 5f electrons and the hybridization of f-electrons with the conduction elections [1]. We track the evolution of classical and quantum critical points in applied field, as a function of pressure, and of the total electron concentration [2]. We simulate the effect of the pressure applied to the real system. We argue, that the main effect of pressure is to change the hybridization strength. We discuss also the effect of the f-level position with the increasing pressure, as well as the possibility of crossing the Hill limit when the overlap between f-orbitals turns out to be nonzero. Our approach explains in a semiquantitative manner the recent experimental results [4].

Support of the National Science Centre (NCN), Grant MAESTRO, No. DEC-2012/04/A/ST3/00342 and of the Foundation for Polish Science (FNP), grant TEAM is acknowledged.

References
[1] M. M. Wysokiński, M. Abram, J. Spałek, Phys. Rev. B **90**, 081114(R) (2014).
[2] M. M. Wysokiński, M. Abram, J. Spałek, Phys. Rev. B **91**, 081108(R) (2015).
[3] M. Abram, J. Kaczmarczyk, J. Jędrak, J. Spałek, Phys. Rev. B **88**, 094502 (2013).
[4] V. Taufour, D. Aoki, G. Knebel, J. Flouquet, Phys. Rev. Lett. **105**, 217201 (2010), H. Kotegawa, V. Taufour, D. Aoki, G. Knebel, J. Flouquet, J. Phys. Soc. Jpn. **80**, 083703 (2011).

Email of the presenting author: marcin.abram@uj.edu.pl

Kondo Alloys: from local to coherent Fermi liquids

José-Luiz Ferreira[1,2], Sébastien Burdin[3,4], Vladimir Dobrosavljevic[5] and Claudine Lacroix[1,2]
[1]*Univ. Grenoble Alpes, Institut NEEL, F-38042 Grenoble, France*
[2]*CNRS, Institut NEEL, F-38042 Grenoble, France*
[3]*Univ. Bordeaux, LOMA, UMR 5798, F-33400 Talence, France*
[4]*CNRS, LOMA, UMR 5798, F-33400 Talence, France*
[5]*Department of Physics and National High Magnetic Field Lab., Florida State University, Tallahassee, FL 32306, USA*

The modification of the electronic structure induced by correlations is at the heart of condensed matter physics. In rare-earth systems one of the most relevant interactions is the antiferromagnetic coupling between local f-orbitals and conduction c-electrons: the Kondo interaction.

In dilute systems the Kondo interaction is well described by the single impurity Kondo model. At very low temperature this model has a universal behavior, that Nozieres in the 70's described as a local Fermi liquid. On the other hand the concentrated regime is quite complex, since RKKY interaction may compete with Kondo effect. However, if magnetic ordering is neglected, the system forms a heavy Fermi liquid and coherence effects among f-orbitals "promote" them to form a large Fermi-surface (FS) together with c-electrons.

Recently it was proposed by two of us[1] that a topological 'Lifshitz-like' transition would separate the local (dilute) and coherent (dense) Fermi liquid regimes, since it is impossible to connect them analytically at zero temperature. This study was conducted in the limit of infinite Kondo coupling. In this limit the transition occurs when the number of electrons in the conduction band is equal to the number of impurities, i.e. of rare-earth atoms.
In order to go beyond the infinite coupling limit, and to get in touch with real systems, we carried out a numerical study of the Kondo Alloy Model in a Bethe Lattice. This model is an interpolation of the single impurity and the lattice hamiltonian using the concentration of magnetic sites and the band filling as control parameters. Moreover in the Bethe lattice, we can vary the coordination number of the lattice.

We used an algorithm inspired by the self-consistent treatment of disorder by Abou-Chacra *et al* [2] and later adapted to strongly correlated systems by Dobrosavljevic and Kotliar [3]. It implements exactly the effects of disorder and gives access to full distributions of the local quantities.

Our results may shed a light in the low temperature physics of rare-earth alloys such as $La_{1-x}Ce_x$[…] or $Lu_{1-x}Yb_x$[…], in which it is possible to achieve both diluted and coherent regimes. These systems are well-known for the appearance of large Non-Fermi Liquid regimes for intermediate concentrations.

References
[1] S. Burdin and C. Lacroix, *Phys. Rev. Lett.* 110, 223406 (2013).
[2] R.Abou-Chacra, P.W. Anderson and D.J. Thouless, J. *Phys. C: Solid State Phys.* 6, 1734 (1973).
[3] V. Dobrosavljevic and G. Kotliar, *Phys. Rev. Lett.* 78, 3943 (1997).

Email of the presenting author: jose-luiz.ferreira@neel.cnrs.fr

Influence of Eu^{2+} magnetic moment order on superconductivity in $Eu_{0.73}Ca_{0.27}(Fe_{0.87}Co_{0.13})_2As_2$ and $Eu(Fe_{0.81}Co_{0.19})_2As_2$

Lan Maria Tran[1], Alain Cousson[2], Arene Goukassov[2], Kamila Komędera[3],
Artur Błachowski[3], Krzysztof Ruebenbauer[3], Jan Żukrowski[4,5],
Zbigniew Bukowski[1], Vinh Hung Tran[1], Andrzej J. Zaleski[1]
[1]*Institute of Low Temperature and Structure Research, Polish Academy of Sciences, ul. Okólna 2, 50-422 Wrocław, Poland*
[2] *Laboratoire Léon Brillouin, CEA-CNRS, CEA Saclay,91191 Gif-sur-Yvette, France*
[3]*Mössbauer Spectroscopy Division, Institute of Physics, Pedagogical University, ul. Podchorążych 2, 30-084 Kraków, Poland*
[4] *AGH University of Science and Technology, Academic Center for Materials and Nanotechnology, Av. A. Mickiewicza 30, 30-059 Kraków, Poland*
[5] *AGH University of Science and Technology, Faculty of Physics and Applied Computer Science, Department of Solid State Physics, Av. A. Mickiewicza 30, 30-059 Kraków, Poland*

AFe_2As_2-based systems (so called 1:2:2 systems, where A = Ba, Ca, Eu, Sr) draw considerable attention, because of some resemblance to the CuO-based superconductors, multiple phase transitions, but mostly because of **possible coexistence of superconductivity (SC) and magnetically ordered phase** and relatively easy tuning of the temperature regions of individual phase transitions (e.g. by chemical substitutions). [1, 2]

These compounds crystallize in the tetragonal $ThCr_2Si_2$-type structure (*I4/mmm* space group). With lowering the temperature, at T_{SDW}, they undergo a structural transition to an orthorhombic phase (*Fmmm* space group), which coincides with a **spin density wave (SDW)** transition of Fe^{2+} magnetic moments.

In this respect, investigated by us $EuFe_2As_2$-based single crystals are no different from the other 1:2:2 systems. However, due to the Eu, with further cooling, it is possible to observe an antiferromagnetic (AF) order of Eu^{2+} magnetic moments. While Eu or Fe content is diluted by e.g. Ca or Co doping it is possible to reach the superconducting (SC) region.

In this contribution we show that there is some influence of the Eu^{2+} magnetic moments on the superconductivity of the FeAs-layers. As examples we present electron transport, magnetization and magnetic susceptibility measurements of $Eu_{0.73}Ca_{0.27}(Fe_{0.87}Co_{0.13})_2As_2$ and $Eu(Fe_{0.81}Co_{0.19})_2As_2$. Both of these compounds show not only typical for the $EuFe_2As_2$ attributes, but also some unusual features such as **re-entrant** behaviour in case of $Eu_{0.73}Ca_{0.27}(Fe_{0.87}Co_{0.13})_2As_2$ (Fig. 1) and a rare phenomenon of **Field-Induced SC (FI-SC)** observed in $Eu(Fe_{0.81}Co_{0.19})_2As_2$ (Fig. 2). [3, 4] Moreover observed features strongly depend on the direction of the applied magnetic field, and so the FI-SC feature is observed only for fields applied perpendicular to the c-axis (Fig. 2).

From our analysis based both on bulk (electron transport, magnetic susceptibility, magnetization) and microscopic (Mössbauer spectroscopy, neutron scattering) measurements, we prove an important influence of the magnetic structure (especially Eu^{2+} magnetic moments) on observed behaviour. Moreover, we propose lowering of **orbital pair breaking effect** as responsible for observation of FI-SC if taking into account a **possible triplet pairing** of superconducting pairs.

We acknowledge the partial financial support by the National Science Center of Poland under projects DEC-2011/03/B/ST3/00446, 2011/01/B/ST3/04553, 2011/01/B/ST5/06397 and the 7th Framework Program: NMI3-II/FP7 – Contract No. 283883.

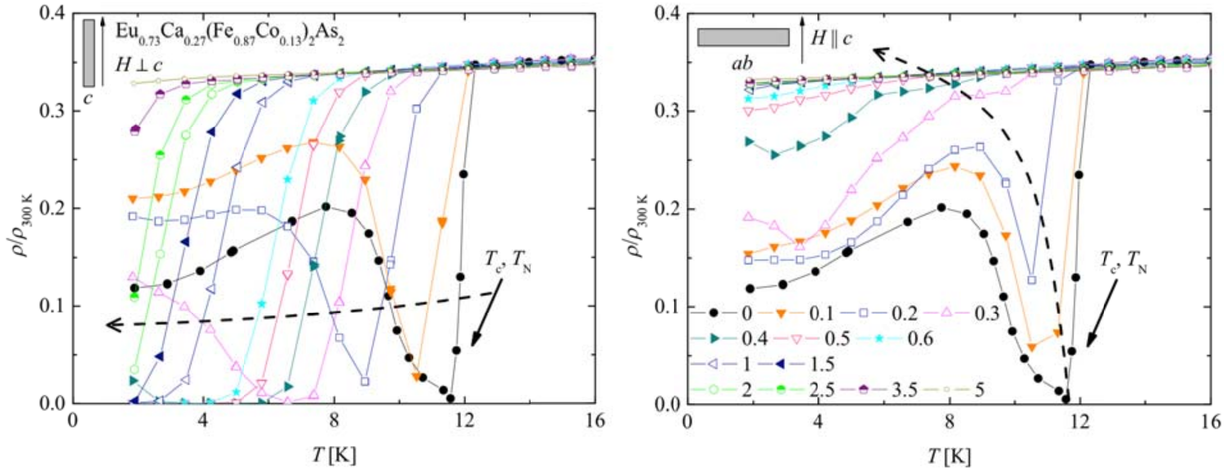

magnetic

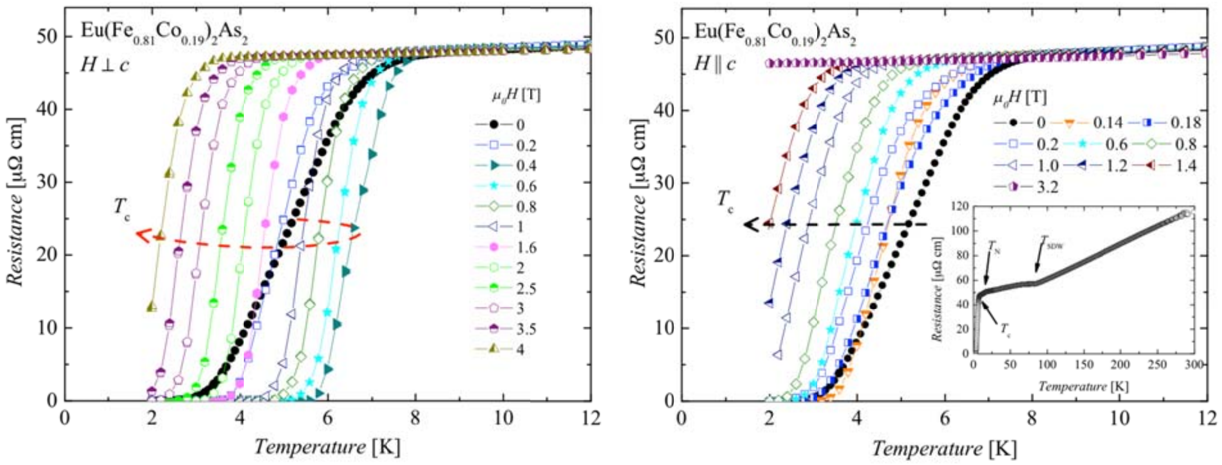

ic fields

References

[1] Lumsden MD, Christianson AD; *J. Phys.* **22** (2010) 203203

[2] Błachowski A, Ruebenbauer K, Żukrowski J**,** Bukowski Z, Rogacki K, Moll PJW, Karpinski J; *Phys. Rev B* **84** (2011) 174503

[3] Tran VH, Zaleski TA, Bukowski Z, Tran LM, Zaleski AJ; *Phys. Rev. B* **85** (2012) 052502

[4] Tran VH, Bukowski Z, Tran LM, Zaleski AJ; *New J. Phys.* **14** (2012) 073052

Email of the presenting author: l.m.tran@int.pan.wroc.pl

Magnetic Measurements on $La_{(1-x)}Sr_xMnO_3$ nanoparticles

Cornelia Hintze[1], Dirk Fuchs[1], Michael Merz[1], Amer Baniodeh[2], Annie Powell[2],
Hilbert von Löhneysen[1]
[1] *Institute for Solid State Physics, Karlsruhe Institute for Technology, Eggenstein-Leopoldshafen, Germany*
[2] *Institute of Nanotechnology, Karlsruhe Institute for Technology, Eggenstein-Leopoldshafen, Germany*

Using a modified Microemulsion technique, weakly agglomerated nanoparticles of pure $La_{(1-x)}Sr_xMnO_3$ particles were prepared. Taking into account the large changes in crystal lattice with respect to bulk single crystal samples, the variation in Curie temperature and magnetization is assessed and discussed.

Email of the presenting author: Cornelia.Hintze@kit.edu

New highly luminescent lanthanide complexes based on pyrazole substituted 1.3-diketones – synthesis and photophysical properties.

Ilya Taydakov
P.N. Lebedev Institute of Physics, Russian Academy of Scienses, S.I. Vavilov Department of Luminescence, Leninskiy pr-t. 53, 119991 Moscow, Russian Federation

Recently we have developed a general synthetic approach to diverse symmetrical and unsymmetrical β-diketones bearing pyrazole moiety. Three main structural types of these compounds were investigated: heterocyclic analogs of dibenzoylmethane (Hdbm, **I**), benzoylacetone (Hbzac, **II**) and benzoyltrifluoroacetone (Hbtfac, **III**). β-Diketone fragment was introduced into different positions of pyrazole ring and other positions were partially substituted by alkyl or fluorinated alkyl groups.

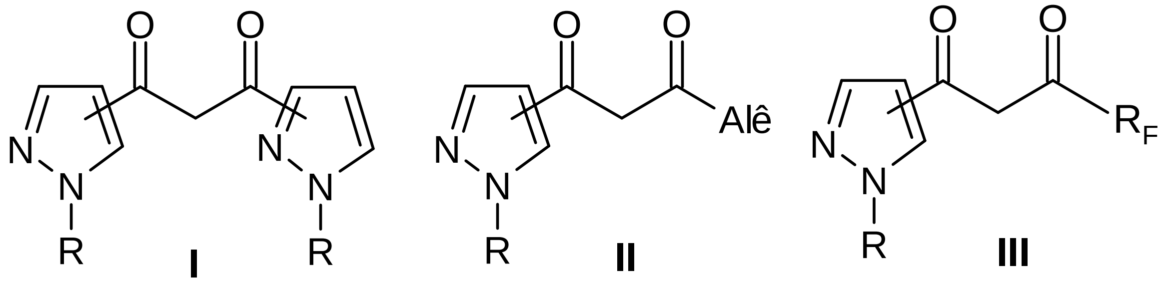

Figure 1. Structural types of ligands.

Some of these compounds were transformed into higly luminescent complexes of Sm^{3+}, Eu^{3+} and Tb^{3+} with different ancillary ligands. Peculiarities of synthesis and luminescent properties of above-mentioned complexes will be discussed in details.

Email of the presenting author: taidakov@gmail.com

Racah materials: role of atomic multiplets in intermediate valence systems

Alexander B. Shick[1], Ladislav Havela[2], Alexander I. Lichtenstein[3], Mikhail I. Katsnelson
[1] Institute of Physics, ASCR, Na Slovance 2, CZ-18221 Prague, Czech Republic
[2] Department of Condensed Matter Physics, Charles University, Ke Karlovu 5,
12116 Prague, Czech Republic
[3] University of Hamburg, Jungiusstrasse 9, 20355 Hamburg, Germany
[4] Radboud University Nijmegen, Heyendaalseweg 135, 6525, AJ Nijmegen, The Netherlands

We address the long-standing mystery of the insulating state of the intermediate valence SmB_6. Within a combination of the local density approximation (LDA) and an exact diagonalization (ED) of an effective discrete Anderson impurity model, the intermediate valence ground state with the f-shell occupation n_{4f}=5.6 is found for the Sm atom in SmB6. This ground state is a singlet, and the first excited triplet state ~3 meV higher in the energy. SmB6 is a narrow band insulator already in LDA, with the direct band gap of ~10 meV. The electron correlations increase the band gap which now becomes indirect. Thus, the many-body effects are relevant to form the indirect band gap, and support the idea of "topological Kondo insulator" in SmB_6.

Also, an actinide analog PuB_6 is considered, and the intermediate valence singlet ground state is found for the Pu atom. We propose that [Sm,Pu]B_6 belong to the new class of the intermediate valence materials with the multi-orbital "Kondo-like" singlet ground-state. Crucial role of complex spin-orbital f[n]-f[n+1] multiplet structure differently hybridized with ligand states in such Racah materials is discussed. Connection between the electronic structure of PuB_6, δ-Pu and Pu115 is established.

Email of the presenting author: shick@fzu.cz

Influence of defects on the dynamical properties of d- and f-electron systems

Urszula D. Wdowik[1], Przemysław Piekarz[2], Krzysztof Parlinski[2], Dominik Legut[3]
[1] *Institute of Technology, Pedagogical University Cracow, Podchorążych 2,*
30-084 Cracow, Poland
[2] *Institute of Nuclear Physics, Polish Academy of Sciences, Radzikowskiego 152,*
31 342 Cracow, Poland
[3] *Nanotechnology Centre & IT4Innovations, VSB-Technical University of Ostrava,*
17. listopadu 15, 708 33 Ostrava, Czech Republic

This contribution presents the recent density functional theory (DFT) studies of the lattice dynamics in the strongly correlated electron system FeO containing Fe-vacancies as major defects. Results of the DFT investigations of the defect-free UC, UC with C-vacancies, and UC with O-impurities are to be presented as well. The current theoretical research highlights the importance of explicit inclusion of strong electron correlation effects and spin-orbit interactions in *ab initio* simulations to predict properly the electronic structure and the vibrational properties of the *d*- and *f*-electron systems. It also uncovers qualitative difference between the lattice dynamics of stoichiometric and defected systems. The Fe-vacancies in FeO are shown to be responsible for significant broadening of the phonon spectra [1] observed in the nuclear resonant inelastic x-ray scattering experiments [2]. On the other hand, the C-vacancies and O-impurities introduce additional vibrational states (localized modes) into the phonon bands of UC. This finding conforms to the experimental results obtained for $UC_{1-x}O_x$ ($x = 0.02$) compound by the neutron time-of-flight technique [3].

References
[1] U. D. Wdowik, P. Piekarz, K. Parlinski, A. M. Oles and J. Korecki, Phys. Rev. B 87 (2013) 121106(R).
[2] V. V. Struzhkin, H. K. Mao, J. Hu, M. Schwoerer-Bohning, J. Shu, R. J. Hemley, W. Sturhahn, M. Y. Hu, E. E. Alp, P. Eng and G. Shen, Phys. Rev. Lett. 87 (2001) 255501.
[3] F. A. Wedgwood, J. Phys. C: Solid State Phys. 7 (1974) 3203.

Email of the presenting author: udw@up.krakow.pl

Excitonic insulator state and condensation in the intermediate valent semiconductor $TmSe_{0.45}Te_{0.55}$

Vardan Apinyan, Tadeusz Kopeć
Institute of Low Temperature and Structure Research (ILTSR),
Polish Academy of Sciences, PO. Box 1410, 50-950 Wroclaw 2, Poland

At ambient conditions, $TmSe_{0.45}Te_{0.55}$ is an indirect semiconductor with weak f-d hybridization and with a gap $\Delta E = 130$ meV, formed between the top of the 4f valence band at Γ-point and the bottom of the 5d conduction band at X-point of the first Brillouin zone. With pressure and at 300 K, this gap can be linearly closed, and an intermediate valent semimetal results. At the low temperatures, pressure leads to an intercepting excitonic insulating phase, as proposed by Mott and Kohn years ago. This fact has been verified with many experimental works.

The excitonic insulator phase is obtained for a given pressure and temperature region, and it exists without any external excitation on the system (light, for example), also, for $T \to 0$. Thus, the excitonic insulator phase is a ground state of matter. Very often, a condensed excitonic phase at low temperatures and high pressure has been realized in the intermediate valent $TmSe_{0.45}Te_{0.55}$, where the excitons with a heavy effective mass strongly bind to phonons. The result is quite surprising, because of the indications of a roton or vortex spectrum (being typical bosonic excitations, related directly to the Bogoliubov-Landau phonon-roton spectrum) with a gap of about 5 K. The principal embarrassment at this point, is that the extension of these measurements under pressure to the region of much lower temperatures are still absent.

In the present work we have answered to the question "what happens at the lower temperatures". Employing the extended Falicov-Kimball model, we have proved that the spontaneous hybridization between the quasilocalized f electrons and itinerant c band is present in the solid state material, which is responsible for the excitonic insulator phase. We have found the critical temperature of the excitonic insulator phase transition. The important result of our theory concerning the excitonic insulator phase is that this state is present even in the case of the totally localized f-band electrons, i.e. when the f-band electron hopping amplitude is vanishing.

At the low temperature region the situation is quite different. Especially, we have examined the breaking of the exciton hybridization state, mediated by the strong bosonic phase fluctuations that appears after introducing the electronic phases in both solid state bands.

In the case of the uniform distribution of the phase variables across the solid state bands, we have found the strong evidence of the phase stiffness in the system. Then, by evaluating the phase stiffness parameter we have found numerically that it is very small: for considered $TmSe_{0.45}Te_{0.55}$ compound it is of order 0.00176 meV. Furthermore, considering the hybridization-symmetry breaking, we have calculated the excitonic condensate transition probability function, the condensate transition critical temperature, and condensate density of states for the realistic system. Comparing with the excitonic pair formation critical temperature, which is of order 186.6 K for $TmSe_{0.45}Te_{0.55}$, the maximum of the exciton BEC transition temperature for $TmSe_{0.45}Te_{0.55}$ is found to be smaller of about two orders of magnitude at $T_c=0.44$ K.

In addition, the excitonic DOS spectra are found gapless, which is the effect of the strong bosonic fluctuations, and the strong phase coherence between different bands in the material.

The principal conclusion that we can derive from our consideration is that the spontaneous hybridization between f and c bands in the solid state is not sufficient for the excitonic condensation at the low temperatures, and contrary, the hybridization-breaking effects should be properly considered, in order to prove the excitonic condensate phase, which is the thermodynamically stable ground state of matter.

Hereafter, in Fig.1, we present the situation of the theory before (the left panel in the picture) and after (the right panel) our investigations in the field. In the left panel the excitonic insulator phase and the excitonic condensate state are considered as the same, while the right panel in the picture shows our correction to the theory and the resulting phase diagram. Different colors in the pictures corresponds to different phases of matter.

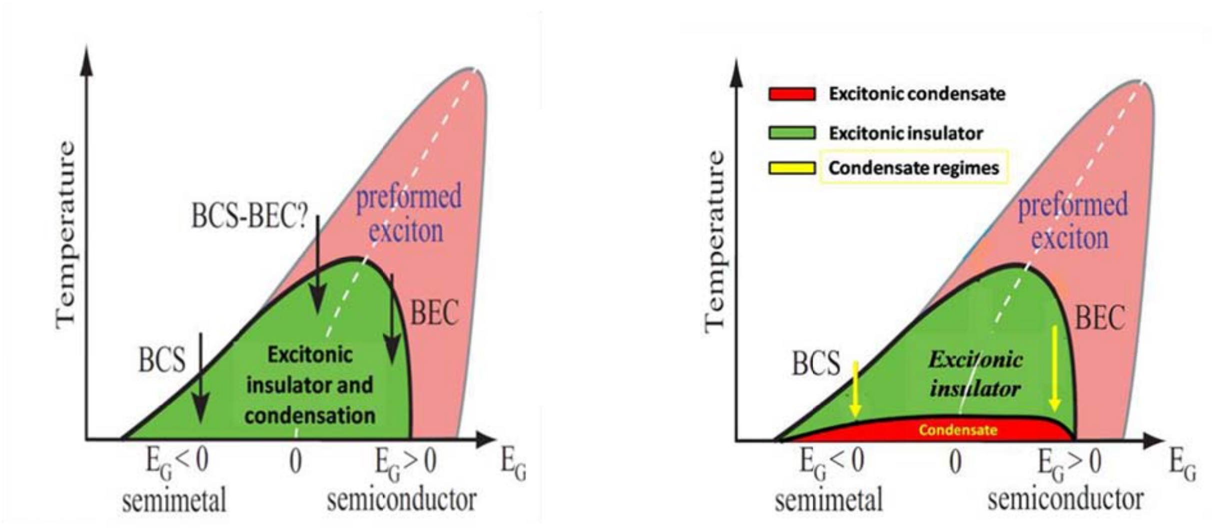

Figure 1. The condensate correction to the general phase diagram (see the left panel) of the excitonic phase transition scenario in the in the intermediate valent semiconductor $TmSe_{0.45}Te_{0.55}$.

Email of the presenting author: v.apinyan@int.pan.wroc.pl

Momentum dependence of a Kondo resonance in $Ce_2Co_{0.8}Si_{3.2}$

P. Starowicz[1], R. Kurleto[1], J. Goraus[2], H. Schwab[3,4], M. Szlawska[5], F. Forster[3,4],
A. Szytuła[1], I. Vobornik[6], D. Kaczorowski[5] , F. Reinert[3,4]
[1]Marian Smoluchowski Institute of Physics, Jagiellonian University, Lojasiewicza 11,
30-348 Kraków, Poland
[2]Institute of Physics, University of Silesia, Uniwersytecka 4, 40-007 Katowice, Poland
[3] Universität Würzburg, Experimentelle Physik VII, Am Hubland,
D-97074 Würzburg, Germany
[4] Karlsruher Institut für Technologie KIT, Gemeinschaftslabor für Nanoanalytik,
D-76021 Karlsruhe, Germany
[5] Institute of Low Temperature and Structure Research, Polish Academy of Sciences,
P.O. Box 1410, 50-950 Wrocław, Poland
[6] CNR-IOM, TASC Laboratory, SS 14, km 163.5, I-34149, Italy

$Ce_2Co_{0.8}Si_{3.2}$ is a hexagonal system and its crystal structure can be classified as a derivative of the AlB_2 type [1]. It shows the properties of a Kondo lattice with characteristic Kondo and coherence temperatures equal to 50 K and 80 K, respectively. Moreover, the system is nonmagnetic down to 0.4 K and exhibits an enhanced electronic specific heat equal $C/T=200$ mJ/(mole$_{Ce}$K^2) at 0.4 K. Finally, below 10 K an evidence of Griffiths phases was found, which should be related to a disorder in Co-Si sublattices [1].

The $Ce_2Co_{0.8}Si_{3.2}$ system was investigated by means of angle resolved photoemission spectroscopy (ARPES) at APE beamline installed at Elettra synchrotron [2]. ARPES data were collected at the temperature of 25 K with photon energies of $h\nu = 25$ eV and 40 eV. The latter photon energy yields an increased photoionization cross section for Ce 4f electrons. For $h\nu = 40$ eV we observed a Kondo peak (KP) ($f_{5/2}^1$ final state) and its spin-orbit partner ($f_{7/2}^1$ final state) and a few dispersing bands. One can distinguish a band with parabolic-like dispersion, which should be a surface state and an electron pocket near the Γ point. The latter is interpreted to be of bulk character.

KP does not reveal any dispersion but its intensity varies considerably with momentum. Maximum of the intensity is found where no band is visible in the experiment while there is a Fermi surface crossing in the theoretical calculations performed with FPLO method. On the other hand KP has a moderate or low intensity for the experimental Fermi vectors. The variation of KP intensity along the FS is interpreted as the evidence of a strong k-vector dependence of the hybridization V_{cf} between conduction band and f electrons. Such a strong V_{cf} variation was predicted theoretically [3-5].

References
[1] M. Szlawska and D. Kaczorowski J. Phys.:Condens. Matter **26**, 016004 (2014).
[2] P. Starowicz, R. Kurleto,, J. Goraus, H. Schwab, M. Szlawska, F. Forster, A. Szytuła, I. Vobornik, D. Kaczorowski and F. Reinert, Phys. Rev. B **89**, 115122 (2014).
[3] H. Weber and M. Vojta, Phys. Rev. B **77**, 125118 (2008).
[4] J. H. Shim, K. Haule and G. Kotliar, Science **318**, 1615 (2007).
[5] P. Ghaemi, T. Senthil and P. Coleman, Phys. Rev. B **77**, 245108 (2008).

Email of the presenting author: pawel.starowicz@uj.edu.pl

Unique hydrogenation properties of R_2Ni_2M compounds with the W_2CoB_2-type structure

Khrystyna Miliyanchuk[1], Ladislav Havela[2], Yuliya Tsaruk[1], Silvie Mašková[2],
Roman Gladyshevskii[1]
[1] *Department of Inorganic Chemistry, Ivan Franko National University of Lviv, Kyryla i Mefodiya St. 6, 79005 Lviv, Ukraine*
[2] *Department of Condensed Matter Physics, Charles University, Ke Karlovu 5, 12116 Prague 2, The Czech Republic*

Hydrides of the intermetallic compounds with the stoichiometry R_2T_2M crystallizing with the tetragonal Mo_2FeB_2-type structure (Pearson symbol *tP*10, space group *P*4/*mbm* (#127)), where *R* is a lanthanide or actinide metal, *T* is a *d*-element, and *M* is a main-group element, have been intensively studied so far. It has been shown that the compounds with the rare-earth metals absorb up to 8 H atoms per formula unit, whereas the uranium-containing compounds remain below the limit of 2 H atoms per formula unit, but their physical properties are extremely sensitive to the concomitant lattice expansion. This group of compounds proved that the compounds of rare-earth metals absorb hydrogen more willingly already at ambient pressure and room temperature, contrary to their uranium counterparts which require elevated temperature and hydrogen pressure. R_2T_2M compounds crystallizing with the orthorhombic W_2CoB_2-type structure (*oI*10, *Immm* (#71)) form another large group of intermetallics including primarily aluminides and stannides of rare-earth and *d*-metals.

The hydrides of R_2Ni_2Al (R = Gd, Er, Lu) and R_2Ni_2Sn (R = Gd, Tb) compounds were synthesized by exposing the activated material to H_2 under the pressure of 0.8 bar at room temperature. In the case of Al-containing compounds, the hydrogen absorption proceeded very rapidly. It started in less then 1 min, and 5 min was sufficient to complete the reaction. The Sn counterparts, on the contrary, exhibit only sluggish hydrogenation kinetics under similar conditions. The process starts only after several hours incubation period and the reaction rate is noticeably lower. The composition of the synthesized hydrides, refined unit-cell parameters, and concomitant lattice expansion due to hydrogenation are given in the Table. The X-ray diffraction peaks for the hydrides were indexed in the space group *Immm* using the W_2CoB_2 structure as a prototype. Hydrogenation results in strongly anisotropic lattice expansion reaching up to 21% and prevailing in *b*-direction.

Table 1. Unit-cell parameters *a*, *b*, *c*, volume *V*, and relative lattice expansion upon hydrogenation for the studied hydrides of the R_2Ni_2M compounds.

Compound	*a* (Å)	*b* (Å)	*c* (Å)	*V* (Å^3)	$\Delta a/a$ (%)	$\Delta b/b$ (%)	$\Delta c/c$ (%)	$\Delta V/V$ (%)
Gd_2Ni_2Al	4.1969(4)	5.4382(5)	8.4484(7)	192.83(3)	–	–	–	–
$Gd_2Ni_2AlH_{5.5}$	3.902(1)	6.331(2)	9.317(3)	230.1(1)	-7.0	16.4	10.3	19.3
Er_2Ni_2Al	4.1499(2)	5.3654(3)	8.2487(3)	183.66(1)	–	–	–	–
$Er_2Ni_2AlH_x$	3.908(1)	5.887(2)	8.875(3)	204.2(1)	-5.8	9.7	7.6	11.2
$Er_2Ni_2AlH_{5.3}$	3.841(1)	6.383(2)	9.106(2)	223.3(1)	-7.4	18.9	10.5	21.6
Lu_2Ni_2Al	4.1158(3)	5.3282(3)	8.1701(4)	179.17(2)	–	–	–	–
$Lu_2Ni_2AlH_{4.8}$	3.726(1)	6.321(1)	8.972(2)	211.3(1)	-9.5	18.6	9.8	17.9
Gd_2Ni_2Sn	4.2822(6)	5.6195(8)	8.3831(10)	201.73(4)	–	–	–	–
$Gd_2Ni_2SnH_{4.2}$	4.034(2)	6.238(3)	9.148(4)	230.2(2)	-5.8	11.0	9.1	14.1
Tb_2Ni_2Sn	4.2712(3)	5.6055(4)	8.3231(5)	199.27(2)	–	–	–	–
$Tb_2Ni_2SnH_{3.8}$	4.022(1)	6.215(1)	9.106(3)	227.6(1)	-5.8	10.9	9.4	14.2

Based on the analysis of the variations of interatomic distances upon hydrogenation a model for the crystal structure of the hydride was suggested. Comparing the crystal structure of the intermetallic compound Er_2Ni_2Al and the lower hydride $Er_2Ni_2AlH_x$, the most pronounced difference in the interatomic distances is observed for the tetrahedra $[Er_3Ni]$, marked as 'H1' on the figure. The centre of the polyhedron has coordinates (8*l*) (0, 0.193, 0.324). The distance between atoms occupying this site (2.3 Å) does not break the "2 Å rule", leading to the theoretical composition of the lower hydride $Er_2Ni_2AlH_4$. Further hydrogen absorption affects most the tetrahedra $[Er_2Ni_2]$ (marked as 'H2'). The coordinates of the centre of the tetrahedron are (4*f*) (0.250,1/2,0). The full occupancy of both crystallographic sites would yield the maximal H content 6 atom per formula unit.

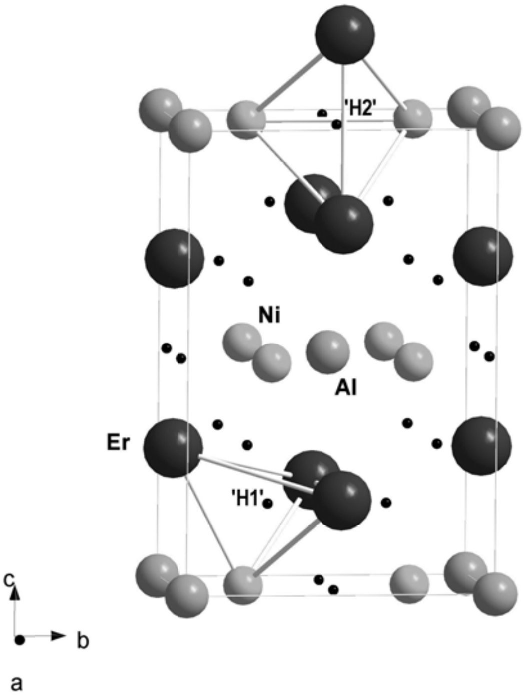

Figure 1. The model of the crystal structure of $Er_2Ni_2AlH_6$.

To conclude, the intermetallic compounds crystallizing with the W_2CoB_2-type structure possess a number of interesting features making further studies of their hydrogenation properties and characterization of the hydrides an important task.

Email of the presenting author: k_miliyanchuk@lnu.edu.ua

Exploring the diversity of $CeCr_2Al_{20}$-type ternary cage aluminides

Michał J. Winiarski[1], Piotr Wiśniewski[2], Dariusz Kaczorowski[2], Jean-Christophe Griveau[3],
Eric Colineau[3], Tomasz Klimczuk[1]
[1] *Faculty of Applied Physics and Mathematics, Gdansk University of Technology,*
Narutowicza 11/12, 80-232 Gdansk, Poland
[2] *Institute of Low Temperature and Structural Research, Polish Academy of Sciences,*
P. O. Box 1410, 50-950 Wroclaw, Poland
[3] *European Commission, Joint Research Centre, Institute for Transuranium Elements,*
Postfach 2340, Karlsruhe, D-76125 Germany

The $CeCr_2Al_{20}$-type group, discovered in the late 60's of the XX century [1], is a wide and diverse family of Al, Zn and Cd-based intermetallics, exhibiting a large versatility towards the composition. In the aluminide group early transition metals can occupy the Cr position and Ce may be replaced by lanthanides, actinides, Sc, Y, Al, Ga, and Ca, and a variety of physical properties and phenomena can be observed depending on the composition.

The work summarizes the results obtained by the presenting author covering the synthesis crystal structure studies, and physical property measurements of various $CeCr_2Al_{20}$ compounds including (La, Ce, Gd, Ho, Lu)T_2Al_{20} (T = Ti-Cr, Nb), (Sc, Y)V_2Al_{20}, and (Th, Np, Pu)$_{1-x}V_2Al_{20}$. Some general trends and dependcies between composition and properties are shown, based both on own and literature data.

In the group of (Sc, Y, Lu)V_2Al_{20} superconductivity with T_c ranging from 0.6 to 1 K was observed. The three Gd(Ti, V, Cr)$_2Al_{20}$ compounds exhibit antiferromagnetic transition with Neel temperatures in the range of 2-3.5 K occurs.

Reference
[1] P. I. Kripyakevich and O.S. Zarechnyuk, Dopovidi Akademii Nauk Ukrainskoi RSR Seria A 30, 364 (1968)

Email of the presenting author: mwiniarski@mif.pg.gda.pl

Preparation of U alloys for EBSD mapping

D. Drozdenko, P. Minarik, M. Paukov, I. Tkach, L. Havela
Charles University, Faculty of Mathematics and Physics, Ke Karlovu 5, 12116 Prague 2, Czech Republic

In the course of investigation of U alloys and their hydrides, microstructure and texture analysis has become important. It is necessary to define grain size, grain boundaries, inclusions, impurity segregation and twinning, but it can give mainly a direct information on phases and their spatial distribution. Here various methods of preparing the U alloys splats for microstructural analysis are discussed, in particular in the context of $U_{x-1}Mo_x$ alloys. The aim of the present study is to optimize the preparation technique for surfaces of U alloys (with various alloying elements).

Uranium metal exists in three allotropic phases (orthorhombic α, tetragonal β, and body-centred cubic γ-phase) [1]. In earlier works it was shown that it is possible to retain the γ-phase down to at room temperature (RT) ultrafast cooling [2]. To reveal presence of small areas of different phases, precise microstructural analysis by Scanning Electron Microscope (SEM) is needed. Moreover, the electron back scatter diffraction (EBSD) provides information about the texture by determining and mapping the crystallographic orientation of grains. For such techniques a high surface quality is a prerequisite and special procedures have to be applied because of the tendency to oxidize rapidly in air [3-6]. An oxide layer on the surface often makes the EBSD mapping unsuccessful and it should be removed. We have attempted several techniques treating the surface for such analyses. The information depth for EBSD is 50-100 nm, so we do not need surface clean in atomic sense, as required e.g. for photoelectron spectroscopy.

In general, the first step of sample preparation for all methods is mechanical polishing. The specimens are sequentially ground on SiC grinding papers (800, 1200, 2000, 4000) using water. Then coarse polishing is performed using 3-µm and 1-µm (and 0.1-µm) diamond abrasive on a nylon lap with a diamond suspension (for 3-µm, 1-µm and 0.1-µm, respectively). In [7], using 1-µm suspension is recommended to minimize the oxidation effect during mechanical preparation. To reveal the microstructure and to remove a surface oxide (the last step of preparation), different methods could be used. Focused Ion Beam (FIB) milling, as part of the SEM Cross Beam, is the one of the possible ion beam milling system. However, sometimes area for investigation prepared by FIB is limited due to formation of uneven "wavy surface". Moreover, this technique is very time consuming. Another method is Ar ion milling in the Precision Ion Polishing System (PIPS). As PIPS is a separate device not attached to SEM, it is necessary to move the specimen from one vacuum chamber to another through air. Therefore oxide formation cannot be avoided. Nevertheless, for different compositions of U alloys the produced surface of a specimen after such preparation procedure could still be different. In Fig. 1 the surfaces of splats of UMo15% and UMo4% (at.%) after mechanical polishing and ion milling in PIPS for 6h are represented. As we can see, for different Mo concentrations the interaction of Ar ions with the surface is different. More importantly, back scattered electrons compose Kikuchi map, from which phases and orientation of grains are revealed, could be observed only in the case of UMo15%. The treatment visualizes grain boundaries, which are more sensitive to ion bombarding and are faster evaporated.

One of the most popular methods for preparing samples for the EBSD analysis is electrochemical etching/polishing [7-9]. Different electrolyte solutions are used. In [9], importance of two electropolishing steps is explained. The first electrolyte used is the solution of 45% ethanol, 27% ethylene glycol, and 27% phosphoric acid [10]. The parameters of electropolishing are: 10–15 V, 5–10 min, RT, the electrolyte is stirred. The samples are rinsed in tap water, then in propanol, warm-air dried, and re-immersed in the unbiased electrolyte. The samples are then re-rinsed and dried with unheated pressurized air. The second electropolishing step is performed to passivate the surface at least for time needed transfer the sample into SEM. The second electrolyte used is a solution of 5% phosphoric acid and 95% de-ionized water [7]. Samples are electropolished at 5 V for 1–2 s at RT in an unstirred bath. Following the second electropolish, the specimens were rinsed with water, rinsed with propanol, and dried with unheated pressurized air. Scott et al. in [8] presented that one step of electopolishing using an electrolyte solution consisting of a mixture of 50% orthophosphoric acid, 30% ethanol and 20% ethylene glycol, followed by ion milling by FIB, is successful for the EBSD sample preparation. Ref. [7] also shows that using 5% orthophosphoric acid is environmentally friendly and sufficient for preparing U surface for EBSD mapping.

Our experience shows that electrochemical etching/polishing (which can be combined with mild final in-situ FIBing for flashing off residual oxides) is a convenient way for preparing U surfaces. The disadvantage is that the parameters should be optimized for different U alloys, as properties of γ-U surfaces (e.g. with more Mo) are very different than for mostly α-U, found in low-doper U. An interesting finding is that upon electropolishing the U surfaces oxidize slower than upon only mechanical polishing.

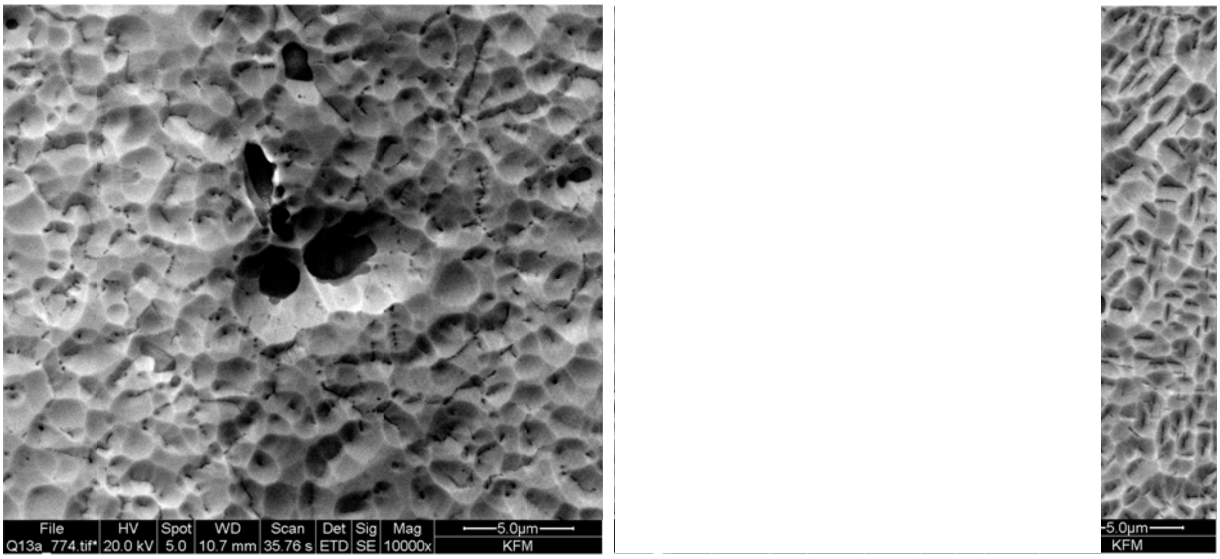

a) b)

Figure 1. SEM image of a) UMo15% (polished up to 1 µm ~20 min, PIPS ~6 h, does diffract) b) UMo4% (polished up to 0.1 µm ~25 min, PIPS ~6 h, does not diffract).

References

[1] L. Morss, N.M.Edelstein, J.Fuger, The Chemistry of the Actinide and Transactinide Elements, 3rd ed., Springer (2006).
[2] I. Tkach et al., J. Alloys and Comp. 534 (2012) 101-109.
[3] G.C. Allen, P.M. Tucker, J. Chem. Soc., Dalton Trans. 5 (1973) 470–474.
[4] G.C. Allen et al., J. Chem. Soc., Faraday Trans. 2 (80) (1984) 991–1000.
[5] G.C. Allen et al. J. Chem. Soc., Dalton Trans. 12 (1974) 1296–1301.
[6] G.C. Allen, R.K. Wild, J. Chem. Soc., Dalton Trans. 5 (1974) 493–498.
[7] Kelly et al., J. of Nuclear Mater. 353(2006) 158-166.
[8] T.B. Scott et al., J. Alloys Comp. 475 (2009) 766-772.
[9] R.J. McCabe and D. F. Teter, J. of Microscopy, 223 (2006) 33–39.
[10] ASM International Handbook Committee 9 (1985) 52.

Email of the presenting author: drozdenko@karlov.mff.cuni.cz

Magnetic properties of double doped UH_3 -based hydrides

M. Paukov[1], I. Tkach[1], D. Drozdenko[1], P. Minárik[1], D. Kriegner[1], Z. Matěj[1], S. Mašková[1], I. Turek[1], M. Diviš[1], M. Cieslar[1], N.-T. H. Kim-Ngan[2], A.V. Andreev[3], L. Havela[1]
[1]*Charles University, Ke Karlovu 5, 12116 Praha 2, Czech Republic*
[2]*Institute of Physics, Pedagogical Univerristy, 30084 Krakow, Poland*
[3]*Institute of Physics, Academy of Sciences of the Czech Republic, Prague, Czech Republic*

Interaction with hydrogen is an important issue related to application of uranium and its alloys. Any contact of α-U with H leads to formation of the stable allotropic form β-UH_3, a dark pyrophoric powder, formed via the metastable α-UH_3. Applications of U metal are typically based on its *bcc* form γ-U, because it is more malleable, ductile and stable with respect to irradiation effects than α-U. It is stable at high temperatures, but it can be retained as pure or in a α-γ composite using a doping (by Mo, Zr, Ti, Nb, Re, Ru, Pd, or Pt). *Bcc* U-Mo and U-Zr alloys form different types of hydrides (high H_2 pressures needed), although both are based on UH_3. The U-Mo alloys lead to amorphous structure based on β-UH_3, which can be characterized as $(UH_3)_{1-x}Mo_x$ (grain size 1 nm). They not only retain the ferromagnetism of β-UH_3 ($T_C \approx 165$ K), but the ordering temperature even increases, exceeding 200 K. Magnetic moments also increase, from 0.9 to 1.1 μ_B/U [1]. The U-Zr alloys lead to crystalline hydrides of the α-UH_3 type, which could be therefore synthesized first time without the β-UH_3 admixture. Besides, those two types one has to include also hydrogenation of U_6T (T = Mn, Fe, Co, Ni), which leads to β-UH_3 type of hydrides, with T_C in the similar range below 200 K. U_6FeH_{17} corresponding to $(UH_{\approx 2.8})_{0.86}Fe_{0.14}$ (magnetic moment 0.79 μ_B/U) and U_6CoH_{18} corresponding to $(UH_3)_{0.86}Co_{0.14}$ (magnetic moment 1.0. μ_B/f.u., i.e. 1.2 μ_B/U) have the Curie temperatures 173 K and 185 K respectively [2,3]. Magnetic properties of α-UH_3 and β-UH_3 are despite different structure very similar. Curie temperatures are in the range between 165 K and 210 K, magnetic moments are around 1.0 μ_B/f.u. The dependences of Curie temperature on concentration of the doping have similar view in cases of Mo and Zr.

Important information on magnetism comes from related lattice expansion, i.e. spontaneous magnetostriction, which depends mostly on the difference of spin moments in paramagnetic and ordered state. To determine the magnetostriction, the temperature dependence of the lattice parameter *a* was measured in the range 10 - 300 K using X-ray diffraction (Fig. 1). The result can be compared with the data of β-UH_3 that was published in [4]. Fig. 1 indicates a large magnetostriction effect below 200 K, yielding the relative volume change $\Delta V/V = 3.2 \cdot 10^{-3}$ [5].

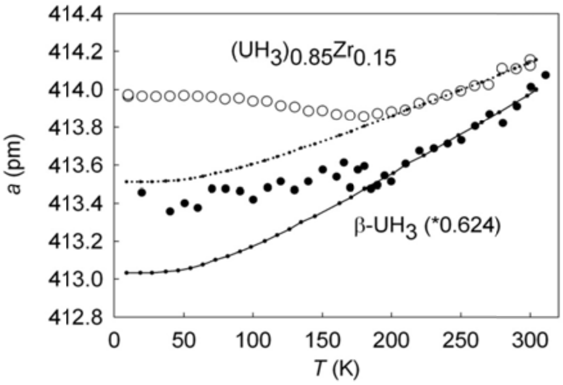

Figure 1. Temperature dependence of the lattice parameter of $(UH_3)_{0.85}Zr_{0.15}$ compared with β-UH_3, (from Ref. 4) with extrapolated dependence from the paramagnetic state. The data on β-UH_3 are rescaled to match approximately those on $(UH_3)_{0.85}Zr_{0.15}$, which allows to compare mutually the magnetostriction and thermal expansion.

Provided the amorphous structure guaranteed by Mo, it can accept other types of dopants in addition. We tested for Ti, Fe, and Zr and investigated variations of magnetic properties. We assumed that the amorphous structure must be more accepting diverse sizes of dopant atoms and we indeed obtained the amorphous structure (Fig. 2.) for the hydrides with Ti, Fe, or Zr doping together with Mo, as $(UH_3)_{0.851}Fe_{0.142}Mo_{0.007}$, $(UH_3)_{0.78}Mo_{0.12}Zr_{0.10}$, $(UH_3)_{0.78}Mo_{0.12}Ti_{0.10}$.

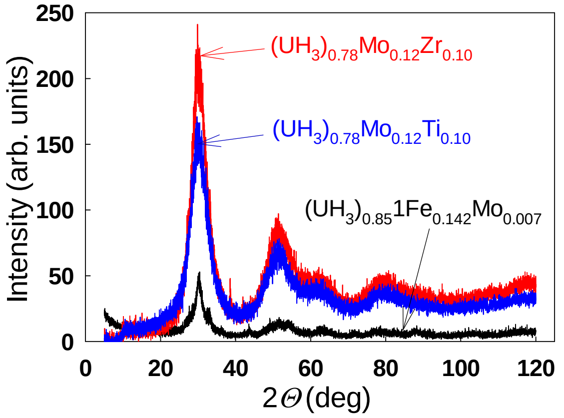

Figure 2. X-ray diffraction pattern of the amorphous hydrides (λ =0.1540562 nm).

Our investigation of magnetic properties of such double doped hydrides shows ferromagnetic ordering with parameters only weakly depending on the dopants. The addition of Zr enhances T_C more than addition of Ti, addition of Fe broadens the transition and enhances magnetization per U atom (Fig. 3).

The work will continue to establish limits of stability of the amorphous phase.

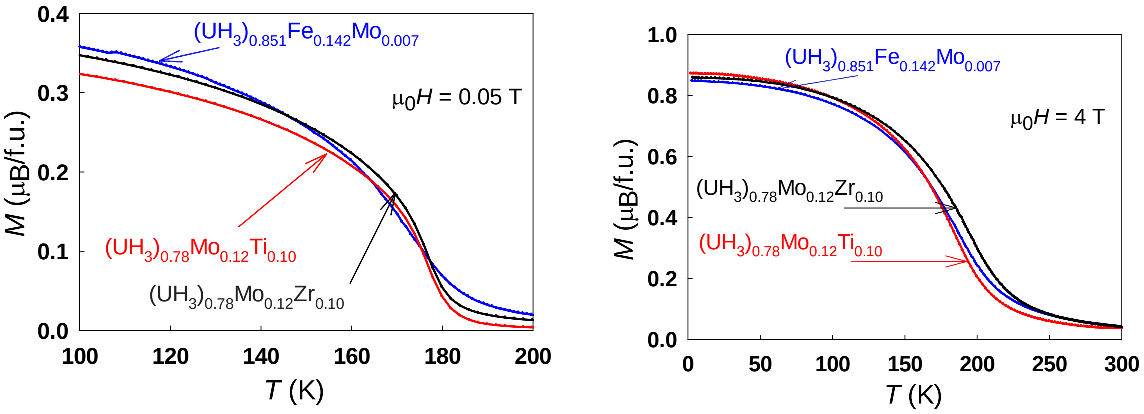

Figure 3. Temperature dependence of magnetization: left - detail in for low magnetic fields illustrating the Curie temperatures, right - in $\mu_0 H$ = 4 T, illustrating the total magnetization.

This work was supported by the Czech Science Foundation under the Grant No 15–01100S. M. Paukov was supported by the Grant Agency of the Charles University under the project No. 1332314. Experiments were partly performed at MLTL (http://mltl.eu), which is supported within the program of Czech Research Infrastructures (project No. LM2011025). Participation of N.-T.H.K-N. was supported by the program MOBILITY 7AMB14PL036 (Czech-Polish bilateral cooperation ID(PL) 9004/R14/R15).

References

[1] I. Tkach et al., *Phys. Rev. B* **88**, 060407(R) (2013).
[2] H. Drulis et al., *Phys. Rev. B* **52**, 9500 (1995).
[3] A.V. Andreev et al., *Phys. Stat. Sol. (a)* **98**, K47 (1986).
[4] A.V. Andreev et al., *J. Alloys Comp.* **267**, 32 (1998).
[5] I. Tkach et al. *Phys. Rev. B* **91** (2015) 115116.

Email of the presenting author: Michael.Paukov@gmail.com

Chemical pressure effect in $SmNiC_2$

Tomasz Klimczuk[1], Prathiba[2], Judyta Strychalska[1], Tuson Park[2]
[1] *Faculty of Applied Physics and Mathematics, Gdansk University of Technology,*
Narutowicza 11/12, 80-233 Gdansk, Poland
[2] *Department of Physics, Sungkyunkwan University, Suwon 440-746, South Korea*

A series of $Sm_{1-x}Ln_xNiC_2$, where Ln=La and Lu, were synthesized by arc-melting method and annealed for 2 weeks at 850°C. Powder x-ray diffraction was used to analyze sample purity and the lattice parameters were calculated using LeBail refinement method. Physical properties were measured by means of magnetic susceptibility, electrical resistivity and heat capacity.

$SmNiC_2$ is a ferromagnet with relatively high Curie temperature (T_C = 17 K). Since Sm is located almost in the middle of the lanthanides, it gives unique opportunity of chemical doping by large La as well as small Lu metal. This way increase (La doping) or decrease (Lu doping) in the unit cell volume is expected, which might be seen as negative or positive “chemical” pressure.

The phase diagram reveals a sudden decrease of the charge density wave formation temperature (T_{CDW}) from 150K for $SmNiC_2$ to 55K for $Sm_{0.75}La_{0.25}NiC_2$. The Curie temperature decreases with both La and Lu substitution in $Sm_{1-x}Ln_xNiC_2$. Interestingly ferromagnetism is observed for $Sm_{0.13}Lu_{0.87}NiC_2$ and Curie temperature T_C = 3.5 K was estimated from the Arrot plot. Further increase of La reveals superconductivity and the highest T_{sc} ~3 K is obtained for pure $LaNiC_2$.

Email of the presenting author: tomasz.klimczuk@pg.edu.pl

XMCD study of ferromagnetism in $YbCu_2Si_2$ under pressure

F. Wilhelm[1], D. Braithwaite[2], S. M. Ramos[2], E. N. Hering[2], G. Lapertot[2], A. Rogalev[1]
[1] ESRF-The European Synchrotron, 71 Avenue des Martyrs, 38000 Grenoble, France
[2] CEA/INAC, 17 Avenue des Martyrs, 38000 Grenoble, France

In rare-earth intermediate-valence (IV) compounds, the interplay between the magnetic and valence instability represents one of the most studied subjects, with the possibility of tuning the system to a magnetic quantum critical point (QCP), where strong spin and/or valence fluctuations are present. The Ce and Yb Kondo lattices are often considered to be electron/hole equivalents, however Yb compounds also offer a favorable opportunity for studying the role of the valence fluctuations in the quantum criticality, since applying pressure is expected to induce larger changes of the valence. $YbCu_2Si_2$ is an ideal prototype Yb system, obeying Doniach's phase diagram. By applying pressure, the system evolves from a paramagnetic state to an ordered one [1], reached at the critical pressure Pc=7-8GPa. Recent a.c. susceptibility measurements under high pressure strongly suggested that the induced magnetic order is ferromagnetic (FM) [2]. Determining the nature of an ordered phase that occurs only above 8 GPa although, is not trivial. A direct confirmation of ferromagnetism in this compound is highly desirable, especially because systems presenting a FM QCP are quite rare. In this work, we report x-ray magnetic circular dichroism (XMCD) measurements at the L_3-edge of Yb in $YbCu_2Si_2$ single crystal at 2K and under pressure up to 15GPa that have been performed at the ESRF ID12 beamline. The amplitude of the XMCD signal is proportional magnetization of the absorbing atom. For pressures higher than 7.5GPa, the field dependence of the XMCD signal shows a typical FM behavior with a tendency to saturate above H=0.5T. Moreover, it was found to be small and almost constant at low pressure, followed by a strong increase above Pc, confirming the FM nature of the ordered phase.

References
[1] K. Alami-Yadria, H. Wilhelm, and D. Jaccard, Eur. Phys. J. B **6**, 5–11 (1998).
[2] A. Fernandez-Pañella, D. Braithwaite, B. Salce, G. Lapertot and J. Flouquet, Physical Review B **84**, 134416 (2011).

Email of the presenting author: wilhelm@esrf.fr

Structure and superconducting transition in U-Pt and U-Pd alloys prepared by splat cooling technique

S. Sowa[1], N.-T.H. Kim-Ngan[1], M. Paukov[2], M. Krupska[1], I. Tkach[2], L. Havela[2]
[1]*Institute of Physics, Pedagogical University, Podchorazych 2, 30-084 Krakow, Poland*
[2]*Faculty of Mathematics and Physics, Charles University, Ke Karlovu 5,*
12116 Prague, Czech Republic

Uranium metal exhibits three allotropic phases: α-U phase below 940 K (orthorhombic structure; space group *Cmcm*, unit cell parameters a = 2.854 Å, b = 5.870 Å, c = 4.937 Å, the mass density ρ = 19.07g/cm^3 and the smallest atomic distance d_{U-U} = 2.837 Å), β-U phase between 940–1045 K (tetragonal structure (P4$_2$/mmm, a = b = 10.52 Å, c = 5.57 Å , ρ = 18.17g/cm^3, d_{U-U} = 2.889 Å) and the γ-U phase (body-centered cubic (*bcc*), A$_2$-type structure) between 1045–1405 K ($Im\bar{3}m$, a = 3.542 Å (when extrapolated to room temperature), ρ=17.94 g/cm^{-3}, d_{U-U} = 3.067 Å). We succeeded to retain the pure γ-U phase down to room temperature with 13 at.% Mo doping (U-13%Mo). It is essential that by using ultrafast cooling we could reduce the required doping content. All U-Mo splats become superconducting below 2.1 K.

The XRD patterns of the so-called intermediate Mo concentration, in the range of 2-10 at. % Mo, consisted of both α and γ reflections. We have thus investigated other two U-T splats with an intermediated T content, i.e. 2-10 at.% Pt and Pd. We show in Fig. 1 the XRD patterns of U-T splats with 5-6at. % T doping (U-6%Mo, U-5%Pd and U-5%Pt). They are very similar indicating a mixed phase. Our results indicate also that by splat cooling, a larger solubility of Pd and Pt in U can be obtained, at least up to 15 at.%, as in our case. Indeed we could stabilize the γ-U phase down to room temperature by doping with 15at.% Pt (combined with splat cooling).

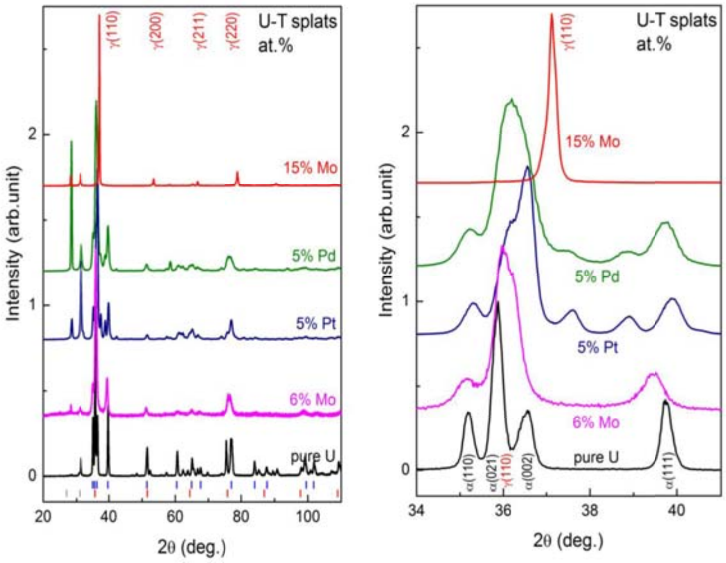

Figure 1. Left: X-ray diffraction patterns of U-T splats. Each curve was normalized to the maximal intensity of most intense peak 2θ = 36^0 – 37^0 and shifted with respect to that for pure-U splat. The (color) vertical sticks indicate the main XRD patterns of orthorhombic (blue) and cubic (red) structures and of the surface impurities (black). Right: A comparison of the low-angle XRD data for U-6%Mo, U-5%Pd and U-5%Pt with those for pure-U splats consisted of mainly orthorhombic α-peaks (α(110), α(021), α(002), α(111)) and for U-15%Mo splat having a single cubic γ(110) reflection in the angle range of 34-41^o.

The investigated samples become superconducting manifested by an abrupt drop in resistivity at T_c (Fig. 2). For U-5%Pd and U-5%Pt splats, only one single resistivity drop was observed at T_c = 0.69 K, with a relatively narrow transition width ΔT_ρ = 0.08 K and 0.02 K, respectively. The U-6%Mo splat reveals clearly two separate features in the resistivity. It was estimated that the first smooth superconducting transition has T_c=1.07 K and ΔT_ρ = 0.60 K, while the second superconducting transition is very abrupt at T_c=0.78 K and with ΔT_ρ = 0.02 K, revealing two different superconducting phases in this splat. The lower T_c was assumed to be associated with the γ-U phase (as it was also revealed by a sizeable specific heat anomaly). Applying external magnetic fields, the superconducting transitions shift towards lower temperatures as expected. The temperature T_c dependence of the critical field $H_c(T)$ for selected U-T splats is shown in Fig. 3. Although it is difficult to be conclusive about the analytical shape from such a few data points, it is visible that neither a quadratic dependence as the temperature approaches 0 K nor a close to linear dependence were revealed for those splats. The critical magnetic fields at zero temperature ($\mu_0 H_c$) estimated from the polynomial fits of the experimental data provide values of 1.8-2.2 T and the critical slopes at T_c of the H_{c2} vs T curves ($-\mu_0(dH_{c2}/dT)_{Tc}$) of 3.2-3.6 T/K.

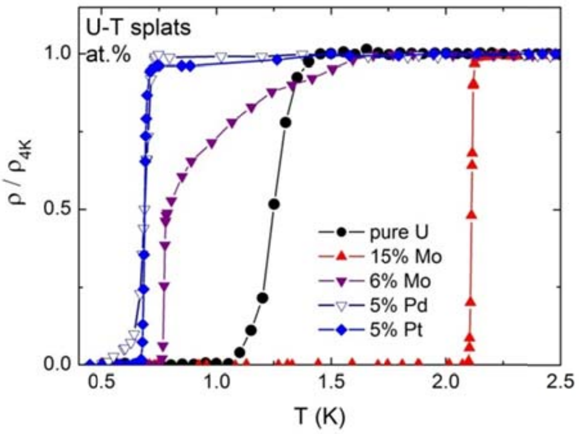

Figure 2. The superconducting transition in splat-cooled U-6%Mo, U-5%Pd and U-5%Pt alloys observed in the resistivity in zero field.

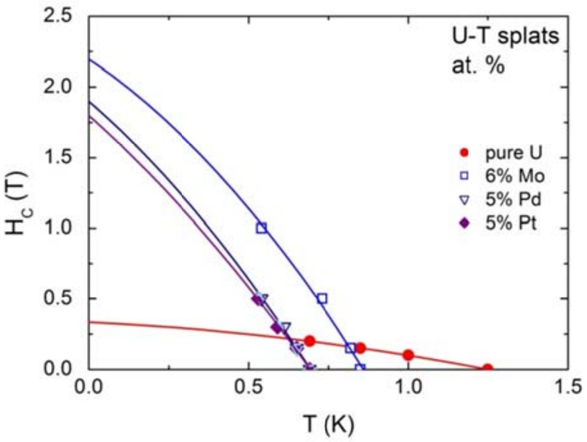

Figure 3. The critical magnetic field H_{c2} vs temperature T_c for the splat-cooled pure-U, U-6%Mo, U-5%Pd and U-5%Pt alloys.

A small broad peak was observed around 0.7 K in the specific heat with the T_c value of 0.72 K and 0.68 K respectively for U-6%Mo and U-5%Pt splat (Fig. 4). The superconducting transition revealed only by one broad specific heat peak in U-6%Mo at the T_c close to that of sharp resistivity jump (0.78 K). In both cases, the specific-heat jumps are much smaller than the calculated values from the BCS theory. Namely, for U-6%Mo the estimated jump is only around 55% of the BCS value. In the case of U-5%Pt, it is still smaller (22%). We suggest that the superconductivity in the specific heat is mainly associated with the γ-U phase.

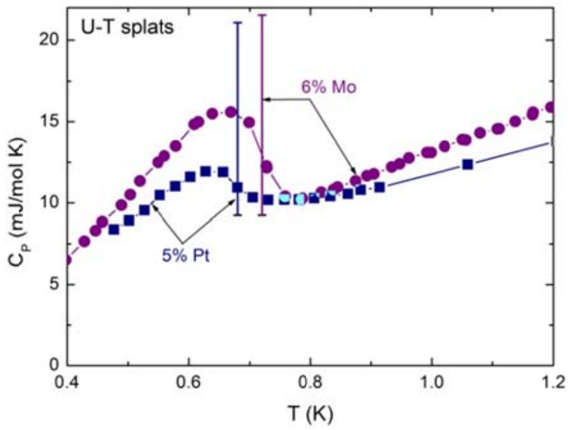

Figure 4. Superconducting phase transitions in U-6%Mo and U-5%Pt splats revealed in the specific-heat in zero field. The vertical bars indicate the theoretical BCS values $\Delta C = 1.43\,\gamma_e T_c$.

Experiments were partly performed at MLTL (http://mltl.eu), which is supported within the program of Czech Research Infrastructures (project No. LM2011025). Participation of Krakow group was supported by the program MOBILITY 7AMB14PL036 (Czech-Polish bilateral cooperation ID(PL) 9004/R14/R15).

Email of the presenting author: sowas.agh@gmail.com

Efficient calculations of *f*-materials relevant for nuclear waste management using DFT+U

George Beridze[1], Yan Li[1], Ariadna Blanca-Romero[1,2], Piotr M. Kowalski[1]
[1]*Institute of Nuclear Waste Management and Reactor Safety (IEK-6), Forschungszentrum Jülich, Jülich, Germany*
[2]*Imperial College London, London, United Kingdom*

Safe management of nuclear waste is a serious problem faced by the countries that utilize nuclear technology [1]. Due to activity of the investigated materials, the experimental work is usually problematic and limited to the conditions that not always resemble the ones expected in a repository. On the other hand, with the modern computational resources and state-of-the-art *ab initio* methods of computational quantum chemistry one can complement the experimental research by providing a valuable atomic-scale insight into the processes that determine the properties of different actinide-bearing materials. However, since properties of *f*-materials are often determined by strongly correlated *f*-electrons, the straightforward application of the existing and widely used quantum chemical methods, such as DFT, can lead to wrong results. For this reason, more accurate, but computationally unfeasible methods such as hybrid functionals, MP2 and CCSD(T) are often proposed for relibale simulations of *f*-materials [2,3]. The high computational cost of these methods limits their applicability to the simples crystalline materials, which prevents investigation of more realistic but chemically complex nuclear materials. In this contribution we will show an assessment of the performance of DFT+*U* method with the hubbard *U* parameter derived *ab initio* [4], for prediction of the structural and thermodynamic properties of actinide- and lanthanide- bearing materials such as simple uranium-bearing molecules and solids [5] and novel nuclear waste forms such as monazite-type orthophosphates ($Ln\mathrm{PO}_4$) [6] and pyrochlores ($Ln_2(\mathrm{Zr,Hf})_2\mathrm{O}_7$) [7]. Our results indicate that an exceptionally good description of materials structures and energetics can be obtained [4, 5] only when the Hubbard *U* parameter is derived *ab initio* for each f-element and structure, using for instance the linear response method (cLDA) [4]. Furthermore, we will show that with the carefull choice of the computational approach it is possible to accuratelly reproduce the available experimental data on the heat capacities and the standard entropies of lanthanide monazites ($Ln\mathrm{PO}_4$) and thus predict these thermodynamic parameters for unmeasured systems, which is of great value for the assesment of stability of novel waste forms [8].

References

[1] M. I. Ojovan, W. E. Lee, *An Introduction to Nuclear Waste Immobilisation,* Elsevier Science, 2005.
[2] X-D. Weng, R. L. Martin, T. M. Henderson et al., Chem. Rev., 2013, 113, 1063.
[3] G. A. Shamov, G. Schreckenbach, and T. N. Vo, Chem. Eur. J. 2007, 13, 4932.
[4] M. Cococcioni and S. de Gironcoli , Phys. Rev. B, 2005, 71, 035105.
[5] G. Beridze and P. M. Kowalski, J. Phys. Chem. A, 2014, 118, 11797.
[6] A. Blanca-Romero, P. M. Kowalski, G. Beridze et al., J. Comput. Chem., 2014, 35, 1339.
[7] Y. Li, P. M. Kowalski, G. Beridze, et al., *submitted.*
[8] P. M. Kowalski, G. Beridze, V. Vinograd, et al., J. Nucl. Mater., *in press.*

Email of the presenting author: g.beridze@fz-juelich.de

Interdiffusion and ion beam mixing effect in bi-layer magnetite-on-Fe films prepared by MBE technique on MgO(001) substrate

M. Krupska[1], N.-T. H. Kim-Ngan[1], S. Sowa[1], Z. Tarnawski[2], A.G. Balogh[3]
[1]*Institute of Physics, Pedagogical University, 30-084 Kraków, Poland*
[2]*AGH University of Science and Technology, Faculty of Physics and Applied Computer Science, 30-059 Kraków, Poland*
[3]*Institute of Materials Science, Technische Universität Darmstadt, 64287 Darmstadt, Germany*

Ion beam techniques (included Ion Beam Analysis (IBA) and Ion Beam Modification of Materials (IBMM)) can be used to investigate as well as modify the surface and interface properties of the materials in a nanometer scale. These methods have been widely used in materials science for improvement material properties, such as adhesion, hardness, interface engineering and fabricationof semiconductor devices by implantation.

We are interested in characterization and modification of magnetite thin films. Due to its interesting electronic and magnetic properties, magnetite has a high potential for technological applications. Moreover, it is viewed as a promising material for the spintronic application at room temperature.

We have prepared a series of single and bilayer thin films of magnetite on MgO(001) substrates by MBE growth. In this work, we focus on investigations of two bilayer films, Fe_3O_4/Fe/MgO(001), with a nominal layer thickness of nx25 nm for each layer (n=1,2,4). For underlying the interdiffusion during the film growth, one film was undergone a post-annealing (sample S5), while another (S9) was without annealing (non-ann.). We have investigated the film structure and properties in the as-deposited state as well as after being modified by 1MeV Ar^+ and Kr^+ ion beam (with different ion influences in the range of 10^{15}-10^{17} ions/cm^2) by means of Rutherford backscattering spectrometry (2 MeV He^+ ion beam, scattering angle of 171^o) and X-ray reflectometry (XRR). For the data interpretation, the computer code SIMNRA was employed. By analysing and making a comparison the data obtained before and after modification, we could be able to underline the ion beam mixing effect in those thin films. The as-grown films is found to consist of a thicker Fe_3O_4 layer (60 nm) and a much thinner Fe layer (29 nm), indicating that the top and bottom part of the Fe layer was oxidized, rather during the growth than due to post-annealing. However, using such a bilayer geometry, on the film surface is always a pure Fe_3O_4 layer.

As example, we show in Fig. 1 the RBS spectra of irradiated Fe_3O_4/Fe/MgO(001) film (S9) by 1MeV Kr^+ ion beam with different ion fluences. The Kr^+ ion irradiation implies such a strong Fe-Mg mixing, revealed by a large non-zero background between the Fe peak and Mg edge as well as a large change in the slope of the Mg-edge. A large change was also observed for the Fe peak. Since the film layers are very thin, we illustrate the ion mixing effect (i.e. the change of the layer thickness and layer concentration) in this film in a enlarged scale, where the layer thicknesses are drawn (in cm) proportionally with respect to the values estimated from the RBS (in nm), shown in Fig. 2. The solid line indicates the original separation between the film and the MgO substrate. Different colours indicate different Mg, Fe and O composition in each layer. Our analysis indicated that the pure Fe_3O_4 layer on the surface was still well preserved under Kr^+ irradiation with $\varphi<3{,}84\times10^{16}$ ions/cm^2 although the layer thickness decreased (d < 13nm). During the talk, the results for sample S5 will be also shown. Some concluding remarks on the film stability will be presented.

The support of the European Regional Development Fund under the Infrastructure and Environment Programme is highly acknowledged.

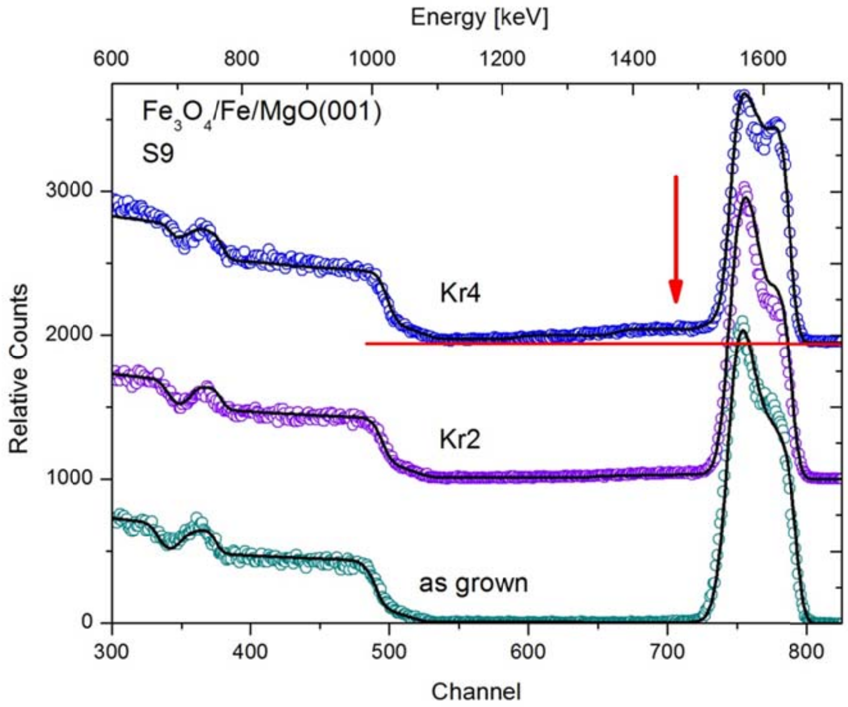

Figure 1. RBS spectra (markers) and the SIMNRA simulated spectra (lines) of the Fe_3O_4/Fe/MgO(001) film (S9) irradiated by 1MeV Kr^+ ion beam with different ion fluences (Kr2=1,68.10^{16} ions/cm^2, Kr4=3,84. 10^{16} ions/cm^2). Red line indicates the zero background of the as-deposited films. The arrow note the strong mixing effect implied a large non-zero background.

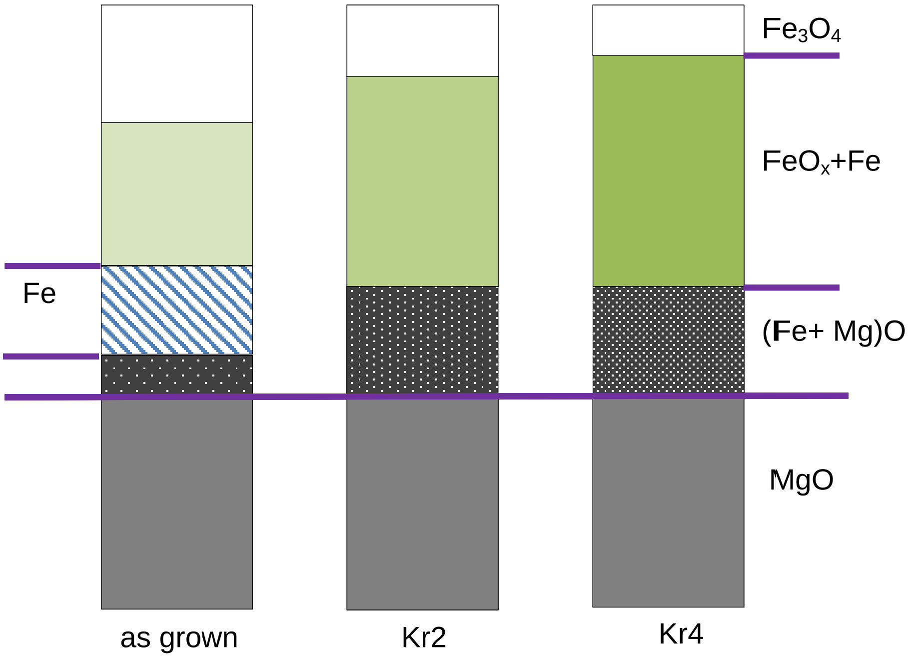

Figure 2. Illustration of ion mixing effect for Fe_3O_4/Fe/MgO(001) film (sample S9) irradiated by a 1MeV Kr^+ ion beam with different ion fluences (Kr2=1,68.10^{16} ions/cm^2, Kr4=3,84.10^{16} ions/cm^2).

Email of the presenting author: krupska.magdalena@gmail.com

La_3Co – superconductivity on the edge of ferromagnetism

Judyta Strychalska[1], Marta Roman[1], Bartlomiej Wiendlocha[2], Agnieszka Kozub[1],
Tomasz Klimczuk[1]
[1] *Faculty of Applied Physics and Mathematics, Gdansk Univeristy of Technology,*
Narutowicza 11/12, 80-233 Gdansk Poland
[2] *Faculty of Physics and Applied Computer Science, AGH University of Science*
and Technology, Aleja Mickiewicza 30, 30-059 Krakow, Poland

A polycrystalline sample of La_3Co was synthesized by arc-melting of stoichiometric amount of lanthanum (purity 99.9 %) and cobalt (purity 99.95 %) and annealed at 500º C for three weeks.

Physical properties were studied by measuring susceptibility, specific heat and resistivity. The temperature dependence of resistivity above transition temperature ($T_c = 6$ K) discloses a metallic-like character ($d\rho/dT > 0$). The residual resistivity ratio is $\rho_{300K}/\rho_{8K} = 6$. Traces of unreacted lanthanum metal is detected by a sudden drop of resistivity below $T_c = 6$ K. The second, sharp drop of $\rho(T)$ at 4.65 K is associated with the transition of La_3Co to the superconducting state.

By plotting H_{c2} versus T and using the WHH expression we obtained upper critical field $\mu_0H_{c2}(0) = 3.5$ T, that implies the superconducting coherence length $\xi(0) = 10$ nm.

A clear heat capacity anomaly is observed below a transition temperature $T_c = 4.44$ K and confirms bulk superconductivity of La_3Co.

The results of measuring the specific heat in magnetic field 3 T determined Sommerfeld coefficient $\gamma = 31.1$ mJ mol^{-1} K^{-2} and Debye temperature $\Theta_D = 133$ K. The electron-phonon coupling constant estimated from the inverted McMillan formula (where $\mu^* = 0.13$) was $\lambda_{ep} = 0.82$. Using γ and the specific-heat-jump value $\Delta C/T_c$ at the superconducting transition temperature, we estimated $\Delta C/\gamma T_c = 1.83$, suggesting intermediate-coupling superconductivity.

Estimated value of zero-temperature lower critical field, complying the demagnetization factor $\mu_0H_{c1}(0) = 17.6$ mT. Using obtained values we calculated a Ginzburg-Landau superconducting penetration depth $\lambda_{GL}(0) = 162$ nm. The Ginzburg-Landau parameter is $\kappa = 16.7$, indicating that La_3Co is a II-type superconductor. We estimated the thermodynamic critical field $\mu_0H_c = 148$ mT.

Email of the presenting author: jstrychalska@mif.pg.gda.pl

Influence of Ba doping of $Na_{0.5}Bi_{0.5}TiO_3$ ceramics on their structural, dielectric and ferroelectric properties

Urszula Lewczuk[1], Jan Suchanicz[2], Konieczny[2], E.M. Dutkiewicz[1,3]
[1] *Institute of Physics, Pedagogical University, ul. Podchorazych 2, 30-084 Krakow, Poland*
[2] *Institute of Technology, Pedagogical University, ul. Podchorazych 2,*
30-084 Krakow, Poland
[3] *Institute of Nuclear Physics PAN, ul. Radzikowskiego 152, 31-342 Krakow, Poland*

Lead oxide based ferroelectrics are most widely used as an element of actuators, sensors and transducers. Among them, $PbTiO_3$-$PbZrO_3$ (PZT) has the best piezoelectric properties, but considering lead toxicity, the lead-free piezoelectric materials have attracted attention from the viewpoint of environmental protection. Furthermore, the RoHS Directive (2002/95/EC) restricts the use of, inter alia, lead. Among the available materials, $Na_{0.5}Bi_{0.5}TiO_3$ (NBT) and NBT-based solid solutions are considered the most promising candidates for replacing lead containing materials.

$(Na_{0.5}Bi_{0.5})_{1-x}Ba_xTiO_3$ (x=0, 0.04 and 0.06) ceramics were prepared by conventional solid state method. The structural, ferroelectric and piezoelectric properties were investigated. The obtained results will be discussed in terms of ions/lattice imperfections, which create local electromechanical fields.

Email of the presenting author: urszula.lewczuk@gmail.com

Properties of barium titanate modified by Co doping

Renata Bujakiewicz-Korońska
Institute of Physics, Pedagogical University, Cracow, Poland

Ceramic compositions in the (1-x)$Ba_{0.95}Pb_{0.05}TiO_3$ - $x$$Co_2O_3$ system (BPTC) with compositions $x < 0.10$ were prepared by conventional ceramic processing technique. They have been characterised by X-ray diffraction, scanning electron microscope, differential scanning calorimetry, dielectric measurements and magnetic studies.

Crystal structure refinement was performed in space group No 99 - P4mm. In the BPTC ceramics, Co^{+3} ions partially occupy the positions of Ti^{+4} ions. The Co-doping causes a small decreasing of the tetragonality of the perovskite lattice and is responsible for a gradual shift of ferroelectric Curie transition towards lower temperatures. Moreover, the diffusive character of the transition between the tetragonal phase to the orthorhombic one was observed. The activation energies for the samples are about 0.9 eV. The temperature conductivity in the range of 400 – 600 K can be ascribed by the migration of oxygen vacancies introduced to compensate the charge deficiency due to Co^{3+} valence at the B-site of the perovskite lattice. Magnetic measurements showed that in the BPTC ceramics with higher Co amounts there are observed an agglomerate of the BT nanopowder matrix and a few cobalt oxide component. Some contribution from weak paramagnetic impurities is visible at temperatures below 10 K.

Additionally, a*b initio* calculations were performed within DFT using GGA and LCAO with localized basis set in the form of spherical functions as implemented in SIESTA 3.2 code together with the spin polarization. The results of the simulations confirmed ferroelectric and magnetic properties of the BPTC.

BPTC seems to be a promising new multiferroic material with a weak coupling between magnetic and ferroelectric properties. Details about possible ways of coupling between them require further experimental investigations and theoretical considerations.

Acknowledgments
The authors acknowledge the CPU time allocation at Academic Computer Centre CYFRONET AGH in Cracow. This work was supported partly by PL-Grid Infrastructure.

References
[1] R. Bujakiewicz-Korońska, A. Kalvane, Y. Zhydachevskii, B. Garbarz-Glos, W. Śmiga, L. Vasylechko, J. Czerwiec, A. Suchocki, A. Kamińska, W. Piekarczyk, Ferroelectrics 436, 62 (2012).
[2] E. Markiewicz, R. Bujakiewicz-Koronska, D. Majda, L. Vasylechko, A. Kalvane, M. Matczak, J. Electroceram. 32, 92 (2014).
[3] R. Bujakiewicz-Koronska, E. Markiewicz, D.M. Nalecz, L.Vasylechko, M. Balanda, M. Fitta, E. Juszynska-Galazka, A.Kalvane, Ceram. Intern. 41, 3983 (2015).

Email of the presenting author: sfbujaki@cyf-kr.edu.pl

High-field study of a $TbFe_5Al_7$ single crystal

A.V. Andreev[1], D.I. Gorbunov[1,2], S. Yasin[2], N.V. Mushnikov[3], Y. Skourski[2],
S. Zherlitsyn[2], J. Wosnitza[2]
[1] *Institute of Physics, Academy of Sciences, 18221 Prague, Czech Republic*
[2] *High Magnetic Field Laboratory, Helmholtz-Zentrum Dresden-Rossendorf, 01314 Dresden, Germany*
[3] *Institute of Metal Physics, Kovalevskaya str. 18, 620990 Ekaterinburg, Russia*

The $TbFe_5Al_7$ compound with a tetragonal crystal structure of the $ThMn_{12}$ type is a highly anisotropic ferrimagnet with Curie temperature T_C = 242 K and compensation point T_{comp} = 84 K [1]. Spontaneous and field-induced phase transitions have been studied on single crystals (grown by Czochralski method in tri-arc furnace) by magnetization and ultrasound measurements in static (up to 14 T) and pulsed (up to 60 T) magnetic fields. $TbFe_5Al_7$ displays the easy-plane anisotropy. In the vicinity of $T = T_{comp}$ the compound exhibits a spontaneous spin-reorientation transition within the basal plane, the easy magnetization direction (EMD) changes from [100] (below T_{comp}) to [110] (above T_{comp}). Along the EMD, the field-induced phase transitions have been observed. The magnetization jump reflects step-wise rotation of the Tb and Fe magnetic moments from one easy axis to another within the basal plane. All the transitions, spontaneous and field-induced, are accompanied by pronounced anomalies in sound velocity and sound attenuation. At low temperatures, $TbFe_5Al_7$ does not reach the forced ferromagnetic state with magnetic moment of 17 μ_B/f.u. even at 60 T field applied along the EMD, only 12.5 μ_B/f.u. is reached along the [110] axis. Therefore, additional magnetization step(s) can be found above 60 T. From the obtained high-field data the Tb-Fe inter-sublattice exchange constant has been determined, $\lambda = 6.7$ T f.u./μ_B, in good agreement with $\lambda = 6.9$ T f.u./μ_B which is deduced from molecular-field theory.

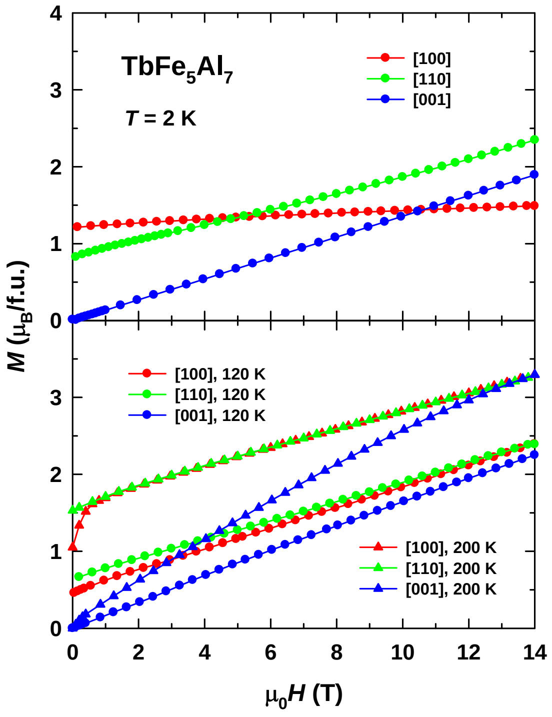

Figure 1. Magnetization curves along the principal crystallographic directions of the $TbFe_5Al_7$ single crystal at several selected temperatures.

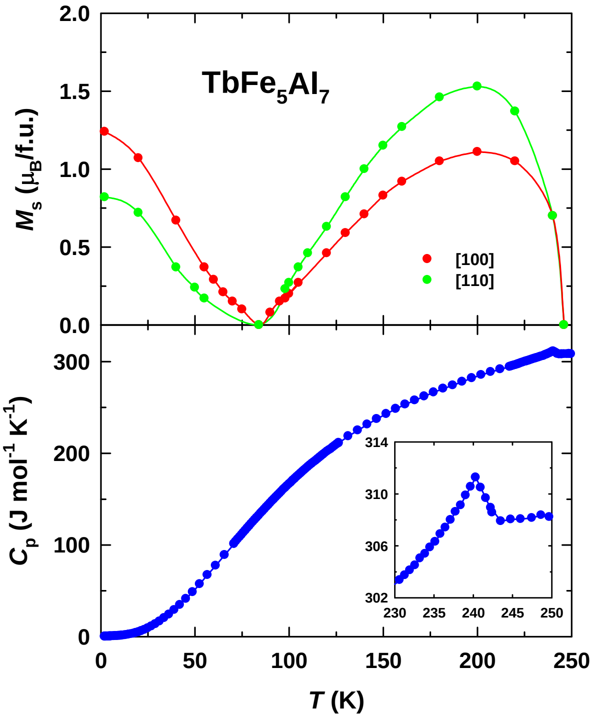

Figure 2. Temperature dependence of M_s along the [100] and [110] axes (top) and temperature dependence of the specific heat (bottom).

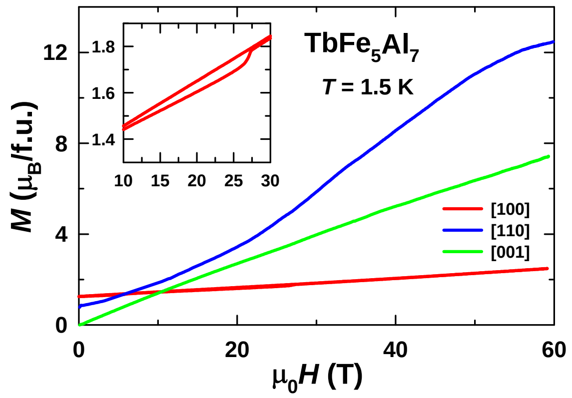

Figure 3. Magnetization curves along the main axes in pulsed fields at 1.5 K. The inset shows details along the [100] axis in the vicinity of the field-induced transition.

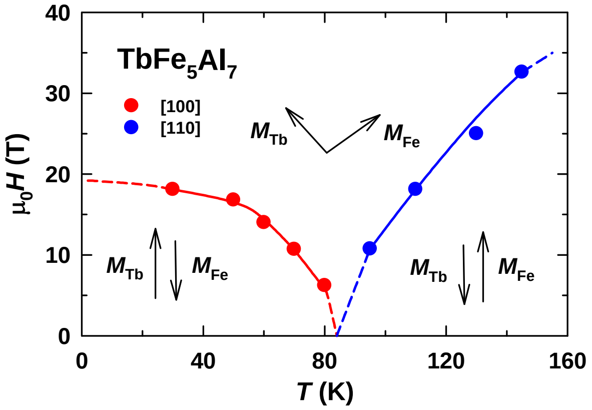

Figure 4. *T–H* magnetic phase diagram for fields along the [100] and [110] axes.

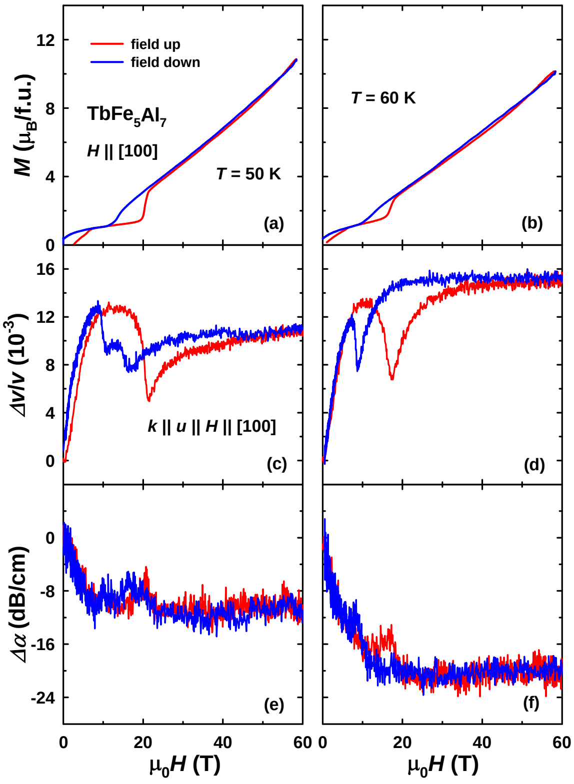

Figure 5. Magnetization (a and b), relative change of the sound velocity (c and d), and sound attenuation (e and f) in fields along the [100] axis at 50 and 60 K.

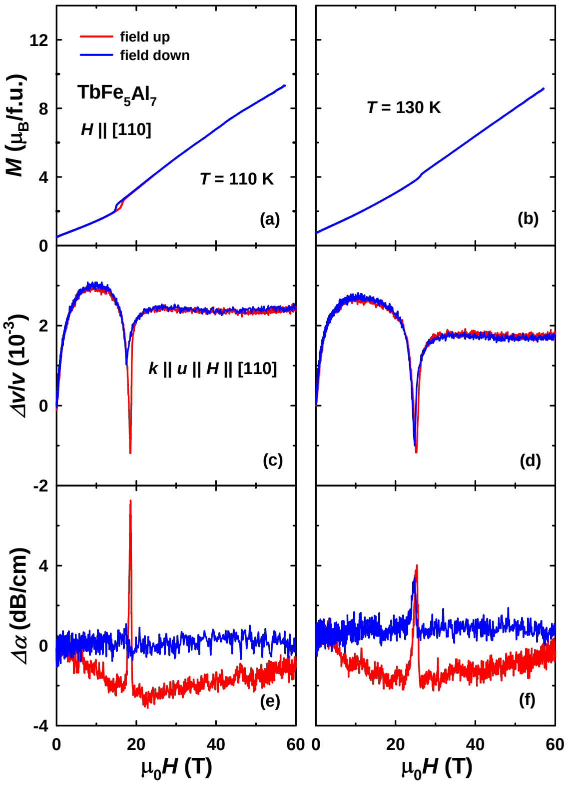

Figure 6. Magnetization (a and b), relative change of the sound velocity (c and d) and sound attenuation (e and f) in fields along the [110] axis at 110 and 130 K.

Reference
[1] D.I. Gorbunov, A.V. Andreev, J. Alloys Comp. 577 (2013) 203.

Email of the presenting author: a.andreev@seznam.cz

Influence of Er-substitution on the Crystal and Magnetic Properties of Ferric Borate Samples

Osman Murat Ozkendir
Mersin University, Faculty of Technology, Energy Systems Engineering, Tarsus, Turkey

The effects of Erbium substitution on the crystal, electric, electronic and magnetic properties of Ferric Borate samples were investigated. The collected data were studied according to the influence of the change in the crystal structure by increasing Er substitutions. The samples were determined as semiconductors showing weak Antiferromagnetic ordering at room the temperature. The magnetic properties were studied by the collected data from the XMCD measurements for the samples. The probes on the electronic structure properties were studied by the collected XANES data. According to the increasing substitution amount of the Er atoms, prominent changes, structural distortions and phase transitions in the crystal structure were observed. In the substituted Ferric Borate samples, iron atoms were defined as the chief role player in the whole crystallographic phenomena.

Email of the presenting author: ozkendir@gmail.com

Screening of magnetic moment at Co impurity in Cu host

Agnieszka L. Kozub[1,2], Jindřich Kolorenč[2], Alexander B. Shick[2]
[1]*Faculty of Applied Physics and Mathematics, Gdansk University of Technology, Gdansk, Poland*
[2]*Institute of Physics, Academy of Sciences of the Czech Republic, Prague, Czech Republic*

Cobalt impurity located in the bulk copper is described within the multi-orbital Anderson impurity model (IAM) that is parametrized to match the LDA electronic structure. The AIM is then solved using the Lanczos method. We concentrate on the many-body description of the ground state and excitation spectra. The calculations yield the nonmagnetic singlet ground state for the impurity atom, where the Co local moment is screened by the bath of conduction electrons. The computed spectral densities (shown in the Figure) are in a good agreement with those obtained using the quantum Monte Carlo method [1].

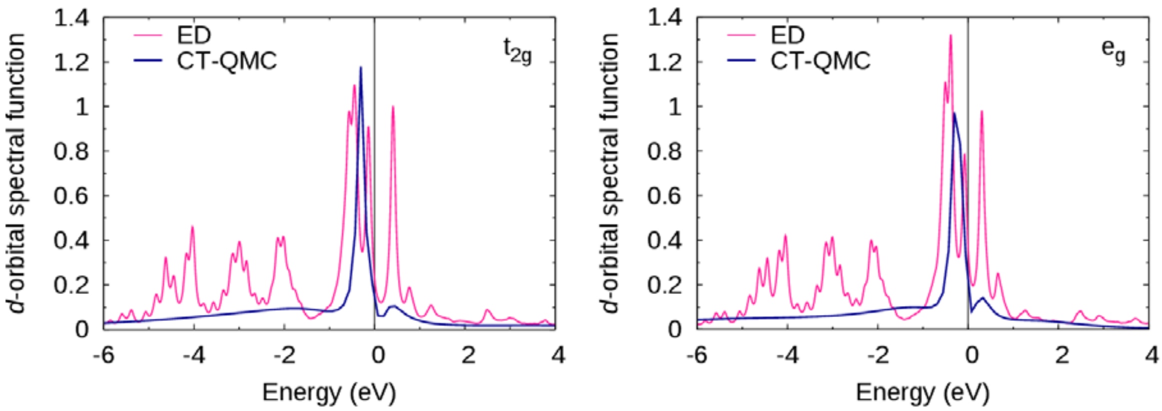

Reference
[1] B. Surer, M. Troyer, P. Werner, T.O. Wehling, A.M. Läuchli, A. Wilhelm, A.I. Lichtenstein, Phys. Rev. B **85**, 085114 (2012).

Email of the presenting author: akozub@mif.pg.gda.pl

Valence fluctuations and magnetism in lanthanide systems

José-Luiz Ferreira[1,2], Sébastien Burdin[3,4] and Claudine Lacroix[1,2]
[1]*Univ. Grenoble Alpes, Institut NEEL, F-38042 Grenoble, France*
[2]*CNRS, Institut NEEL, F-38042 Grenoble, France*
[3]*Univ. Bordeaux, LOMA, UMR 5798, F-33400 Talence, France*
[4]*CNRS, LOMA, UMR 5798, F-33400 Talence, France*

The connection between magnetism and valence fluctuations in Ytterbium- and Cerium-based compounds is analyzed using an extended version of Periodic Anderson Model [1]. The model includes a repulsive Coulomb interaction (U_{fc}) among conductions (s, p and d orbitals) and localized (f) electrons. We treat this model in a combination of a mean-field approximation for the U_{fc} term and a Hubbard-I scheme for the f orbitals in the limit of large f-f repulsion.

We find that U_{fc} repulsion induces either a 1st order valence transition or a crossover depending on system parameters. We discuss the effects of external and Weiss internal magnetic fields and we clarify their relation with valence fluctuations. We compare our results with experimental data from x-ray scattering, focusing in particular on $YbCu_2Si_2$ [2], $YbMn_6Ge_{6-x}Sn_x$ [3] and $Eu(Rh_{1-x}Ir_x)_2Si_2$[4].

References:
[1] Y. Onishi and K. Miyake, J. Phys. Soc. Jpn. **69**, 3955 (2000).
[2]A. Fernandez-Pañella *et al.*, Phys. Rev. B **86**, 125104 (2012).
[3]T. Mazet *et al.*, Phys. Rev. Lett. **111**, 096402 (2013).
[4] S. Seiro and C. Geibel, Phys. J. Phys.: Condens. Matter 23, 375601 (2011).

Email of the presenting author: jose-luiz.ferreira@neel.cnrs.fr

Electronic properties of $CeNi_9In_2$ compound

R. Kurleto[1], P. Starowicz[1], J. Goraus[2], S. Baran[1], Yu. Tyvanchuk[3], Ya. M. Kalychak[3], A. Szytuła[1]
[1] *Marian Smoluchowski Institute of Physics, Jagiellonian University, Lojasiewicza 11, 30-348 Krakow, Poland*
[2] *Institute of Physics, University of Silesia, Uniwersytecka 4, 40-007 Katowice, Poland*
[3] *Department of Analytical Chemistry, Ivan Franko National University of Lviv, Kyryla and Mephodiya 6, 79005 Lviv, Ukraine*

We would like to portray the electronic properties of $CeNi_9In_2$ compound. Previous reports [1,2,3] delivered experimental evidence suggesting that a mixed (MV) valence state occurs in this system.

A shape of measured resistivity as a function of temperature resembles that of a typical metal except for a small concavity. In order to perform an analysis of the experimental data we have fitted a model proposed by Freimuth [4] for systems with unstable f shell. The obtained spin fluctuation temperature equals $T_{sf} = 157$ K, while the values of f-level mean position with respect to the Fermi energy and a parameter related to hybridization strength reach the values of $T_0 = 355$ K and $b \cdot J_{sf} = 45{,}2 \cdot 10^{-5}\ \Omega \cdot m \cdot K$, respectively. At low temperatures (below 38 K) we have observed that the measured resistivity follows the behavior, which is typical of a Fermi liquid (FL). To verify that we have calculated Kadowaki – Woods ratio, which is of the same order as in the case of transition metals.

X-ray Photoelectron Spectroscopy (XPS) combined with an application of Gunnarsson-Shönhammer theory [5] allowed us to determine a mean f level occupation and a hybridization strength. We have obtained $n_f = 0.94$ and $\Delta = 104$ meV, for occupation and hybrydization respectively.

So as to describe valence band we have used Ultraviolet Photoelectron Spectroscopy (UPS). A sharp coherent peak, named a Kondo peak, is absent in the collected spectra, in particular at low temperature. Spectral density measured with application of He-II radiation is dominated by two broad maxima – one at about -0.6 eV and the second less intense at about -1.8 eV. It exhibits slightly higher intensity close to the Fermi energy as compared to the spectrum collected with He-I radiation. The difference of He-II and He-I spectra shows higher intensity in the range between -0.3 eV and the Fermi energy. Such a difference reflects spectral intensity related to Ce 4f electrons. Its shape is compatible with much broadened $f_{5/2}^1$ and $f_{7/2}^1$ peaks, which would correspond to a Kondo peak and its spin-orbit splitting partner, respectively. We also present theoretical calculations (FPLO method) of density of states (DOS) in order to provide comparison with experimental data.

References
[1] O. Moze, S. Mentink, G. Nieuwenhuys, K. Buschow, Journal of Magnetism and Magnetic Materials 150 (1995) 345 – 348.
[2] A. Szytuła, S. Baran, B. Penc, J. Przewoźnik, A. Winiarski, Y. Tyvanchuk, Y. Kalychak, Journal of Alloys and Compounds 589 (2014) 622 – 627.
[3] R. Kurleto, P. Starowicz, J. Goraus, S. Baran, Yu. Tyvanchuk, Ya. M. Kalychak, A. Szytuła, Solid State Communications, 206 (2015) 46-50.
[4] A. Freimuth, J. Magn. Magn. Mat. 68 (1987) 28.
[5] J. C. Fuggle, F. U. Hillebrecht, Z. Zołnierek, R. Lässer, C. Freiburg, O. Gunnarsson, K. Schönhammer, Phys. Rev. B 27 (1983) 7330–7341; O. Gunnarsson, K. Schönhammer, Phys. Rev. B 28 (1983) 4315–4341.

Email of the presenting author: rkurleto@gmail.com

Magnetic spiral order in iron pnictides FeAs and FeSb

A. K. Jasek[1], K. Komędera[1], A. Błachowski[1], K. Ruebenbauer[1], J. Żukrowski[2,3],
Z. Bukowski[4], A. Krztoń-Maziopa[5]
[1] *Mössbauer Spectroscopy Division, Institute of Physics, Pedagogical University, ul. Podchorążych 2, PL-30-084 Kraków, Poland*
[2] *AGH University of Science and Technology, Academic Center for Materials and Nanotechnology, Av. A. Mickiewicza 30, PL-30-059 Kraków, Poland*
[3] *AGH University of Science and Technology, Faculty of Physics and Applied Computer Science, Department of Solid State Physics, Av. A. Mickiewicza 30, PL-30-059 Kraków, Poland*
[4] *Institute of Low Temperature and Structure Research, Polish Academy of Sciences, ul. Okólna 2, PL-50-422 Wrocław, Poland*
[5] *Warsaw University of Technology, Faculty of Chemistry, ul. Noakowskiego 3, PL-00-664 Warsaw, Poland*

Iron pnictides FeAs and FeSb exhibit very complex magnetic order pattern due to the competition between super-exchange covalent coupling and itinerant magnetism. Generally one observes anti-ferromagnetic order in the form of incommnsurate planar spirals propagating along one of the crystallographic axes. There are two spirals differing by the shape of the spiral in the plane perpendicular to the propagation axis.

FeAs crystallizes within *Pnma* symmetry group. It was found that the spin spiral propagating along the *c*-axis leads to the complex variation of the hyperfine magnetic field amplitude with the spin orientation varying in the *a*-*b* plane. The magnitude of the hyperfine field pointing in the direction of the local magnetic moment depends on the orientation of this moment in the *a*-*b* plane. Patterns are vastly different for iron located in the $[0\,k\,0]$ positions and for iron in the $[0\,k+\frac{1}{2}\,0]$ positions within the orthorhombic cell. Lattice softens upon transition to the paramagnetic state at 69.2 K primarily in the *a*-*c* plane as seen by iron atoms. This effect is quite large considering lack of the structural transition. Two previously mentioned iron sites are discernible in the paramagnetic region till 300 K by different electron densities on the iron nuclei. The anisotropy of the iron vibrations developed at the transition to the paramagnetic state increases with the temperature in accordance with the harmonic approximation, albeit tends to saturation at high temperatures indicating gradual onset of the *quasi*-harmonic conditions [1]. Adjacent figures show unit cell of FeAs and spiral shapes.

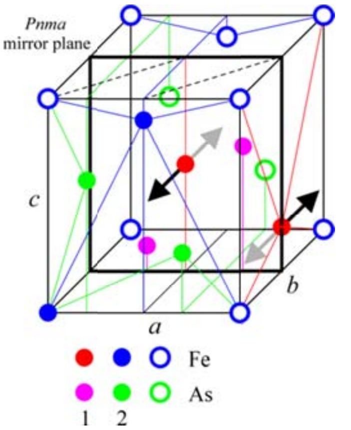

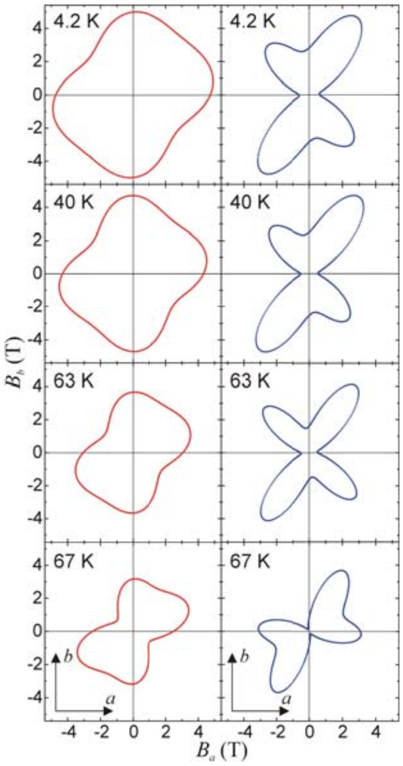

The $Fe_{x+1}Sb$ compound has been synthesized close to stoichiometry with x = 0.023(8). basically it conforms to the *$P6_3/mmc$* symmetry group with some interstitial iron present. The anti-ferromagnetic ordering temperature was found as 232 K i.e. much higher than for the less stoichiometric material. Regular iron was found to occupy two different positions in proportion 2:1. They differ by the electric quadrupole coupling constants and both of them exhibit extremely anisotropic electric field gradient tensor (EFG) with the asymmetry parameter $\eta \approx 1$. The negative component of both EFGs is aligned with the *c*-axis of the hexagonal unit cell, while the positive component is aligned with the <120> direction. Hence, a model describing deviation from the *P6₃/mmc* symmetry group within Fe-planes has been proposed. Spectra in the magnetically ordered state could be explained by introduction of the incommensurate spin spirals propagating through the iron atoms in the direction of the *c*-axis with a complex pattern of the hyperfine magnetic fields distributed within *a*-*b* plane. Hyperfine magnetic field pattern of spirals due to major regular iron is smoothed by the spin polarized itinerant electrons, while the minor regular iron exhibits hyperfine field pattern characteristic of the highly covalent bonds to the adjacent antimony atoms. The excess interstitial iron orders magnetically at the same temperature as the regular iron, and magnetic moments of these atoms are likely to form two-dimensional spin glass with moments lying in the *a*-*b* plane. The upturn of the hyperfine field for minor regular iron and interstitial iron is observed below 80 K. Magneto-elastic effects are smaller than for FeAs, however the recoilless fraction increases significantly upon transition to the magnetically ordered state [2]. Figures below show unit cell of FeSb with the proposed deformation of the iron planes, magnetic spiral shapes and corresponding average hyperfine field distribution.

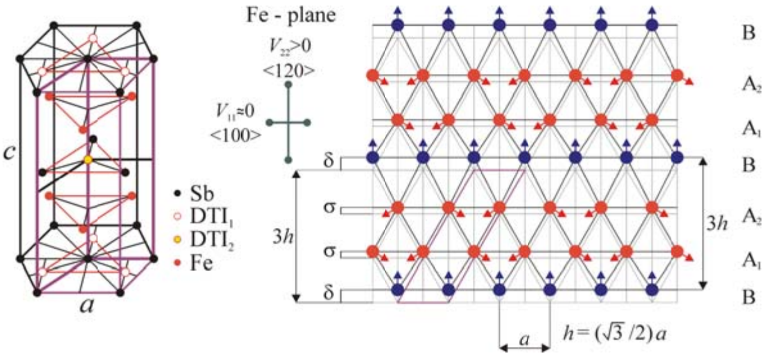

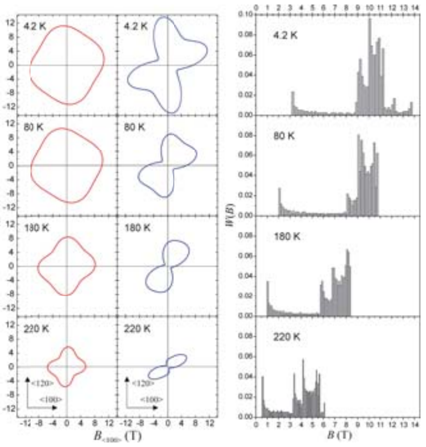

This project was financially supported by the National Science Center of Poland under the Grant No. DEC-2011/03/B/ST3/00446.

References
[1] A. Błachowski, K. Ruebenbauer, J. Żukrowski, and Z. Bukowski, J. Alloys Comp. **582**, 167 (2014).
[2] K. Komędera, A. K. Jasek, A. Blachowski, K. Ruebenbauer, and A. Krztoń-Maziopa, arXiv:1406.7767 (2014).

Email of the presenting author: aleksjasek@gmail.com

The use of ultrafast cooling for phase stabilization and phase modification in f-electron alloys

N.-T.H. Kim-Ngan[1], M. Paukov[2], I. Tkach[2], S. Sowa[1], M. Krupska[1],
Z. Tarnawski[3], L. Havela[2]
[1]*Institute of Physics, Pedagogical University, Podchorazych 2, 30 084 Krakow, Poland*
[2]*Faculty of Mathematics and Physics, Charles University, Ke Karlovu 5,*
12116 Prague, Czech Republic
[3]*AGH University of Science and Technology, Faculty of Physics and Applied Computer Science, al. Mickiewicza 30, 30 059 Krakow, Poland*

The rapid quenching of certain alloys from the melt could form completely extended solid solutions, new metastable crystalline phases and amorphous solid phases. The splat cooling system (HV splat cooler by Vakuum Praha) in the Department of Condensed Matter Physics, Faculty of Mathematics and Physics, Charles University has an estimated cooling rate of 10^6 K/s, when the molten metal was dropped between two massive copper pistons. The resulting splat sample has a shape of irregular disc approx. 20 mm in diameter and 100-200 μm in thickness (Fig. 1). The technique can be used in similar situation as melt spinning, its advantage is a small amount of material needed. It can give amorphous alloys in the case of deep eutectics, or it can be used to suppress reactions relying of material transport, as diffusion.

Using the advantage of ultrafast cooling, we succeeded to retain the high-temperature cubic γ-U phase in U-T alloys down to room temperature in a combination with alloying with 13-15 at.% T concentration (T = Mo, Pt, Pd, Nb) or by 30 at.% Zr. It is crucial that the γ-U structure was stabilized especially in the as-formed state without any additional sample treatment, which can be ascribed to homogeneous distribution of alloying elements.

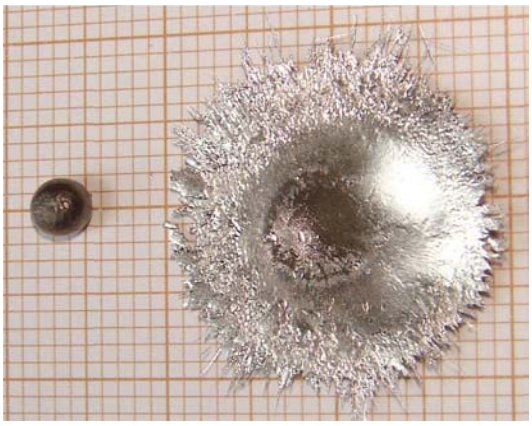

ed sample
lk-sample
) prepared

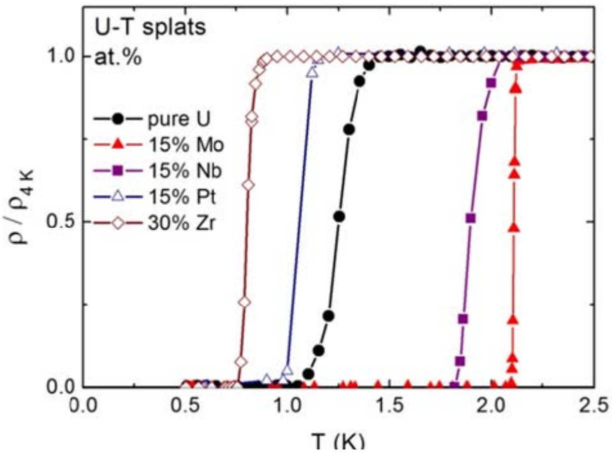

onducting
(T = Mo,
field. For
alized to

We have then characterized the low-temperature properties of the obtained splat-cooled samples. All U-T splats become superconducting with T_c in the range of 0.6 K – 2.1 K [1]. In all cases, a sharp resistivity drop was observed at T_c with a small superconducting transition width ΔT_ρ (Fig. 2). The sharpest superconducting transition was observed in U-15 at.% Mo splat (ΔT_ρ = 0.02 K), which is a conventional BCS superconductor. A sharp resistivity drop was surprisingly revealed at 1.24 K for pure-U splat consisted of α-U phase, whereas only a small broad feature related to superconducting transition was observed in the specific heat.

Using ultrafast cooling we are able to reduce the required content of dopants Mo/Zr/Nb for stabilization of the γ-U phase, retaining a high temperature structure to low temperatures. Moreover, ultrafast cooling can reach much higher solubility of Pt/Pd in U, reaching far beyond the equilibrium solubility even at high temperatures. Thus we could stabilize the γ-U phase with 15at.% Pt alloying, while maximum Pt solubility does not exceed 5at.%. All splat-cooled alloys are very stable when exposed to ambient conditions. We also found that the cubic γ-U phase is very stable if exposed to hydrogen atmosphere at pressures below 1 bar and at room temperature, even if for many days. Hydrogen can be slowly absorbed into U-Mo alloys when a critical H_2 pressures (> 4.5 bar) is exceeded, forming different types of UH_3 related hydrides [2]. The products lack the pyrophoricity of normal UH_3, which ignites easily in air at room temperature. Hydrogen can be easily desorbed by heating to 500 °C in vacuum. Thus our study revealed a new and simple technique with a technological significance for production the γ-U phase in a powder form: by a combination of hydrogenation, followed by crushing and then hydrogen desorption in a vacuum.

In fact, our very first attempt with splat cooling was undertaken on YCo_2. We expected the compound could be partially amorphized (similarly to that e.g. by swift heavy-ion irradiation) and if so we would be able to tune its electronic and magnetic properties. No amorphization is observed, indicating that such ultrafast cooling is still slower than crystallization. However, the SEM image revealed a formation of regular nano-thread of YCo_2 splat. XRD patterns indicate the presence of spurious YCo_3 phase (Fig. 4) originally absent in the precursor.

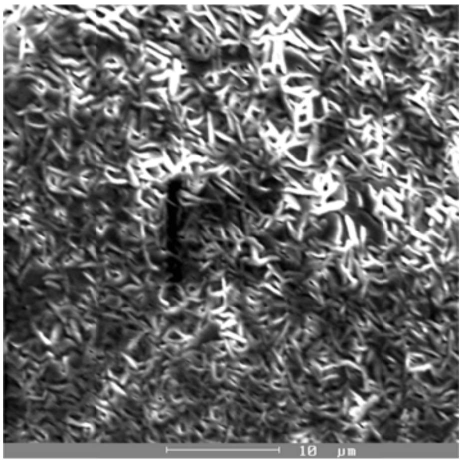

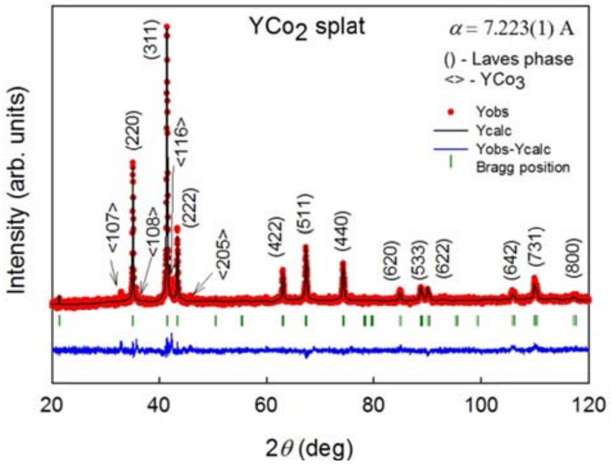

led YCo_2
reads.

ate a fully

Experiments were partly performed at MLTL (http://mltl.eu/), which is supported within the program of Czech Research Infrastructures (project No. LM2011025). Participation of Krakow group is supported by the program MOBILITY 7AMB14PL036 (Czech-Polish bilateral cooperation ID(PL) 9004/R14/R15). We highly acknowledge the support from prof. V. Sechovsky for this splat-cooling research and his valuable discussions and comments.

References
[1] I. Tkach, N.-T.H. Kim-Ngan, A. Warren, T. Scott, A.P. Goncalves, L. Havela, Physica C 498 (2014) 14.
[2] I. Tkach, S. Maskova, Z. Matej, N.-T. H. Kim-Ngan, A. V. Andreev, L. Havela, Phys. Rev. B 88 (2013) 060407(R).

Email of the presenting author: tarnawsk@up.krakow.pl

Thermopower, electrical resistivity and thermal conductivity of the $CeNi_2(Si_{1-y}Ge_y)_2$ alloys

T. Toliński[1], K. Synoradzki[1], M. Koterlyn[2,3], G. Koterlyn[4], R. Yasnitskii[3]
[1]*Institute of Molecular Physics, Polish Academy of Sciences, Poznań, Poland*
[2]*Institute of Physics, K. Wielkiego University, Bydgoszcz, Poland*
[3]*Faculty of Electronics, Ivan Franko National University of L'viv, Ukraine*
[4]*Western Scientific Center of the National Academy of Sciences of Ukraine and Ministry of Education and Science of Ukraine, L'viv, Ukraine*

The compounds of the composition MT_2X_2 (M – Ce, U; T – transition metal; X – Si, Ge) are known to exhibit many of the anomalous behaviours resulting from the hybridization between the f electrons and the conduction states. It includes heavy fermions (HF), superconductivity, fluctuating valence, magnetic ordering, and non-Fermi-liquid (NFL) behaviour [1,2].

We report our studies of the intermediate compositions between $CeNi_2Si_2$ and $CeNi_2Ge_2$, i.e. the alloys $CeNi_2(Si_{1-y}Ge_y)_2$. While $CeNi_2Si_2$ is a well confirmed fluctuating valence system [3] the behaviour of the HF $CeNi_2Ge_2$ indicates on exotic behaviours like NFL and superconductivity [4,5]. It is due to the proximity of this compound to the antiferromagnetic Quantum Critical Point (QCP). The Kondo temperature of $CeNi_2Ge_2$ is about 30 K and the onset of superconductivity is strongly sample-dependent and still not confirmed as a bulk effect [6].

Polycrystalline samples of $CeNi_2(Si_{1-y}Ge_y)_2$ were prepared by arc-melting of the constituent elements in a purified argon atmosphere. The electrical resistivity, thermopower, and thermal conductivity were measured using the Physical Property Measurement System (PPMS, Quantum Design) in the temperature range 2 – 400 K. To use the four-probe method, bar-shaped samples were obtained with the wire saw.

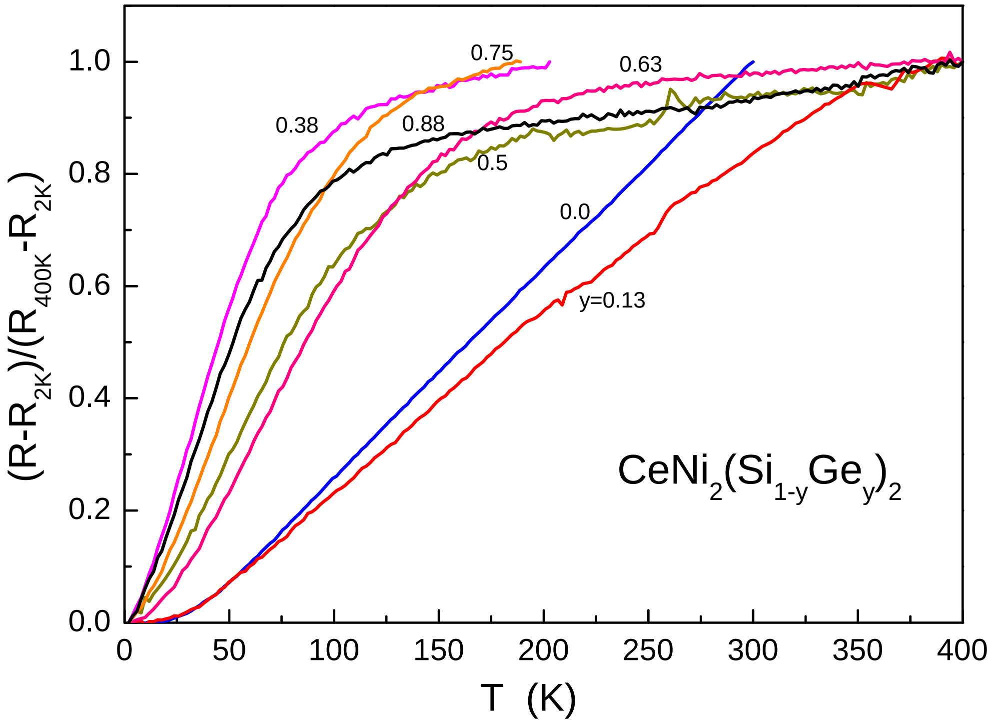

Figure 1. Normalized electrical resistance measured for various Ge content y.

The normalized resistance data of $CeNi_2(Si_{1-y}Ge_y)_2$ (Fig. 1) reveals that the change of the temperature dependence of the resistivity towards the typical metallic behaviour occurs already below y~0.3, i.e. a tendency to saturation persists up to significant substitutions of Ge by Si. It is also visible that the transition between $CeNi_2Si_2$ and $CeNi_2Ge_2$ is not a simple monotonic change. A comparison with the behaviour of the thermal conductivity and the thermopower will be also addressed in the present report.

Fig. 2 shows an example of the thermal conductivity of $CeNi_2(Si_{1-y}Ge_y)_2$ for y = 0.13 and y = 0.88. It can be observed that the increase of the Ge amount essentially modifies the temperature dependence of the thermal conductivity for $T > 50$ K. In the case of thermopower we mainly observe a shift of the peak present at 100 K towards higher temperatures for increasing content of Si.

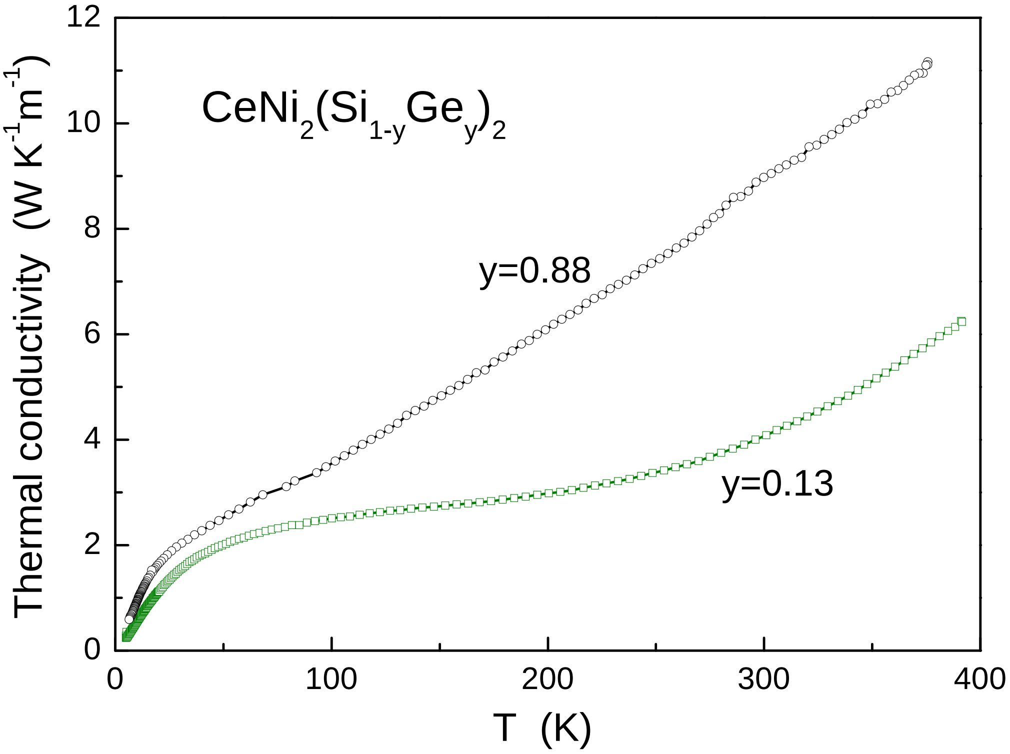

Figure 2. Thermal conductivity of $CeNi_2(Si_{1-y}Ge_y)_2$ for y = 0.13 and y = 0.88.

References
[1] T. Endstra, G.J. Nieuwenhuys, J.A. Mydosh, Phys. Rev. B 48 (1993) 9595.
[2] M.D. Koterlyna, R.I. Yasnitskii, G.M. Koterlyn, B.S. Morokhivskii, J. Alloys Compd. 348 (2003) 52.
[3] M. Koterlyn, I. Shcherba, R. Yasnitskii, G. Koterlyn, J. Alloys Comp. 442 (2007) 176.
[4] P. Gegenwart, F. Kromer, M. Lang, G. Sparn, C. Geibel, F. Steglich, Phys. Rev. Lett. 82 (1999) 1293.
[5] R. Küchler et al. Phys. Rev. Lett. 91 (2003) 066405.
[6] C. Bergmann et al. Phys. Stat. Sol. B 247 (2010) 694.

Email of the presenting author: tomtol@ifmpan.poznan.pl

Magnetic studies of $TmCo_2$ singlecrystal

Jakub Šebesta[1], Jiří Prchal[1], Marie Kratochvílová[1], Jaroslav Valenta[1],
Michal Vališka[1], Vladimír Sechovský[1]
[1] *Charles University in Prague, Faculty of Mathematics and Physics, Department of Condensed Matter Physics, Ke Karlovu 5 121 16 Praha 2, Czech Republic*

Magnetic properties of RCo_2 compounds has been subject of studies already in the second half of last century [1-7]. However, in recent years these materials are becoming interesting again because of new magnetic state recently discovered in RCo_2 ferrimagnets (R={Gd,…, Tm} [8,9]) in paramagnetic range called "parimagnetism". The parimagnetism is explained like a short range anti-parallel interaction between magnetization of Co clusters and magnetic moments of rare-earth atoms. It could be observed in paramagnetic region of the temperature dependence of AC magnetic susceptibility like a small anomaly, which is connected with flipping of Co magnetization along rare-earth moment, as it was estimated by microscopic methods (XMCD and SANS) [8,10-12]. The characteristic temperature was denoted as flipping temperature T_f. The importance of $TmCo_2$ compound comes from its position at the end of the series of ferrimagnetic compounds. Firstly it was prepared as a polycrystalline sample. In the measured data of magnetization/specific heat/electrical resistivity there was observed an anomaly at the temperature 3.6 K which was denoted as Curie temperature. Another anomaly appears at 4.6 K with unknown origin. One more anomaly was observed around 35 K in the AC-magnetic susceptibility data and since it behaves in the same way as for previously known cases of $ErCo_2$ and $HoCo_2$ (especially high sensitivity on external magnetic field [8,12]) it is expected that this anomaly is also connected with parimagnetic behavior and characterizes the flipping temperature T_f. There were found discrepancies between our measured data based on the polycrystalline sample and the results presented in literature[1-6,13] namely concerning the different ordering temperatures and behavior of Co magnetism. It was also found that $TmCo_2$ is a special case among the family of RCo_2 compounds with respect to relation of the characteristic temperatures (T_C, T_f). Our results moreover point to almost no response to the applied hydrostatic pressure of both T_C and T_f.

To clarify the discrepancies we have tried to grow the single crystals of this compound by using the flux growing method and the Bridgmann method. As a result of several attempts of the growing, we got few single crystals. In measurements on the same single crystalline sample we observed appearance of parimagnetic behavior similar to the previously measured data on polycrystalline sample. One can also observe a sample dependence of ordering temperature, which sometimes does not correspond to the ordering temperature of polycrystal. There is also an evidence of effect of the annealing process. These features should be connected with discrepancies in the literature and with problematic preparation. We will present experimental data evidencing the exceptionality of $TmCo_2$ from point of view of the measured results.

References:
[1] GIGNOUX D. et al., Physical Review B 14, 162-171,(1976)
[2] GRATZ E. et al., Journal of Physics-Condensed Matter 7,: 597-610 (1995)
[3] RESEL R. et al., Solid State Communications 95, 735-738, (1995)
[4] DUBENKO I.S. et al., Journal of Magnetism and Magnetic Materials 150, 304-310, (1995)
[5] BARANOV N.V. et al., Journal of Alloys and Compounds 252, 32-40, (1997)
[6] NAKAMA T. et al., Physical Review B 60, 511-522, (1999)
[7] OESTERRE H. et al., Journal of Applied Physics 44, 2350-2354, (1973)
[8] HERRERO-ALBILLOS J. et al., Physical Review B 76, 094409, (2007)

[9] MÍŠEK M. et al., Journal of Applied Physics 111, 07E132, (2012)
[10] HERRERO-ALBILLOS J. et al., Journal of Physics-Condensed Matter 21, 216004, (2009)
[11] BARTOLOME F. et al., European Physical Journal B 86, 489, (2013)
[12] BONILLA C. M. et al., Journal of Physics-Condensed Matter 26, 156001, (2014)
[13] BARANOV N.V. et al., Physical Review B 73,: 104445, (2006)

Email of the presenting author: sebesta.j@email.cz

Synthesis and magnetic properties of the GaN nanoceramics doped with transition metals

Zuzanna Piotrowska, Michał Babij, Andrzej J. Zaleski
Institute of Low Temperature and Structure Research, Polish Academy of Sciences,
P.O. Box 1410, 50-370 Wroclaw, Poland

Nowadays, the study of III-V ferromagnetic semiconductors with high Curie temperature generates intense interest because of their possible application in spintronics.. Gallium nitride has been intensively investigated in last two decades, mainly as an optical material, in the form of single crystals as well as nanocrystals and thin films. However, there are very few publications reporting measurements performed on the GaN nanoceramics, which is relatively easy to obtain and easy to dope. In 2007, apart from magnetic properties also superconducting behavior of undoped GaN was reported with $T_C = 6.5$ K [1].

GaN nanosized powders were synthesized from corresponding oxides by treating them with ammonia in 850^{o}C. So obtained samples were characterized by the X-ray (XRPD) and electron microscopy (TEM) methods (Fig. 1). Gallium nitride nanocrystalline ceramics doped with transition metals (Fe, Mn) were obtained by low temperature high pressure (LTHP) technique (8 GPa at 850^{o}C).

Preliminary magnetization measurements of some doped gallium nitride nanoceramics are presented in this paper. It was found that for instance GaN:10%Fe shows antiferromagnetic correlations and AF transition below about 75K (Fig. 2). These correlations are suppressed by steady magnetic field what is seen from AC magnetization measurements (Fig. 3). Samples doped with 5%Mn exhibited paramagnetic behavior.

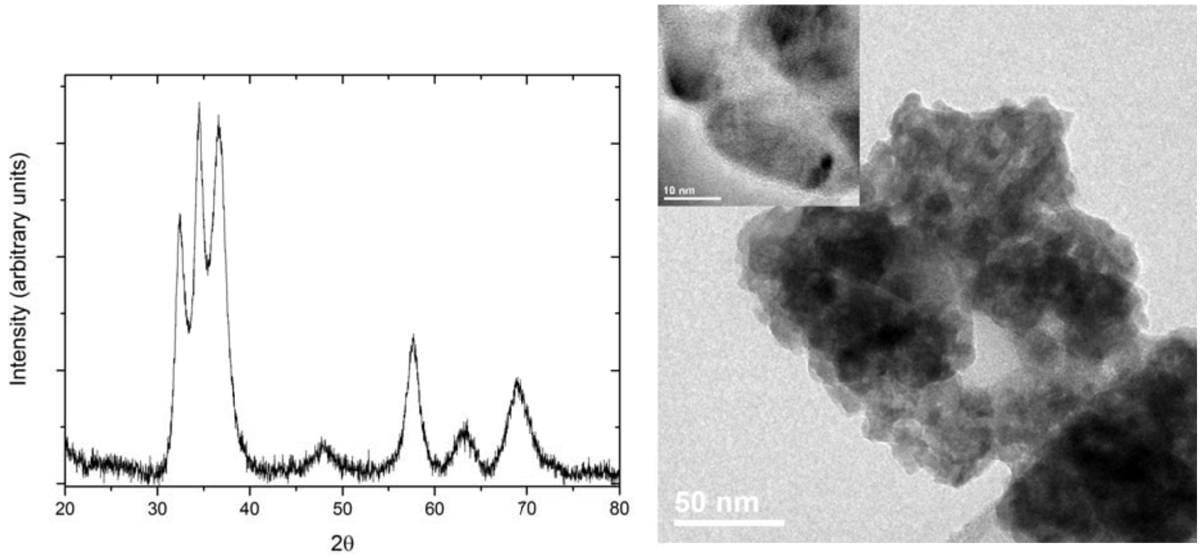

Figure 1. X-ray pattern of GaN:5%Mn nanocrystalline ceramic (left) and TEM picture of GaN nanopowders (right).

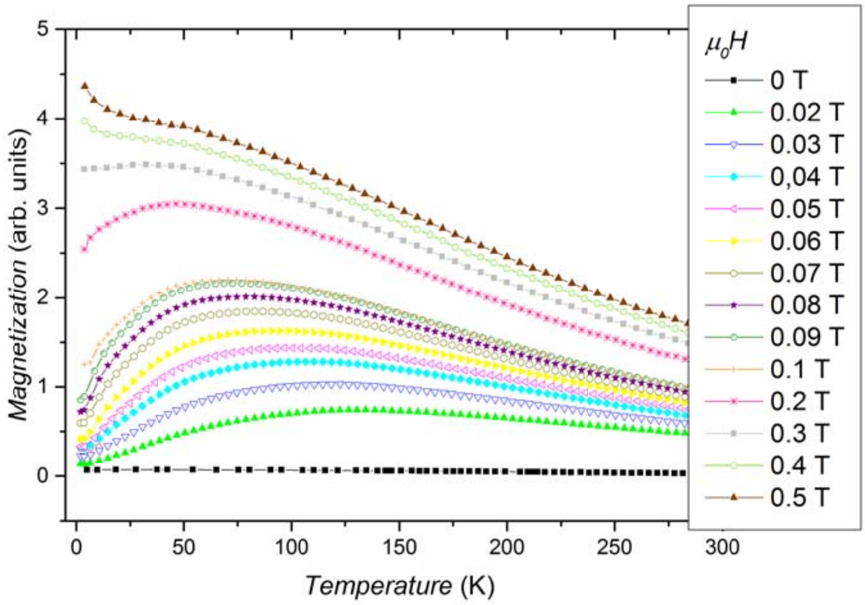

Figure 2. DC magnetization vs temperature for different external fields for GaN:10%Fe nanoceramic prepared from the nanopowders sintered at 850°C.

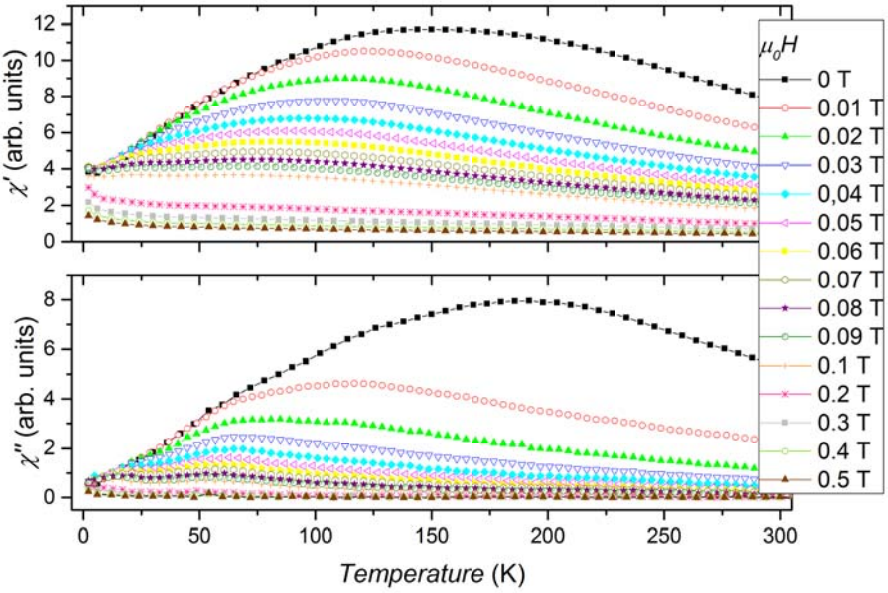

Figure 3. AC magnetization for the same sample as above.

Reference

[1] Zaleski A. J., Nyk, M., & Strek, W. (2007). Magnetic studies of GaN nanoceramics. *Applied physics letters*, *90*(4), 042511.

Email of the presenting author: z.piotrowska@int.pan.wroc.pl

Magnetism and its suppression in $CeCo_{0.715}Si_{2.285}$

J. Moudřík[1], J. Valenta[1], J. Prokleška[1], I. Císařová[2], J. Pospíšil[1] and V. Sechovský[1]
[1]*Charles University in Prague, Faculty of Mathematics and Physics, Department of Condensed Matter Physics, Ke Karlovu 5, 121 16 Prague 2, Czech Republic*
[2]*Charles University in Prague, Faculty of Science, Department of Inorganic Chemistry, Hlavova 2030/8, 128 43 Prague 2, Czech Republic*

Cerium cobalt silicides attract long ongoing attention due to the richness of different ground states and their rather easy tuning by external (field, pressure) and internal (alloying, hydrogenation) parameters. The ground states of up-to-date known compounds range from a 'simple' antiferromagnet (CeCoSi, P4/nmm; however, having a spin-density-wave gap under pressure, and indications of a magnetic quantum critical point [1]), intermediate valence/weak ferromagnetism in $CeCo_{9+\delta}Si_{4-\delta}$ system (I4/mcm [2]) to Pauli paramagnet behavior ($CeCoSi_2$, Cmcm [3]), Kondo paramagnetic behavior ($Ce_2Co_{0.8}Si_{3.2}$, P6/mmm [4]) and an alleged superconductor ($CeCoSi_3$, I4mm [5]). In the presentation we report on the preparation and characterization of the novel compound $CeCo_{0.715}Si_{2.285}$ and its magnetic properties.

The single crystal of $CeCo_{0.715}Si_{2.285}$ has been grown by a modified Czochralski pulling method in a tri-arc furnace under a high-purity argon atmosphere. The obtained ingot has been annealed at 900 °C for one week under high vacuum. The single crystal has been oriented by Laue method and cut up to samples of a suitable shape with a fine wire saw. Specific heat and resistivity measurements were carried out using a commercial physical property measurement system (PPMS) while magnetization measurements were performed in a magnetic property measurement system (MPMS), both from Quantum Design, Inc.

The tetragonal structure (space group 121, I-42m) of the studied compound was determined from single crystal diffraction measurements. It is noteworthy that the unit cell is extremely elongated along [001] direction (a = 4.12Å, c = 32.84Å). The structure determination from the single crystal diffraction is in agreement with powder diffraction data as well. The quality of the crystal was checked by Laue X-Ray diffraction, the phase purity was confirmed by a measurement with a scanning electron microscope equipped with an EDX spectroscopy option.

Temperature dependence of the specific heat of the $CeCo_{0.715}Si_{2.285}$ reflects a typical Debye behavior at high temperatures, at low temperatures the specific heat exhibits two anomalies, at T_N = 10.5 K and at T^* = 9.5 K, respectively (Fig. 1). Similarly to the specific heat data, two corresponding anomalies are observed in temperature dependence of the electrical resistivity.

To determine the nature of the ordered state below T_N measurements of magnetic field dependence of magnetization and electrical resistivity were performed. Below T_N the compound exhibits a strong hysteresis of magnetization with respect to varying magnetic field or temperature as well as a strong anisotropy with easy axis corresponding to the [001] direction. The magnetization is saturated above 1 T and stayed unchanged up to 14 T, which was the maximum field applied within our study. The saturated value of magnetization, however, is considerably reduced (0.26 μ_B/Ce) with respect to the free Ce^{3+} ion value of 2.54 μ_B. Besides, the compound exhibits quite interesting behavior in low magnetic fields below 500 mT – it undergoes numerous magnetic field induced phase transitions when magnetic field is applied in [001] direction (Fig. 2). Below the temperature of 11 K firstly two phase transitions appear at 34 mT and 18 mT, further on, with decreasing temperature the transitions shift to higher magnetic fields and new transitions appear. At temperatures below 2.5 K the number of transitions is again reduced while still being shifted to higher magnetic fields.

The exhibited step-like behavior of magnetization is similar to the behavior of the so-called "devil's staircase" systems (e.g. CeSb [6], $CeRh_3Si_2$ [7], etc.) or $CeCoGe_3$ [8]. Numerous magnetic phase transitions are also manifested in magnetic field dependence of electrical resistivity, however, the step-like behavior is more pronounced in the magnetization data.

The similarity with respect to the $CeTX_3$ group of compounds was a motivation to the hydrostatic experiment. The measurement of electrical resistivity under pressures up to 3 GPa shows a slow suppression of the magnetic ordering of ~1 K/GPa at low pressures leading to rough estimation of magnetism suppression at 6-8 GPa. The results of currently ongoing high pressure experiments will be presented as well.

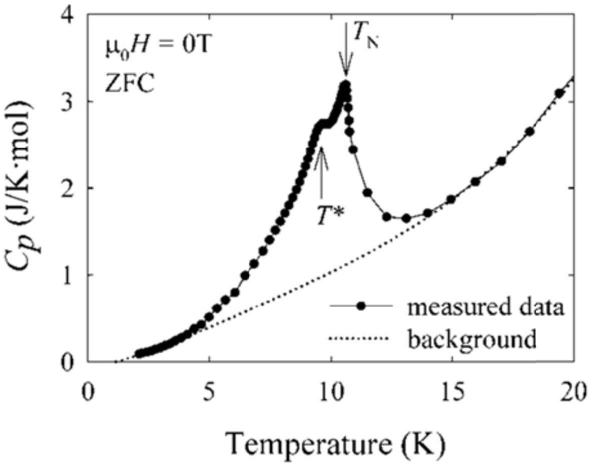

Figure 1. Heat capacity curve with marked T_N and T^* measured at zero field.

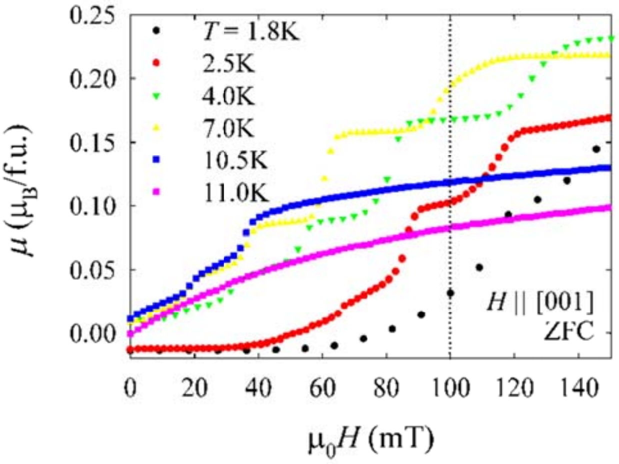

Figure 2. Magnetization curves measured at different temperatures along [001] direction.

Experiments were performed in MLTL (see: http://mltl.eu), which is supported within the program of Czech Research Infrastructures (project no. LM2011025).

References

[1] E. Lengyel, M. Nicklas and C. Geibel, Phys. Rev. B **88**, 155137 (2013).
[2] M. Giovannini, M. Hadwig, R. Pasero, E. Bauer, G. Hilscher, M. Reissner, P. Rogl and H. Michor, J. Phys. Condens. Matter **22**, 135601 (2010).
[3] M. Pelizzone, H.F. Braun and J. Muller, J. Magn. Magn. Mater. **30**, 33 (1982).
[4] M. Szlawska and D. Kaczorowski, J. Phys. Condens. Matter **26**, 016004 (2014).
[5] P. Haen, P. Lejay, B. Chevalier, B. Lloret, J. Etourneau and M. Sera, J. Less-Common Met. **110**, 321 (1985).
[6] J. Rossat-Mignod, P. Burlet, J. Villain, H. Bartholin, W. Tcheng-Si, D. Florence, O. Vogt, Phys. Rev. B **16**, 440 (1977).
[7] D. Kaczorowski and T. Komatsubara, Phys. B Condens. Matter **403**, 1362 (2008).
[8] A. Thamizhavel, T. Takeuchi, T.D. Matsuda, Y. Haga, K. Sugiyama, R. Settai, Y. Onuki, J. Phys. Soc. Japan **74**, 1858 (2005).

Email of the presenting author: valeja@mag.mff.cuni.cz

Electronic band structure calculation and physical properties of the non-centrosymmetric superconductor Th_7Co_3

M. Sahakyan, V.H. Tran
Institute of Low Temperature and Structure Research, Polish Academy of Sciences,
PO. Box 1410, 50-950 Wroclaw 2, Poland

The non-conventional superconductors are the subject of ongoing theoretical and experimental investigations. We should underscore that among of these materials, the high T_C cuprates, the FeAs-based compounds and heavy fermion superconductors have been studied in more detail, during the last years. In the above mentioned superconductors the symmetry of the Cooper pairs is related to the spin-singlet or to the spin-triplet configurations of the spins of fermionic particle.

Recently, there are many works in which it is suggested that the lack of the inversion symmetry could lead to the mixed state of the spin-singlet and spin-triplet configurations of the superconducting pairs, and as a consequence, an assymetric spin-orbit coupling (ASOC) is enhanced, which removes the degeneracy related to the spin, and the parity conservation will be violated by the Pauli principle. As non-centrosymmetric superconductor, e.g. $CePt_3Si$, UIr and $CeRuSi_3$, have been examined so far and the ASOC effect was also considered. However, in these materials the superconductivity, and also the magnetic properties are related with the strong correlation effects, between d and f orbital electrons, and the spin fluctuations could also be responsible for the non-conventional pairing. On the other hand, some non-centrosymmetric materials, in which the strong electron correlations are absent, as in the case of Li_2Pt_3B and Re_6Zr, have been reported. Non BCS-type superconductivity and the role of the spin-orbit coupling would be very important in these superconductors. Therefore, the effect of ASOC would be examined in different non-centrosymmetric superconductors exhibiting weak correlations.

In the present work we examine the superconductor Th_7Co_3 with the critical temperature of order 1.9 K. This superconductor crystallizes in a hexagonal structure (space group $P6_3mc$). Due to the absence of the inversion symmetry center and the electronic correlations are presumably weak, it is highly desired to explore physical properties both, theoretically and experimentally, and furthermore to compare the obtained results.

To the best of our knowledge, the superconducting properties of this superconductor were not well examined. The influence of lack of inversion center on the physical properties of the superconductor Th_7Co_3 was not studied as well. In this paper the results of magnetization, electrical resistivity, and specific heat measurements of Th_7Co_3 are presented. The thermodynamic characteristics of the superconducting state are evaluated.

We have performed also the electronic band structure calculations for the Th_7Co_3 compound using the FP-LMTO method. We get the electronic density of states (DOS), from which it is suggested that the contribution, coming from the Th-6d orbital is twice higher than the contribution from Co-3d orbital. Thus, we can suppose that the superconducting state is related deeply with the electronic state $6d_27s_2$, which is coinciding with the experimental result. By using the total value of the DOS at the Fermi level, we have calculated the Sommerfeld coefficient, which is in well accordance with the experimental value. The self-consistent band structure calculations for the compound Th_7Co_3 were performed too, in which the effect of the ASOC is pronounced, i.e., the degeneracy of the spin-up and spin-down bands is removed.

Email of the presenting author: m.sahakyan@int.pan.wroc.pl

^{57}Fe and ^{151}Eu Mössbauer spectroscopy of $(Eu_{0.72}Ca_{0.28})(Fe_{1.64}Co_{0.36})As_2$ iron-based superconductor

K. Komędera[1], L. M. Tran[2], A. K. Jasek[1], A. Błachowski[1], K. Ruebenbauer[1], J. Żukrowski[3,4], Z. Bukowski[2], A. J. Zaleski[2]
[1]*Mössbauer Spectroscopy Division, Institute of Physics, Pedagogical University, ul. Podchorążych 2, PL-30-084 Kraków, Poland*
[2]*Institute of Low Temperature and Structure Research, Polish Academy of Sciences, ul. Okólna 2, PL-50-422 Wrocław, Poland*
[3]*AGH University of Science and Technology, Academic Center for Materials and Nanotechnology, Av. A. Mickiewicza 30, PL-30-059 Kraków, Poland*
[4]*AGH University of Science and Technology, Faculty of Physics and Applied Computer Science, Department of Solid State Physics, A. Mickiewicza 30, PL-30-059 Kraków, Poland*

The compound $EuFe_2As_2$ is one of the parent compunds of the iron-based superconductors belonging to the most stable chemically '122' family. The parent compound exhibits development of the iron-based longitudinal incommensurate spin density wave (SDW) at about 192 K with almost simultaneous tetragonal distortion from the rhombohedral symmetry. The SDW propagates along the *a*-axis. Europium orders anti-ferromagnetically at about 19 K with moments aligned with the *a*-axis. There is no transfer field on iron due to the divalent europium ordering [1]. Upon doping with cobalt in the iron planes one observes gradual suppression of SDW with the emergent superconducting state (SC). Eventually one reaches overdoped region with neither SDW nor SC. Traces of SDW could survive to the overdoped region. The mixed state has some filamentary character with non-magnetic superconducting filaments and normal metal with SDW. Europium partially transforms to trivalent non-magnetic state due to the chemical pressure, while magnetic moments of the remaining divalent Eu tilt in the *a-c* plane preserving anti-ferromagnetic order. One observes some transfer field on iron due to the Eu order. Eu orders in the SC state as well. Eu^{3+} experiences some transfer field from Eu^{2+}, too. A tetragonal distortion is suppressed by doping [2]. In order to suprees SDW and create SC one can apply hydrostatic pressure and/or doping of any involved element.

We have studied doubly doped compound in order to look upon europium dilution. The compound $CaFe_2As_2$ is a parent compound as well with the SDW onset at about 175 K [1]. Mössbauer spectra of ^{57}Fe contain two electric quadrupole split components at high temperature. The minor component has very broad lines. The major component has slightly larger spectral shift (isomer shift) and much larger quadrupole splitting at room temperature than the parent compound $EuFe_2As_2$ [1]. Hence, the electron density on iron nuclei is lowered due to doping, while the increase in the quadrupole splitting is likely to be caused by the chemical disorder induced by dopants. Traces of SDW order appear in the spectrum collected at 80 K. About 44 % of the sample volume contains SDW, while remainder is free of the iron induced 3d magnetism at 80 K. Spectrum obtained close to the ground state, i.e., at 4.2 K consists of two components as well. About 73 % of the sample volume exhibits SDW and some hyperfine field transferred from the ordered Eu^{2+} magnetic moments. Remainder of the iron nuclei experiences a transferred hyperfine field of about 1.1 T due to the divalent europium magnetic order. The latter minor component does not exhibit 3d magnetic order and it is responsible for filamentary superconductivity typical for 'Eu-122' iron-based superconductors [2].

^{151}Eu Mössbauer spectra were obtained at three temperatures. Dominant contribution to the spectrum is due to Eu^{2+} ions – about 92 %. Remainder is due to non-magnetic Eu^{3+} ions. Spectral shifts (isomer shifts) are typical for above ionic configurations and comparable to shifts in the parent compound $EuFe_2As_2$ [2]. Quadrupole coupling constants of the axially symmetric electric field gradient (EFG) tensor $\varepsilon = \frac{1}{4}(c/E_0)eQ_gV_{zz}$ behave similarly in the non-magnetic region [2]. The hyperfine magnetic field B=26.9(1) T is seen in the spectrum collected at 4.2 K on the Eu^{2+} ions. It is slightly smaller than the field of 27.4(1) T in the parent $EuFe_2As_2$ [2]. Both fields are practically saturation fields. Hence, a decrease is likely to be due to the magnetic dilution of the divalent Eu ions caused by Ca-substitution. The anomaly in the quadrupole coupling constant and line width observed at 4.2 K for trivalent europium is likely to be an artefact caused by the transferred hyperfine magnetic field from the ordered divalent Eu^{2+} ions. The angle between hyperfine field on Eu^{2+} and the main component of EFG on the same ion amounts to 30(4)° at 4.2 K. The main component of EFG is oriented along the *c*-axis, while the hyperfine field is aligned with the Eu^{2+} magnetic moment. Hence, the magnetic moment of divalent europium is tilted by 30(4)° from the *c*-axis, while in the parent compound is perpendicular to the *c*-axis [2]. For superconducting $Eu(Fe_{1.63}Co_{0.37})As_2$ with similar Co concentration one has θ=44(1)° at 4.2 K, while for the overdoped $Eu(Fe_{1.42}Co_{0.58})As_2$ one gets θ=29(3)° at 4.2 K [2]. Therefore, a dilution of the europium by calcium has similar effect to dilution of iron by cobalt as far as Eu behavior is concerned. Both dopants lead to the reorientation of the Eu^{2+} magnetic moment toward the *c*-axis.

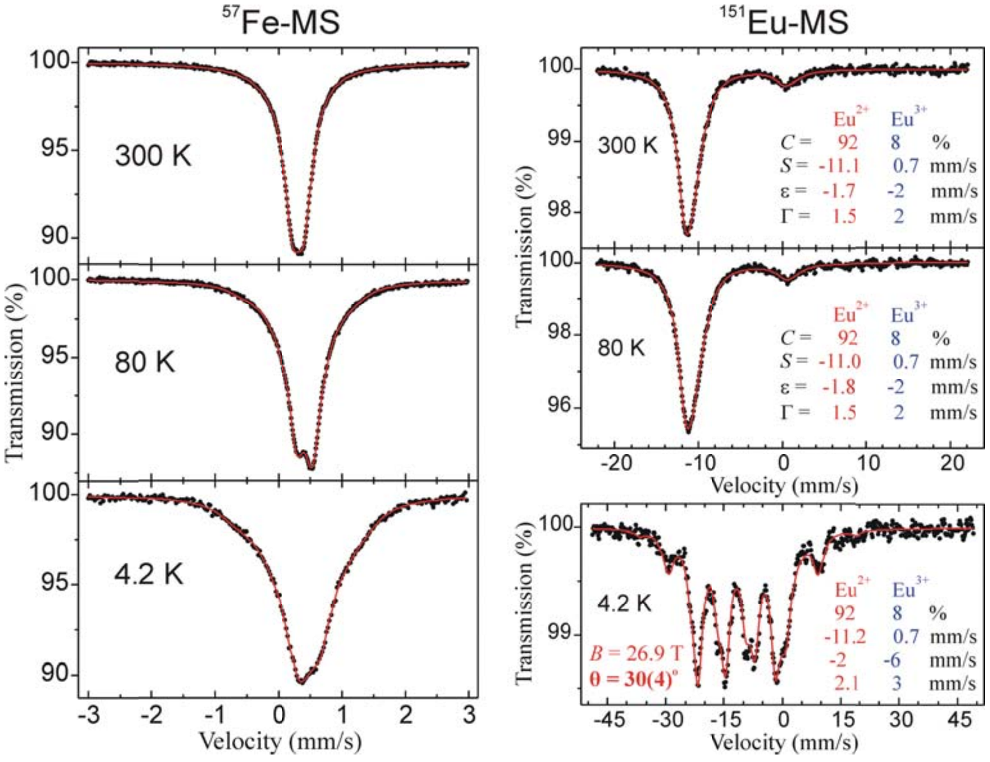

This project was financially supported by the National Science Center of Poland under the Grant No. DEC-2011/03/B/ST3/00446.

References

[1] A. Błachowski, K. Ruebenbauer, J. Żukrowski, K. Rogacki, Z. Bukowski and J. Karpinski, Phys. Rev. B **83**, 134410 (2011).
[2] A. Błachowski, K. Ruebenbauer, J. Żukrowski, Z. Bukowski, K. Rogacki, P. J. W. Moll and J. Karpinski, Phys. Rev. B **84**, 174503 (2011).

Email of the presenting author: kamilakom@op.pl

Mössbauer effect studies of first and second order magnetite single crystals

A. Kozłowski[1], J. Żukrowski[2], Z. Tarnawski[1], I. Biało[3], Z. Kąkol[1]
[1] *Department of Solid State Physics, Faculty of Physics and Applied Computer Science, AGH University of Science and Technology, 30-059 Kraków, Poland*
[2] *Academic Centre for Materials and Nanotechnology, AGH University of Science and Technology, 30-059 Kraków, Poland*
[3] *Faculty of Geology, Geophysics and Environmental Protection, AGH University of Science and Technology, Kraków, Poland*

Probably none of the naturally occurring minerals was utilized by the mankind more in its pristine form than magnetite. But its profound role in civilization notwithstanding, magnetite displays yet another fascinating face: the Verwey transition, the first order phase transformation at T_V of ca 125 K signaled by the huge peak in heat capacity, the resistivity drop of two orders of magnitude on heating across T_V and the anomalies in most of physical characteristics. Owing to these spectacular properties and entangled interactions participating in the transition, magnetite became a test ground for many experimental and theoretical techniques in solid state physics, not necessarily connected with 3d metal oxides. But despite this unieversal and continuous interest and despite the fact that the long standing puzzle - the low temperature structure- has been recently resolved („trimeron lattice“) [Senn], many aspects of physics of this material are still not understood and are still the challange for solid state physics. These still unsolved, or unclear, problems are, e.g.:

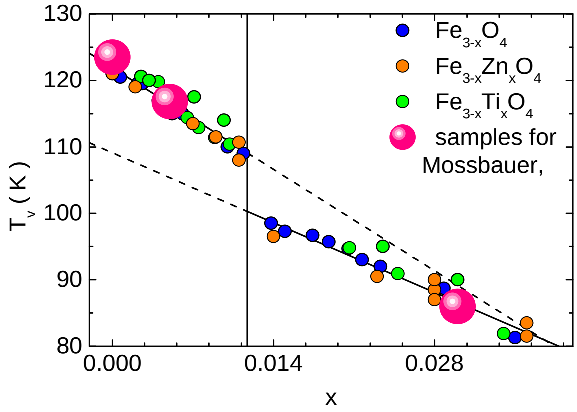

Figure 1. The composition of the measured $Fe_{3-x}Zn_xO_4$ on top of the universal T_V vs. x curve. Note the characteristic break signalling the change of the verwey transition from first (lower x) to the second order.

- the reason for the drastic change of the Verwey transition character from first-order („first-order magnetite“) for stoichiometric magnetite and with low doping/nonstoichiometry level in $Fe_{3-x}M_xO_4$ (M is primarily Zn or Ti, or just iron vacancy; first-order Verwey transition occurs when $x<0.012$, see Fig. 1) to the continuous character („second-order magnetite“, $0.012 < x < 0.036$), and its connection with the trimeron lattice,
- the problem linked to the one above: the reason for the low temperature ($T<T_V$) heat capacity excess in second-order order magnetite on top of that in the first-order samples [Kozl, Kolodz],
- the three components of the transition: charge and orbital orderings and the lattice distorsion, all, possibly decoupled [Lorenzo] and surviving, in the form of short range order, up to high temperatures [Bosak].

We have recenty suggested [Kakol] that all the above problems may be intimately linked and connected with yet another interesting phenomenon: a magnetic field induced changing of monoclinic *c* axis in low *T* phase of magnetite („axis switching“). Namely, trimeron lattice may be unstable against small reorganization of atomic structure caused by doping/ nonstoichiometry in the 2-nd order regime resulting in many electronic states of comparable energy, i.e. of high entropy and leading to a substantial specific heat. To check this conjecture, the technique that can see both the individual atom surroundings (electric field gradient), charge (isomer shift) and the individual atom magnetic field was applied: Mössbauer spectroscopy.

The samples, single crystalline $Fe_{3-x}Zn_xO_4$ (x=0, 0.005, 0.03, see Fig. 1) were skull melter grown and subsequently annealed for stoichiometry. Oriented samples were thinned out to the form of 100 μm thick platelet ((001) plane) perpendicular to gamma quanta beam.The ^{57}Fe measurements were performed in the transmission geometry using a constant acceleration type spectrometer with a ^{57}Co in Rh source kept at room temperature and the absorber placed in a closed cycle refrigeration system at several temperatures both above and below T_V.

The representative results are shown in Fig. 2. While the spectra at $T>T_V$ are very similar, the change of symmetry to low T monoclinic has a profound effect on the spectra. In particular, those for the second order ample (x=.03) do not show subtle line splitting suggesting some considerable lattice disorder.

The spectra were analyzed within the transmission integral approximation assuming two components at $T>T_V$ and five components at $T<T_V$, in accord with the simplified P2c symmetry. The tetrahedrally coordinated Fe is very well visible both at $T>T_V$ and $T<T_V$, with only minor change of parameters at T_V. It is thus, obvious that the tetrahedral iron cations can not change their valance at T_V as found a few years ago in [Rozenberg]. It was suggested there, based on Mössbauer studies under pressure, that apart from the Verwey transition there is also a crossover to normal spinel lattice that proceeds at the same temperature $T_{CC} = T_V$ as the Verwey transition under ambient pressure, but where T_{CC} grows when pressure is increased (contrary to T_V, which lowers with pressure). Normal to the inverse spinel transition, that would naturally explain the Verwey transition, would result in Fe^{+3} to Fe^{+2} change, rejected by our data.

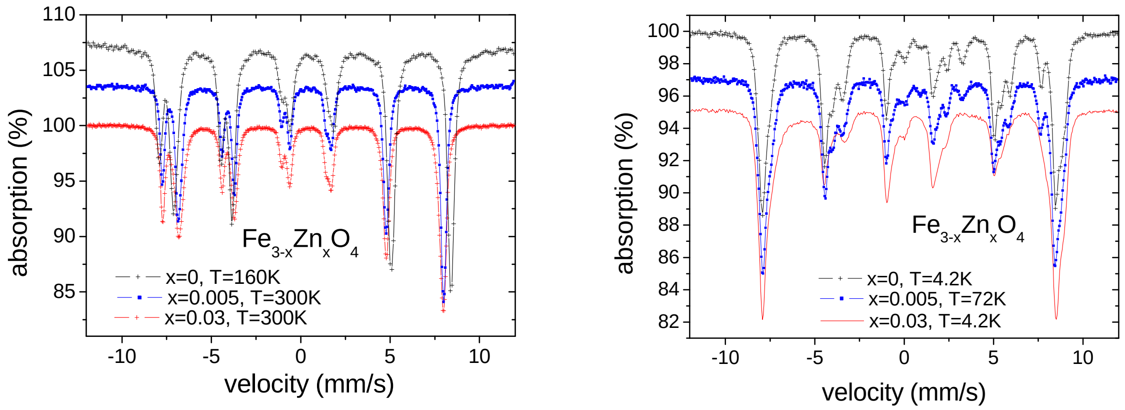

Figure 2. Mossbauer effect spectra of Zn doped single crystalline magnetite. The spectra in the first panel are characteristic for high temperature cubic symmetry and clearly different than in right panel, in monoclinic phase.

References

[Bosak] A. Bosak, et. al. Phys. Rev. **X4**, 011040 (2014).
[Kozl] A. Kozłowski, Z. Kąkol, et. al, Phys. Rev. **B54**, 12093 (1996).
[Senn] Mark S. Senn, Jon P. Wright, J. Paul Attfield, Nature **481**, 173 (2012).
[Kolodz] T. Kołodziej, et. al. Phys. Rev. **B85**, 104301 (2012).
[Kakol] Z. Kąkol, A. Kozłowski, et. al, Phil. Mag., **95**, 633 (2015).
[Lorenzo] J. E. Lorenzo et. al., Phys. Rev. Lett. **101**, 226401(2008).
[Rozenberg]. G. Kh. Rozenberg, et. al. Phys. Rev. **B75**, 020102 (2007). M. P. Pasternak, Hyp. Inter. **222**, 99 (2013).

Email of the presenting author: kozlow@agh.edu.pl

Electrochemical properties of cathode-electrolyte gradient system for use in proton-conducting fuel cells PCFC

Andrzej Kruk, Ewa Durda, Kazimierz Przybylski
AGH University of Science and Technology, Faculty of Materials Science and Ceramics,
al. Mickiewicza 30, 30-059 Krakow, Poland

Proton-conducting solid oxide fuel cells (PCFC) are very promising energy generators distinguished by high efficiency and very low emission of toxic gas. An important aspect is to select a suitable cathode material working with high temperature proton conductor electrolyte. The most desirable cathode material for protonic fuel cell should present both electronic and protonic conductivity which allows for the expansion of the triple phase boundary from the electrode/electrolyte/gas interface to the cathode bulk. Conductivity is realized by small pollaron hopping mechanism. One way of achieving such type of conductivity is to produce composite cathode consisting of both protonic and electronic conducting phases. In addition, use of a composite cathode reduces problems with the thermal expansion coefficient mismatch between the electrode and the electrolyte materials.

A potential solution to these problems is the use of suitable materials of the gradient structure. In this study, a cathode-electrolyte gradient system was obtained by using $Ba_{0.99}Ce_{0.95}Dy_{0.05}O_{3-\delta}$ (BCDy) and $La_{0.6}Sr_{0.4}Co_{0.2}Fe_{0.8}O_{3-\delta}$ (LSCF48) as the electrolyte and cathode material respectively. The system was composed of ceramic layers with linearly differing content of electrolyte and cathode powders with weight ratios: 100:0, 80:20, 60:40, 40:60, 20:80 and 0:100, respectively. The sinters were compressed into a pellet under 250 MPa pressure and sintered in 1373 K for 5 hrs in air. To verify the chemical stability and phase of BCDy and LSCF48, XRD analysis was carried out. The results indicated that no secondary phases were formed. Measurement of electrical properties of the sample were carried out by electrochemical impedance spectroscopy method which indicated improvement of electrical properties compared to the conventional cathode-electrolyte system.

Email of the presenting author: a.kruk@poczta.fm

Reentrant spin-glass state and magnetocaloric effect in the $Ce(Cu_{0.675}Ni_{0.375})_4Mn$ alloy

Karol Synoradzki[1], Tomasz Toliński[1]
[1]*Institute of Molecular Physics Polish Academy of Sciences, Poznań, Poland*

From our previous study on the isostructural $Ce(Cu_{1-x}Ni_x)_4Mn$ system we have found that in the middle range of Ni concentration the samples exhibit two consecutive magnetic transitions. From magnetization data, we identify the higher temperature transition as a cluster ferromagnetic transition and the lower one as a spin glass transition [1]. In the present study we have carried out detailed magnetic measurements to understand the low temperature magnetic anomaly and to verify the proposed reentrant spin glass (RSG) state.

For these studies we choose the $Ce(Cu_{0.625}Ni_{0.375})_4Mn$ sample. This alloy crystalizes in the hexagonal crystal structure (space group P6/mmm) with lattice parameters a = 5.118(1) Å and c= 4.114(6) Å. Frequency-dependent ac susceptibility, dc susceptibility, dc magnetization relaxation, heat capacity, and electrical resistivity measurements were carried out from 2 to 300 K in a Quantum Design Physical Property Measurement System (PPMS).

Fig. 1 shows the magnetic behaviour of the $Ce(Cu_{0.625}Ni_{0.375})_4Mn$ alloy. In probing field of 1 kOe, two consecutive magnetic transitions can be clearly resolved in the ZFC and FC dc magnetic susceptibility. A sharp increase at $T_C \sim 120$ K is followed by a peak at $T_f \sim 30$ K in the ZFC magnetization. Additionally, double peak structure with clear frequency dependence occurs in both the real χ' and imaginary χ" part of the ac susceptibility, which is typical of spin glass behaviour. However, almost stable in time dc magnetization at T = 2 K suggests that the SG state does not show a true reentry with the complete disappearance of the ferromagnetic phase below the SG transition. Therefore, in low temperature $Ce(Cu_{0.625}Ni_{0.375})_4Mn$ exhibits features characteristic for both the spin-glass and ferromagnetic phases.

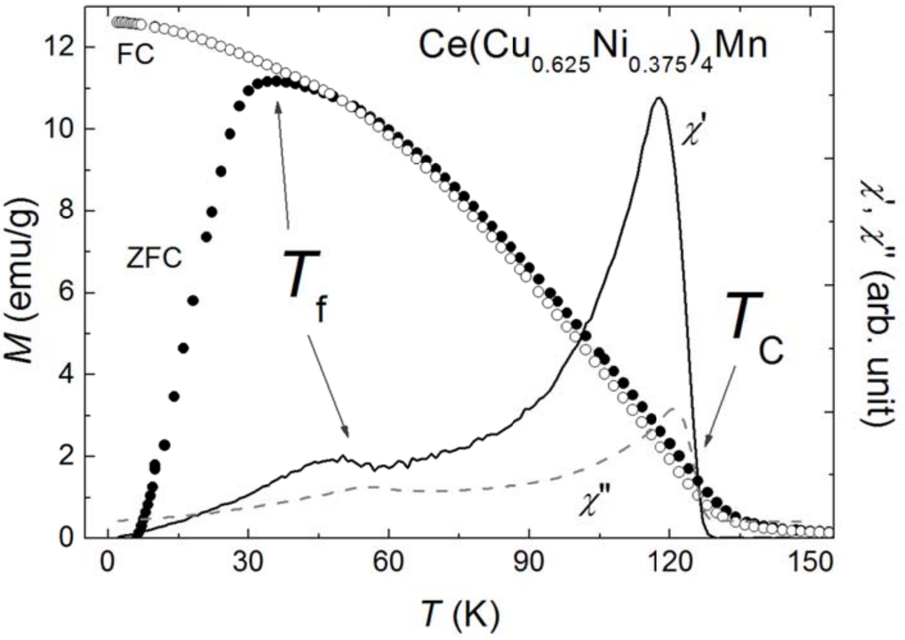

Figure 1. Temperature dependence of FC and ZFC dc magnetization (points, left axis) and ac magnetization (lines, right axis).

On the base of the magnetization curves $M(H)$ data it is possible to determine the magnetocaloric (MC) effect. It was found that the maximum value of the magnetic entropy change $|-\Delta S|$ has reached the highest value of 0.8 J/(kg K) at ΔH = 50 kOe (Fig. 2). The magnetocaloric effect in the studied alloy is weak, which makes this material unattractive for the MC application. However, a peak of $|-\Delta S|$ is around 90 K, i.e. between the Curie and freezing temperature. Therefore, the overall effect on the graph (Fig.2) is a broad peak corresponding to the sum of those two transitions, which improves the relative cooling power (RCP = $|-\Delta S_{MAX}| \times \delta T_{FWHM}$) value.

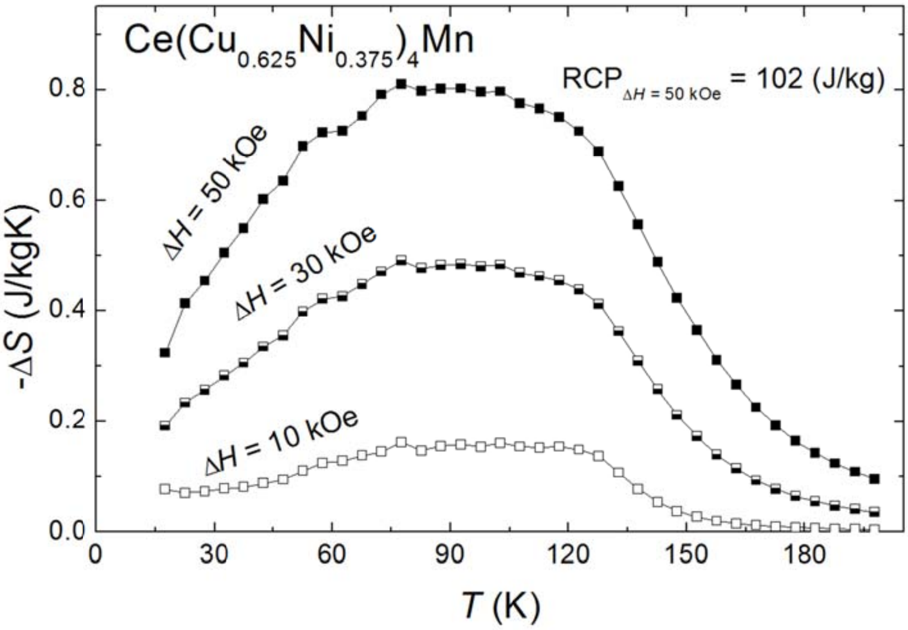

Figure 2. Magnetic entropy change $-\Delta S$ of Ce(Cu$_{0.625}$Ni$_{0.375}$)$_4$Mn sample at various magnetic fields.

Reference

[1] K. Synoradzki, T. Toliński, Acta Phys. Pol. A 126, 300 (2014).

Email of the presenting author: karol.synoradzki@ifmpan.poznan.pl

New quaternary iron-rich compounds U-Fe-Ge-Sn

Margarida Henriques[1,2], António Pereira Gonçalves[2]
[1] *Institute of Physics, ASCR, Na Slovance 2, 18221 Prague, Czech Republic*
[2] *C2TN, Instituto Superior Técnico, Universidade de Lisboa, P-2695-066 Bobadela, Portugal*

Single crystals of two new iron-rich uranium-based quaternary compounds were prepared by the solution growth method, using Sn as flux and starting from the U, Fe and Ge elements mixed in a ratio 1:2:4. The resulting crystals were analyzed by scanning electron microscopy coupled with energy dispersive X-ray spectroscopy. Single crystal X-ray diffraction was undertaken in order to solve their crystal structures.

$UFe_6Ge_2Sn_4$ crystallizes in the primitive hexagonal $HfFe_6Sn_6$ – type structure (space group *P*6/*mmm*) with lattice parameters a = 4.2639(5) Å and c = 8.5969(7) Å. In this quaternary structure, the U, Fe and Ge atoms occupy a single atomic position each that is fully ordered. The Sn atoms are positioned in two inequivalent crystallographic sites, 2*d* and 2*e*, showing occupation of 1 and 0.91 respectively.

$U_2Fe_7Ge_3Sn$ was found to crystallize in a tetragonal lattice (space group *I*4/*mmm*) having lattice constants a = 4.0163(6) Å and c = 24.3030(4) Å. The asymmetric unit is similar to the one of $Eu_2Pt_7P_3Al$ and consists of a unique Wyckoff position for U, three for Fe, two for Ge, and one for Sn. This last atom was located within the unit cell by difference Fourier analysis, with the final refined occupation being 0.12. For all other atoms, the refinement of occupancy rates did not indicate any deviation from 1 in all the atomic positions.

Email of the presenting author: henriques@fzu.cz

Study of Ti, V and their oxides-based thin films in the search for hydrogen storage materials

Z. Tarnawski[1], K. Zakrzewska[2], N.-T. H. Kim-Ngan[3], M. Krupska[3], S. Sowa[3],
K. Drogowska[1], L. Havela[4], A.G. Balogh[5]

[1]AGH University of Science and Technology, Faculty of Physics and Applied Computer Science, 30-059 Kraków, Poland

[2]AGH University of Science and Technology, Faculty of Computer Science, Electronics and Telecommunication, 30-059 Kraków, Poland

[3] Institute of Physics, Pedagogical University, 30-084 Kraków, Poland

[4]Faculty of Mathematics and Physics, Charles University, Ke Karlovu 5, 12116 Prague, Czech Republic

[5]Institute of Materials Science, TechnischeUniversität Darmstadt, 64287 Darmstadt, Germany.

We are interested in the hydrogen storage ability and the effect of hydrogen sorption on the crystal and electronic structure and physical properties of Ti, V and their oxides-based thin films. Thin film processing is in fact an alternative method that synthesizes nanostructured materials in specific compositions which could provide a size-reduction to the nanoscale. Besides, it provides a possibility to investigate the surface or interface contributions to the hydrogenation thermodynamics.

Thin film series consisted of Ti, V, TiO_2 and V_2O_5 layer with different layer geometries and thicknesses have been prepared by the sputtering technique. The film chemical composition, layer thickness and structure were determined by combined analysis of X-ray diffraction, X-ray reflectometry, Rutherford backscattering and optical spectrometry. The hydrogen depth profile of selected films upon hydrogen charging at 1bar and/or hydrogenation at pressure up to 102 bar was determined by using secondary ion mass spectrometry and nuclear reaction analysis using a N-15 beam. The highest hydrogen storage with a concentration up to 50 at.% was found in the pure Ti and Ti-contained layer, while it amounts to around 30% in the metallic Ti-V-Ni layer. Hydrogen can diffuse through the TiO_2 layer without accumulation, but can be stored in the VO_2 layer in some cases. Hydrogen can remove the preferential Ti orientation in the films and induce a complete transition of V_2O_5 into VO_2 in the films.

We show in Fig. 1 the RBS spectrum of as–deposited Ti-V-Si/Si(111) film. It is characterized by a large and wide peak at energy range of 1050 and 1300 keV corresponded to Ti-, V- and Ni signals from the film. Hydrogen charging leads to surface oxidation of the film revealed by an appearance of a quite sharp O-peak at energy of 620 keV. The film structure can be considered to consist of 2 different regions: 1) the oxidized layer with a total thickness of 48 nm, 2) the main part of the film is the pure metal layers of a total thickness of 103 nm. We investigated that the total thickness of the Ti-V-Ni/Si(111) film does not change by hydrogen charging.

Fig. 2 presented hydrogen profile determined from N-15 experiments for Ti-V-Ni/Si(111). Before hydrogen charging, Ti-V-Ni layer reveals small amount of hydrogen (~4 at.%) distributed quite homogenously within the whole film up to 100 nm deep from the film surface. On the surface (up to the thickness of 10-15 nm) a quite high concentration of 15 at.% of hydrogen is found. Hydrogen charging causes an enormous increase of hydrogen amount up to 32 at.% in the film. However, the hydrogen profile reveals that the hydrogen gather mostly in the deepness of the range of 50-100 nm, i.e. in the deep layer consisted of pure Ti-V-Ni metal.

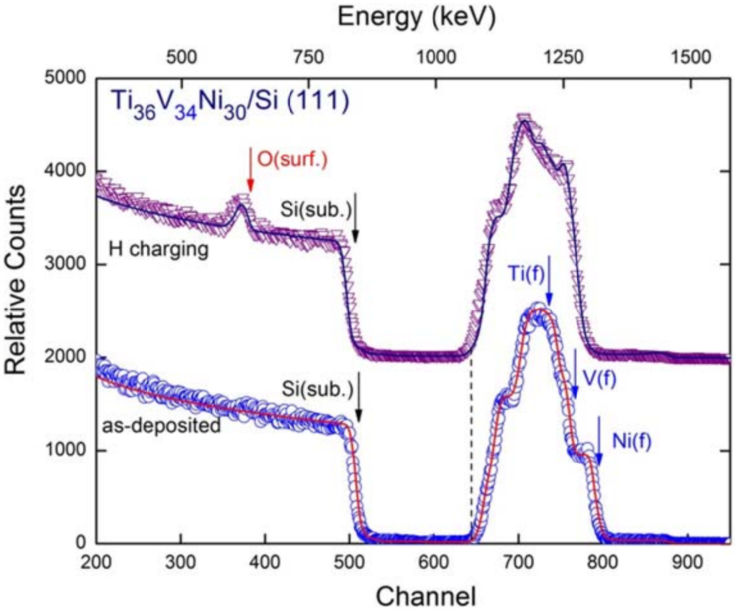

Figure 1. Random RBS (markers) and SIMNRA (lines) simulated spectra for 151 nm $Ti_{36}V_{34}Ni_{30}$/Si(111) film before and after hydrogen charging. RBS experiments were performed with the incident He^+ ion energy of 1.7 MeV and the backscattering angle of 171°. The film is denoted by its nominal chemical composition in the as-deposited state. The curves were normalized and shifted for a clarity. Ni(f), V(f) and Ti(f) denoted respectively the Ni-, V- and Ti signal in the film. The Si signal from the Si substrate is labeled as Si(sub.). The surface oxidization upon hydrogen charging is revealed by an appearance of oxygen signal (O(surf.)). The vertical dotted line indicates that the film thickness (or the peak width) does not change upon hydrogenation.

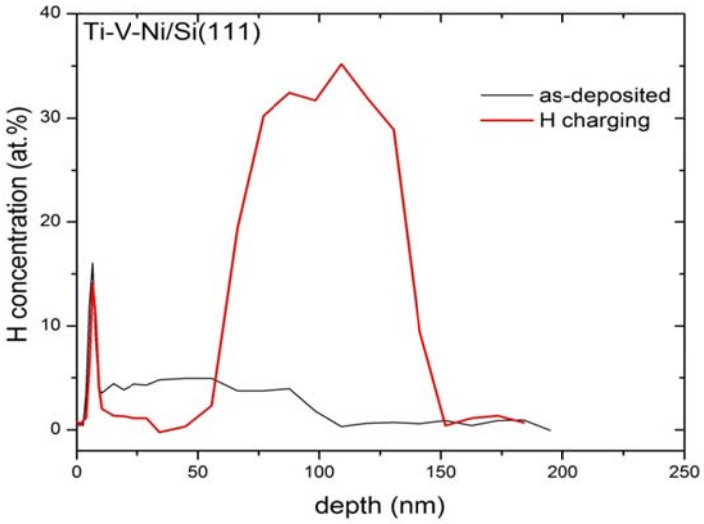

Figure 2. Hydrogen profiles of Ti-V-Ni layer on Si(111) before (as-deposited) and after hydrogen charging revealing a large hydrogen storage (~32 at. %) in the deep metallic Ti-V-Ni layer.

The support of the Czech-Polish cooperation (Czech-polish project ID(CZ) 7AMB14PL036 (ID(PL) 9004/R14/R15)) is highly acknowledged. N.-T.H.K-N. acknowledges the support of the European Regional Development Fund under the Infrastructure and Environment Programme.

Email of the presenting author: tarnawsk@agh.edu.pl

Magnetic phase transition in antiferromagnetic $SrMnO_3$ and K_2CoF_4 perovskites

D. M. Nalecz, R. J. Radwanski, R. Bujakiewicz-Koronska
Institute of Physics, Pedagogical University, Podchorazych 2, 30-084 Krakow, Poland

Compounds of the type ABO_3 perovskite structure are primarily studied in terms of dielectric properties. The popular systems like $BaTiO_3$, $CaTiO_3$, $PbTiO_3$, $LiNbO_3$ contain transition metal ion in the B site. These cations which $3d^0$ electron configuration have empty d shell. The same perovskite structure is also formed by compounds containing a magnetically active ions such as Mn^{4+} and Co^{2+}, that have an open 3d shell. These ions have three and seven electrons in the incomplete 3d shell, respectively forming strongly correlated $3d^3$ and $3d^7$ electron systems. Stoichiometric $SrMnO_3$ shows, depending of the preparation, three polymorphic structures: cubic perovskite (space group Pm-3m, No. 221) containing 1 formula units, and two hexagonal polymorphs 4H and 6H containing 4 and 6 formula units, respectively. They are antiferromagnetic with Néel temperature between 230-280 K. K_2CoF_4 crystalizes in the layered perovskite structure and is antiferromagnet below T_N of 107 K.

Despite of very different ions and their different valencies, there is interesting fact that the electronic structures of these compounds are correlated. The Mn^{4+} and Co^{2+} ions have the same atomic-like ground term ^4F, but the effect of the octahedral crystal field, associated with the octahedral ligand (O^{2-} and F^{1-}) surroundings, is exactly opposite as the Mn^{4+} ion can be regarded as 3-electron system whereas the Co^{2+} ion as the 3-hole system. In a consequence subterm $^4A_{2g}$ (the orbital singlet) is the ground subterm in case of $SrMnO_3$ whereas subterm $^4T_{2g}$ (orbital triplet) is the ground subterm in case of K_2CoF_4. Their 4-fold and 12-fold degeneracies are partly removed by the spin-orbit interactions and fully removed in the magnetic state.

We have calculated low-energy electronic structure of $SrMnO_3$ and K_2CoF_4 [1] both in paramagnetic and the antiferromagnetic state. Magnetic properties of $SrMnO_3$ are predominantly determined by the low-energy, atomic like electronic structure of Mn^{4+} ions whereas magnetism in K_2CoF_4 is associated with Co^{2+} ions. From the calculated low-energy electronic structure we have obtained the temperature dependence of the specific heat with a λ-type peak marking the magnetic phase transition.

We are going to show the calculated temperature dependence of the heat capacity of K_2CoF_4 and $SrMnO_3$. These dependence which contains the 3d contribution $c_e(T)$ as a result of the temperature evolution of the electronic structure, and the lattice contribution under assumptions of Debye temperature values as 400K for K_2CoF_4 and 600K for $SrMnO_3$. The calculated specific heat are in good agreement with experimental points taken from [2-5]. It is worth to note that our approach describes magnetic properties of these compounds being in agreement with their insulating ground state (it is great problem in band theories) [6].

References

[1] R. J. Radwanski, D. M. Nalecz, Phase Transitions, 86, 131-137 (2013)
[2] H. Ikeda, I. Hatta, and M. Tanaka, J. Phys. Soc. Jpn. 40, 334–339 (1976)
[3] I. Hatta and H. Ikeda, J. Phys. Soc. Jpn. 48, 77–85 (1980)
[4] *R.* Søndenå, S. Stølen*, P.* Ravindran*,* T. Grande, Phys Rev B. 75, 214307-1 (2007)
[5] A. A. Belik et al., Phys Rev B. 84, 094438 -1-094438-6 (2011)
[6] D. J. Singh, in Correlated Electrons: From Models to Materials vol. 2, Eds: E. Pavarini, E. Koch, F. Anders and M. Jarrell, Forschungszentrum Jülich, 2.2-2.24 (2012) ISBN 978-3-89336-796-2

Email of the presenting author: sfnalecz@cyf-kr.edu.pl

Really first principles calculations - Quantum Atomistic Solid State Theory (QUASST) for UPd_2Al_3, UGa_2 and UO_2

R. J. Radwanski[1,2], D. M. Nalecz[1], Z. Ropka[2]
[1] *Institute of Physics, Pedagogical University, Podchorazych 2, 30-084 Krakow, Poland*
[2] *Center of Solid State Physics, Snt Filip 5, 31-150 Krakow, Poland*

There is a long-lasting debate within the magnetic community about the role played by *f* electrons, in particular after the arisen problem of the extraordinarily large specific heat at low temperatures for intermetallic compounds known in last thirty years ($CeAl_3$ 1976) as the heavy-fermion problem. There are two schools, a smaller localized crystal-field community and a dominant itinerant community claiming the dominant role of hybridization of f and conduction electrons. In the first the number of f electrons is integer, in the other - is noninteger. This problem can be traced on UPd_2Al_3, as an example. The uniqueness of UPd_2Al_3, discovered in 1991 in a group of Prof. Steglich, relies in the coexistence of the heavy-fermion (h-f) phenomena, the large magnetic moment of about 0.85-1.5 μ_B in the antiferomagnetic state below T_N =14.3 K and the superconductivity below 2 K. In band calculations **all** f electrons (Kubler 1991, Fulde/Zwicknagl) are considered as itinerant. Within the crystal-field (CEF) approach, which we have extended to the Quantum Atomistic Solid State Theory (QUASST), **some** f electrons are treated as localized. Within the localized CEF approaches there is a discussion about the tetravalent (U^{4+} = **two** localized f electrons) (e.g. Steglich group 1992, Divis 1996) or preferred by us [Radwanski 1992] trivalent (U^{3+} =**three** localized f electrons) uranium state in UPd_2Al_3. Some authors (Fulde, Zwicknagl) after important theoretical works with all delocalized *f* electrons recently have admitted the existence in UPt_3 and in UPd_2Al_3, two famous heavy-fermion compounds, of two localized f electrons coming out with a so-called dual model of 5f electrons. In the dual model **two** f electrons are treated as fully localized whereas the **third** f electron is partially localized and partially itinerant. One of the present authors (RJR) has claimed at the very beginning on the existence of the three localized f electrons, i.e. of the U^{3+} ion in UPd_2Al_3, in contrary to strong opposition of the "itinerant" community or of "two-localized-f-electrons" community. However, there is experimental evidence for crystal-field excitations (Krimmel *et al.* [1] which we have fitted with the $5f^3$ configuration. We claim, that the experimental excitations are like fingerprints of the $5f^3$ configuration in UPd_2Al_3.

Much the same debate goes over description of UGa_2. UGa_2 is a very unique uranium compound being ferromagnet with T_c=125 K. The U^{3+} description by Radwanski and Kim-Ngan (JMMM 140-144 (1995) 1373) was covered by a $5f^2$ claim (Phys. Rev. B 53 (1996) 9658) and later by a dual f-electron model (2001). Recent studies [2] on the single-crystal specimen of UGa_2 have revealed a surprised increase of Tc with pressure but confirmed the strong ferromagnetic properties with a moment of 3.07 μ_B, 10% larger than the previous experimental value. Magnetization curves have revealed very strong anisotropy with the moments lying along the a axis in the hexagonal plane (like in UPd_2Al_3). The ferromagnetic state allows for the evaluation of the macroscopic anisotropy parameters. We have derived a new slightly-modified set of crystal-field (CEF) parameters in order to account for the observed larger magnetic moment. We have calculated the splitting of the lowest CEF state in the ferromagnetic state to be 98 K what we claim was seen in the inelastic-neutron scattering experiments and interpreted as a magnon gap of 7-8 meV (Ref. 37 in [2]).

In these two compounds the ground state is Kramers doublet. In UPd_2Al_3 and UGa_2 these Kramers doublet are splitted by internal magnetic spin-spin interactions in the magnetically-ordered state. These splittings are 2 and 12 meV, being roughly proportional to the magnetic-ordering temperature. In our view in heavy-fermion compunds is splitting is very small. In our view the heavy-fermion phenomena have a source in crystal-field spin-like neutral excitations to the Kramers conjugate state of a strongly-correlated odd-number electron system like the Ce^{3+} ($4f^1$), Yb^{3+} ($4f^{13}$) and U^{3+} ($5f^3$) configuration (all these ions are Kramers ions; the U^{3+} ion itself is a really **heavy-fermion** system with strongly-correlated atomic-like 89 electrons). The formation of the ionic-like configuration $5f^3$ (U^{3+}) is manifestation of the strong electron-correlations at the atomic scale. In metallic UPd_2Al_3 three localized 5f electrons coexist with conduction electrons.

We also have studied UO_2. It is predominantly ionic compounds with the tetravalent uranium state. It orders antiferromagnetically below 30 K. We have derived crystal-field interactions and described its temperature dependence of the specific heat in the whole temperature range, including λ-type peak at T_N=30 K.

Within the Quantum Atomistic Solid State theory (QUASST), claiming the preservation of the atomic-like states in a solid, we consistently have explained the ground-state properties and thermodynamics, both in the paramagnetic and magnetic state, together with the reproduction of the λ-type peak at the phase transition. In QUASST we look for solutions with an integer number of f electrons in contrary to a 5f-ligand hybridization model. Of course, we do not claim that CEF explains everything (surely CEF itself cannot explain the formation of a magnetic ordering), but surely the atomic-like 4f/5f/3d cation is the source of the magnetism of a whole solid. The atomic-scale magnetic moment is determined by local effects known as crystal field and spin-orbit interactions as well as very strong electron correlations. These strong electron correlations are predominantly of the intra-atomic origin and are taking into account, in the first approximation, via on-site Hund's rules. These strong correlations lead to many-electron version of the CEF approach.

Finally, we use a name "f electrons", as often is used in literature. Of course, f electrons are not special electrons but it means electrons in f states. f states have well defined characteristics, like the orbital quantum number *l*. By identifying quantum states in a solid we can identified f electrons, in particular their number. We also can say, that QUASST says that any theoretical description of compounds containing a 3d/4f/5f atom is necessary to start from evaluation of the conventional interactions. The solid-state compounds within the QUASST are practical laboratory for the atomic physics and quantum mechanics.

Finally, we add that existing controversies are very vital for development of Science and Physics provided that everybody, researchers and editors, follow scientific rules. It not always is the case, but it is the reality. However, discoveries of mysteries of God is a real pleasure and for it we are doing Physics.

References

[1] A. Krimmel, A. Loidl, R. Eccleston, C. Geibel, F. Steglich, J. Phys.: Condens. Matter **8**, 1677 (1996).
[2] A. K. Kolomiets et al., Phys. Rev. B **91** (2015) 064405.
[3] J. Sichelschmidt, V. A. Ivanshin, J. Ferstl, C. Geibel, F. Steglich, Phys. Rev. Lett. **91**, 156401 (2003).

Email of the presenting author: rjradwanski@gmail.com

Ab initio phonon dynamics in the layered ternary diselenide KNi_2Se_2

Magdalena Mędala, Grzegorz Jagło, Urszula D. Wdowik
Institute of Technology, Pedagogical University, ul. Podchorazych 2,
30-084 Cracow, Poland

Dynamical properties of KNi_2Se_2 lattice are investigated within density functional theory and the approximation of harmonic phonons. Partial phonon densities of states indicate that Ni and Se vibrations span the entire spectral range extending to 27 meV, whereas K vibrations are limited to 11–18 meV. It is shown that inelastic neutron scattering spectra reflect the dynamics of Ni atoms within [Ni_2Se_2] blocks and the high-energy Eg mode is hardly observed in the Raman spectra due to its low intensity. The electronic contribution to the heat capacity of 47 mJ mol^{-1} K^{-2} is estimated at very low temperatures. A comparison between the experimental and calculated heat capacities indicates significant enhancement of the conduction-band effective mass at low temperatures [1].

Reference

[1] G. Jaglo, M.Mędala, U. D. Wdowik, Phys. Lett. A 379 (2015) 183–186.

Email of the presenting author: mmedala@up.krakow.pl

Characterization of lead titanate thin films prepared by sol gel process

E. El Moussafir, R. Adhiri, M. Moussetad , Y. Guaaybess
Laboratoire de l'Ingénierie et Matériaux, Faculté des Sciences Ben M'sik, B. P. 20800, Casablanca, Morocco

Ferroelectric materials are of high interest for a numerous applications, including non-volatile memories, dynamic random access memories, electro optic switches, pyro electric detectors, etc. and considerable attention has recently focused on the development of the technology for their growth in thin films.

Lead titanate ($PbTiO_3$) PT sol–gel derived thin films have been prepared on glace substrates using lead acetate trihydrate, and titanium isopropoxide as precursors along with 2-methoxyethanol as solvent and acetic acid as catalyst by spin coating method. Techniques including X-ray diffraction (XRD), scanning electron microscopy (SEM), electrical and ferroelectric hysteresis measurements have been performed for layer characterization.

E-mail of the presenting author: elmoussafir@hotmail.fr

The resonance transition in spin-crossover molecular nanomagnets

A. Maksymov[1,2], Iu. Gudyma[2], L. Spinu[1]
[1] *Advanced Material Research Institute (AMRI) and Department of Physics, University of New Orleans, New Orleans, LA 70148, USA*
[2] *Department of General Physics, Chernivtsi National University, Chernivtsi 58012, Ukraine*

The increasing needs of contemporaneous nanoelectronics require a new class of materials being able to provide the high-performance processing of large amounts of data and their storage on high-density media. The recent researches of new informational materials have shown that the properties of spin-crossover compounds are well suited for designing new devices able to satisfy the increasing requirements in information technology. The spin-crossover compounds are the new class of coordination inorganic complexes with d^4 to d^7 electronic configuration of metal ion orbitals, situated in the center of the octahedral ligand field [1]. The main property, which makes these molecular magnetic materials promising is bistability controlled by external physical fields. The bistable properties of spin-crossover complexes are related to the existence of low-spin and high-spin configuration of degenerated d-orbitals of metal ion, which takes places due to action of crystal field of the surrounded ligand. The degeneration of d-level lead to the appearance of t_{2g} and e_g sublevels where the electrons may be distributed with different spin configuration depending on the ratio of their energy and energy gap between the t_{2g} and e_g sublevels. Usually such kind of distribution provides the existence of two states that have magnetic nature. If the energy of electron-electron repulsion is less than energy gap the electrons will by situated on the t_{2g} sublevels with antiparallel spins. In this case the low-spin (LS) state with minimal magnetic moment and diamagnetic properties is realized. In the case if value of energy of electron-electron repulsion becomes the same as the energy gap the paramagnetic high-spin (HS) state is realized, and in according to Hund's rule the electrons will be redistributed in such a way that first will try to occupy all free sublevels and then will be pairing.

In the most cases the spin-crossover system is fully described by the behavior of fraction of high-spin molecules. This behavior depends on the action of physical fields (magnetic, light irradiation, temperature, pressure and other). On short time intervals this action is non-regulate and initializes the fluctuation of system parameters which may be described as noise action. The studying of stochastic behavior of spin-crossover system provoked by interaction with environment was developed in the works [2]. The main idea consists in describing the interaction with environment as contact with heat bath. The mathematical tools used are based on stochastic Langevin dynamics in the connection with a set of Fokker-Plank equations.

In this work we carried out the macroscopic studies of system dynamics, where the focus is done on the system with simultaneous action of noise and periodic external signal [2]. Such coupling of external periodic and stochastic forces allows providing the studying of stochastic resonance phenomenon in spin-crossover system with the transition controlled by light irradiation. In this case the theoretical description of system dynamics is based on the phenomenological kinetic equations in terms of competing photoexcitation and relaxation processes following the equations:

$$\frac{dn_H}{dt} = f_{exc}(n_H,t) - f_{rel}(n_H,t) + A\cos\left(\frac{2\pi}{T}t + \phi_0\right) + \xi(t). \qquad (1)$$

This equation describes the evolution of HS fraction of spin-crossover molecules n_H where photoexcitation and relaxation is described as:

$$f_{exc}(n_H,t)=\beta(1-n_H),\quad f_{rel}(n_H,t)=n_H\exp(-\alpha n_H) \tag{2}$$

Here, β is the probability per time unit of the transition from LS state to HS one determined by the intensity of light irradiation and absorption cross-section of optically active element; α is self-acceleration factor of relaxation defined by the cooperative effects in the system described by intersites interaction, the relative atomic concentration and inverse temperature. The periodic signal is characterized by the amplitude A, period T and initial phase ϕ_0 which for simplicity is considered as zero. The stochastic term $\xi(t)$ describes the additive noise which includes all background irregularities presenting in the system. This stochastic term corresponds to the following statistical characteristics

$$\langle\xi(t)\rangle=0$$

$$\langle\xi(t)\xi(t')\rangle=2\varepsilon^2\delta(t-t'), \tag{3}$$

where ε^2 is intensity of additive noise.

The characteristic of stochastic resonance phenomenon in spin-crossover system described by Eq. (1) with the conditions (2) and (3) is given by spectral power amplification (SA) obtained from numerical simulations of system dynamics following the relation:

$$SA=\frac{|X(\omega_0)|^2}{|f(\omega_0)|^2}. \tag{4}$$

where $X(\omega_0)$ is the Fourier transform of simulated stochastic trajectory averaged over ensemble of 300 particular trajectories, and $f(\omega\ )$ is the Fourier transforms of input periodic signal. In order to estimate the spectral amplification was taken into account the Fourier components at frequency ω_0 which corresponds to input frequency of input periodic signal. The obtained results of spectral amplification for the system initially located in HS state ($n_H=1$) were shown in Fig. 1.

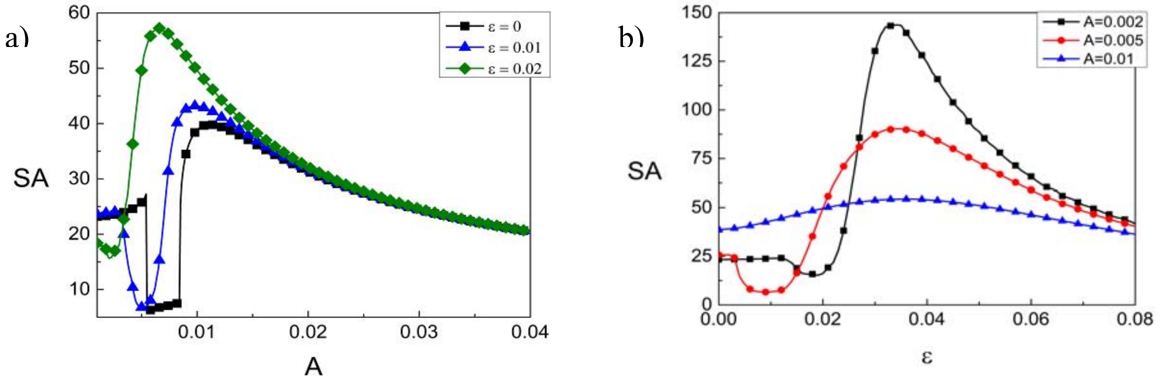

Figure 1. The signal amplification as a function of amplitude of periodic signal for indicated values of noise (a) and as a function of noise intensity at fixed amplitudes (b). Other system parameters are $\beta=0.081$, $\alpha=5.14$.

As it may be observed, the resonant transition between LS and HS states, which corresponds to the main peak in the SA dependencies, occurs for the certain values of noise and amplitude of periodic signal. The fall down of dependencies for small values of amplitude and noise shown in Fig.1 (a) and (b) respectively is related to the resonant transition from initial HS to LS state.

References

[1] *Spin Crossover in Transition Metal Compounds I-III*. P. Gütlich, H. Goodwin (eds), Berlin/Heidelberg: Springer (2004).
[2] Iu. Gudyma, A. Maksymov, M. Dimian, Phys. Rev. E **90**, 052135 (2014) and references therein.

Email of the presenting author: maxyartur@gmail.com

Magnetic disaccommodation in La-Co substituted strontium M-type hexaferrites

P. Hernández-Gómez[1], Xiansong Liu[2], J. M. Muñoz[1], C. Torres[1] and O. Alejos[1]
[1]*Univ. Valladolid, Dpto. Electricidad y Electrónica, 47071 Valladolid, Spain*
[2]*Univ. Anhui, School of Physics and Materials Science, Hefei 230039, PR China*

Hexagonal ferrites have been widely used as permanent magnets owing to their appropriate magnetic properties as big saturation magnetization, large uniaxial magnetic anisotropy, and high Curie temperature, as well as their low manufacturing cost [1]. Regarding magnetic properties, the magnetic after-effect processes have to be taken into account in order to minimize the losses. In addition, the study of this kind of processes provides information about the underlying mechanisms governing the dynamic behavior of Bloch walls [2]. Among the different techniques available, the magnetic disaccommodation measurements are a powerful tool in the detection of this kind of phenomena. It consists in the time variation of the mobility of domain walls after a magnetic shock, and is shown by a temporal evolution of the magnetic permeability after a demagnetization stage, and the relaxation time which characterizes each relaxation process is strongly temperature-dependent. This relaxation phenomenon has been observed firstly in spinel ferrites [2], but is also present in hexaferrites [3] and garnets [4]. Magnetic relaxation has been measured in M-type polycrystalline Sr hexaferrites with substitutions of La and Co. Two different initial compositions were investigated; one of them with equal substitution of La and Co, i.e. $Sr_{1-x}La_xFe_{12-x}Co_xO_{19}$ (x=0.05 to 0.20), and other with different amount of substituting cations: $Sr_{1-x}La_xFe_{12-y}Co_yO_{19}$ (x=0.09, y=0.08; x=0.13, y=0.11; x=0.16, y=0.13) which exhibit increased magnetic properties [5]. The samples have been prepared by means of standard ceramic techniques, presintered at 1250º C in air, dry-milled, pressed in disk form, sintered 4h in air at 1350º C, and then rapidly quenched to provide the presence of crystal vacancies. XRD measurement reveal the formation of single phase magnetoplumbite In the temperature range between 80 and 420 K, the magnetic disaccommodation, has been measured with an automated system based on an LCR bridge. The results have been represented as isochronal curves, i. e, the relative variation of the initial permeability after sample demagnetization between an initial time t_1= 2 s and different window times t_2 = 4, 8, 16, 32, 64 and 128 s in the form

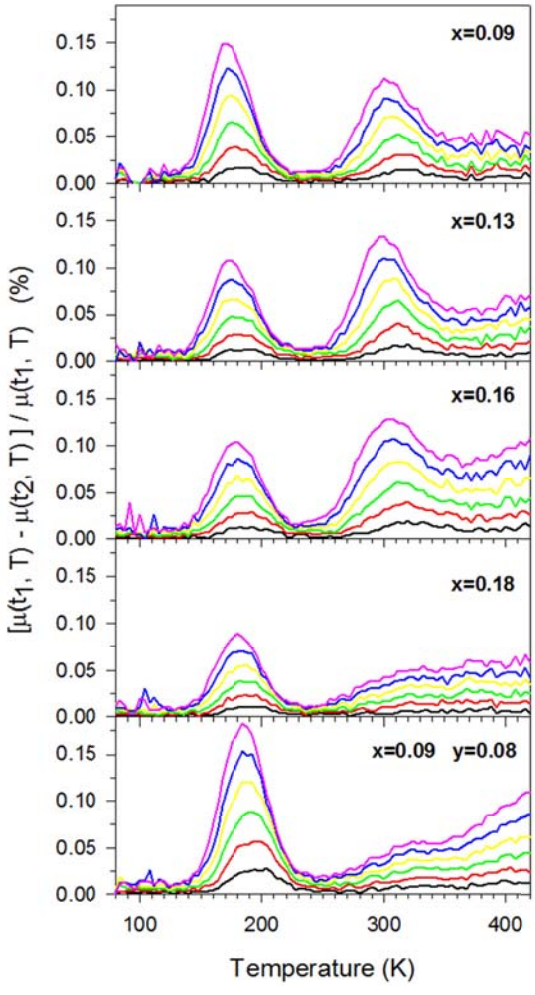

$$\frac{\mu(t_1,T)-\mu(t_2,T)}{\mu(t_1,T)}(\%) \qquad (1)$$

When the time window (t_2-t_1) is of the same order of magnitude that the relaxation time at a specified temperature, this curve exhibits a maximum. In this way, isochronal spectra disclose the different after-effect processes in the temperature range tested, and the characteristic parameters of the relaxation process, as activation energy, can be obtained.

The isochronal disaccommodation spectra in hexaferrites show the presence of different relaxation processes namely A_0 process at 500 K, A peak at 380 K, B at 300 K, C at 240 K, D at 165 K and F at 90 K [3]. A close inspection reveals strong similarities, regarding the metallic sites, among cubic and hexagonal close packed structures. For this reason it is feasible the assumption that the relaxation processes detected in hexagonal ferrites are caused from similar underlying mechanisms responsible for the magnetic after-effects in spinel ferrites, and the presence of additional relaxation processes can be due to the existence of additional interstitial sites in the crystallographic structure. For $Sr_{1-x}La_xFe_{12-x}Co_xO_{19}$ samples we can observe the B and D peaks, whereas A peak has very low amplitude, and A_0 process can be inferred from inspection of some spectra. The increase in doping rate causes a progressive diminution of relaxation processes, especially in B peak, and a shift of D process peak temperature to higher values. At the higher substitution rate analyzed the disaccommodation processes are small, and further doping will suppress them, in a similar way than observed in cobalt doped magnetite. Electronic F process is completely suppressed, as observed also in several doped magnetite systems, caused by the destruction of the crystalline periodic potential. Mössbauer investigations of La^{3+}-Co^{2+} substitution M-type ferrite samples revealed that most of the Co^{2+} cations enter into the structure by substituting in the octahedral 2a sites, and then causing the observed diminution of B peak amplitude, and making energetically unfavourable the A process. In addition, local neutrality favors the presence of the divalent ferrous cation in the vicinity of La^{3+} thus enhancing the D relaxation process which takes place in face-sharing octahedral $4f_2$ in R blocks. On the other hand, substitution of part of Sr^{2+} with La^{3+}, and Co^{2+} instead Fe^{3+} has to be taken into account, as it distort the hexaferrite structure. With this in mind, increased doping rate almost suppresses B peak, due to the small amount of Fe^{2+} in 2a sites occupied by cobalt, and also modifies the D peak in two ways: increasing its characteristic activation energy due to lattice distortion and lowering its amplitude, because the unit cell is smaller and then the presence of localized ferrous cations in $4f_2$ sites is less probable in favour of interstitial diffusion of anisotropic cations via lattice vacancies, thus increasing the high temperature A_0 process. Concerning $Sr_{1-x}La_xFe_{12-y}Co_yO_{19}$ samples, the effect observed with doping rate is similar. In this case we can see that D peak is prominent, and B peak is strongly diminished, even for the lower substitution rate analyzed. In this case, the amount of Co^{2+} is lower than La^{3+} substitution, thus favouring a higher amount of Fe^{3+} changing its valence to Fe^{2+} thus enhancing the D process and almost suppressing the B process regarding $Sr_{1-x}La_xFe_{12-x}Co_xO_{19}$ samples. The increased amount of ferrous cations can not enter completely in the $4f_2$ sites due to higher ionic radium of Fe^{2+} (0.61 Å) regarding Fe^{3+} hence increasing the diffusion of interstitial ferrous cations at high temperatures, i.e, the A_0 relaxation.

Financial support of Universidad de Valladolid and Junta de Castilla y León is acknowledged.

References

[1] H. Kojima in: Ferromagnetic Materials vol. 3, ed. E.P. Wohlfarth (North-Holland, Amsterdam, 1982) 305.
[2] F. Walz, V.A.M. Brabers, S. Chikazumi, H. Kronmüller and M. O. Rigo, Phys. Stat. Sol. B, 110 (1982) 471.
[3] P. Hernández-Gómez et al., J. Magn. Magn. Mat. 272–276 (2004) e1843.
[4] P. Hernández-Gómez et al., Mat. Sci. Forum, 514-516 (2006) 319.
[5] X. Liu et al., Adv. Mater. Res. 284-286 (2011) 2311.

Email of the presenting author: pabloher@ee.uva.es

Dielectric properties of graphene based composites

Ł. Jarosiński[1], A. Rybak[2], Cz. Kapusta[1]
[1] *AGH University of Science and Technology, Faculty of Physics and Applied Computer Science, Department of Solid State Physics, 30-059 Krakow, Poland*
[2] *ABB Corporate Research Center, 31-038 Krakow, Poland*

Graphene is used as a filler material to nanocomposites in order to improve their thermal and electrical properties. That kind of composites can be responsible for heat dissipation from electrical devices. Therefore, nanocomposites with such application should be insulators. Graphene based composites are usually used as a electrically conductive composites. An important role in the assembly of electronic devices is played by polymers (e.g. epoxy resin) used for their construction. The thermal conductivity of polymers is low and it can be improved by addition of thermally conductive particles into the polymer matrix. For this purpose, graphene has been considered as a adequate filler, due to its excellent thermal conductivity (~ 5000 W/mK). However, graphene-based composites show a high electrical conductivity even at a low filler load, which considerably limits their application in electronic devices.

The aim of the present work is to produce and characterize insulating graphene/polymer composites. It can be achieved by adding a second filler: silica that maintain the insulating properties. That kind of hybrid composites combines the advantages of both, the graphene sheets and silica powder, resulting in composites that not only show high thermal conductivity, but also retain electrically insulating properties. In this work electrical resistivity, dielectric breakdown and permittivity was investigated. For instance, the thermal conductivity of hybrid filler composite with only 2 wt.% graphene reaches 1.54 W/mK and the volume resistivity is about 10^{16} Ω·cm. Dielectric breakdown (Fig. 1) is about 20 kV/mm to composite with low graphene content (about 0,25%). The obtained results show a high potential for applications of such nanocomposites for electrical insulations with enhanced thermal conductivity.

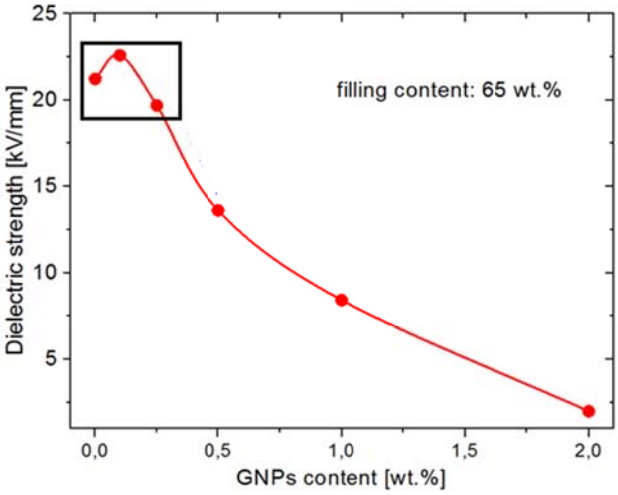

Figure 1. Dielectric breakdown of graphene/silica based composites

Email of the presenting author: lukasz.jarosinski@yahoo.pl

Studies of visual attention and emotion in physics problem solving

Paweł Kazubowski, Władysław Błasiak, Małgorzata Godlewska, Roman Rosiek,
R. Sajka, Dariusz Wcisło
Institute of Physics, Pedagogical University, Podchorazych 2, 30-084 Krakow, Poland

The authors present methods of measurement of biophysical parameters of university students and pupils during the process of problem solving. The aim of the research was to monitor such parameters like: blood volume pulse, skin conductance, respiration measured by BioGraph Infiniti, and oculography parameters measured by SMI HighSpeed 1250^{TM} eyetracker during the process of solving several problems in physics.

The poster presents different parameters as well as different ways of data visualization useful in research on didactics of physics. The oculographical results are presented in the form of heat maps, scan paths, key performance indicators and others.

Email of the presenting author: pawel.kazubowski@gmail.com

Crystal structure, electron band structure and magnetostriction of the $Tb_{0.27}Dy_{0.73}(Fe_{0.7-x}Ni_xCo_{0.3})_2$ intermetallics (x=0, 0.1, 0.2)

M. Szklarska-Łukasik[1], P. Stoch[2], J. Pszczoła[1]
[1] *Faculty of Physics and Applied Computer Science, AGH University of Science and Technology, Al. Mickiewicza 30, 30-059 Kraków, Poland*
[2] *Faculty of Materials Science and Ceramics, AGH University of Science and Technology, Al. Mickiewicza 30, 30-059 Kraków, Poland*

The crystal structure, electron band structure and magnetostriction of nickel substituted $Tb_{0.27}Dy_{0.73}(Fe_{0.7-x}Ni_xCo_{0.3})_2$ intermetallics were studied by powder X-ray diffraction, FLAPW (Full – potential Linear Augmented Plane Waves) calculations and by standard strain gauge masurements.

Compounds with a composition parameter x = 0, 0.1, 0.2 were synthesized by arc-melting procedure. Analysis of the X-ray diffractograms revealed a single-phase composition with a cubic Laves Fd3m, $MgCu_2$-type crystal structure. The unit cell parameter a(x) decreases linearly with the composition parameter.

Band-type calculations for Fe, Co and Ni were performed considering densities of states (DOS) and newly introduced their distribution functions (DDOS). Fig. 1 shows exemplary calculation results for the $Tb_{0.27}Dy_{0.73}(Fe_{0.7}Co_{0.3})_2$ compound, i.e. the starting composition of the series.

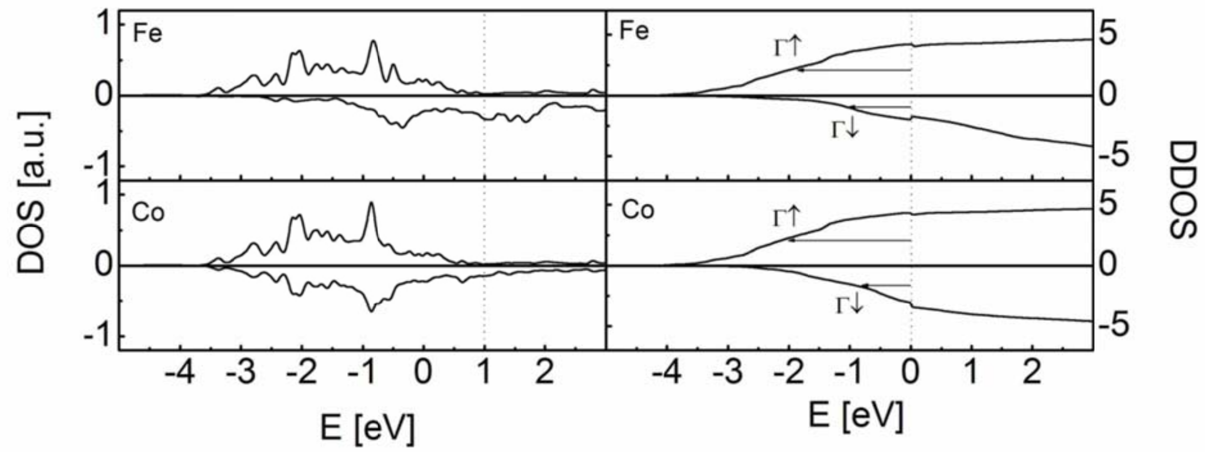

Figure 1. Individual densities of states (DOS) and distribution functions (DDOS) of 3d electrons for Fe and Co as functions of energy E for the $Tb_{0.27}Dy_{0.73}(Fe_{0.7}Co_{0.3})_2$ exemplary compound. Fermi energy corresponds to zero value. The subband half-widths $\Gamma^{\uparrow}$ (majority subband) and $\Gamma^{\downarrow}$ (minority subband) are marked by horizontal arrows.

FLAPW calculated magnetic moments m_{Fe}, m_{Co} and weighted magnetic moment m_M of the transition metal sublatice reduce with x.

The giant magnetostriction parameters $\lambda_{||}$ (parallel to the applied magnetic field) and $\lambda_{\perp}$ (perpendicular to the applied magnetic field) were measured against the magnetic field intensity and the composition parameter.

Both the $\lambda_{||}$ parameter and the absolute value of the $\lambda_{\perp}$ parameter slightly decrease with the m_M – reducing. Additionally shape and volume magnetostriction parameters were determined.

Email of the presenting author: monikaszklarska@gmail.com

Crystal structure and electrical properties of the $Tb_{0.27}Dy_{0.73}(Fe_{1-x}Al_x)_2$ compounds

B. Winiarska[1,2], J. Chmist[1], P. Guzdek[3], J. Pszczoła[1]
[1]AGH University of Science and Technology, Faculty of Physics and Applied Computer Science, Al. Mickiewicza 30, 30-059 Kraków, Poland
[2]The Henryk Niewodniczański Institute of Nuclear Physics, Polish Academy of Sciences, ul. Radzikowskiego 152, 31-342 Kraków, Poland
[3]Institute of Electron Technology, Kraków Division, Zabłocie 39, 30-701 Kraków, Poland

Studies of the polycrystalline $Tb_{0.27}Dy_{0.73}(Fe_{1-x}Al_x)_2$ intermetallic ferrimagnets (x=0, 0.1, 0.2), prepared by arc melting technique, are reported. All compounds of the series crystallize within cubic $MgCu_2$ – type, Fd3m Laves phase. The unit cell edge increases considerably and linearly against the composition parameter x. Consequences of the Fe/Al replacing in the transition metal sublattice were studied.

The four probe dc electrical measurements of the electrical resistivity were performed against temperature. Only samples verified as crack-free were used for electrical resistivity measurements.

Residual ρ_0, phonon ρ_f and magnetic ρ_m resistivities were separated from the measured electrical resistivity ρ using both the Matthiessen and Bloch-Grüneisen formulas.

Fig.1 shows exemplary resistivities for the $Tb_{0.27}Dy_{0.73}Fe_2$ compound.

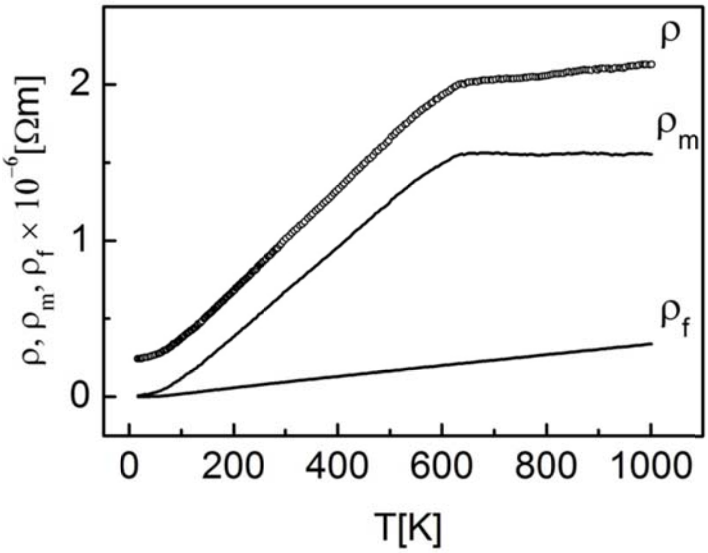

Figure 1. The total electrical resistivity ρ and its phonon ρ_f and magnetic ρ_m contributions observed vs. temperature for the $Tb_{0.27}Dy_{0.73}Fe_2$ compound.

Parameters ρ_0 and θ_D (Debye temperature) were also determined. Residual resistivity ρ_0 considerably increases and Debye temperature θ_D considerably decreases with x. Moreover, using $\rho_m(T)$ dependencies the Curie temperatures were obtained. The Fe/Al replacing in the $Tb_{0.27}Dy_{0.73}(Fe_{1-x}Al_x)_2$ series reduces the Curie temperature value.

Email of the presenting author: Barbara.Winiarska@ifj.edu.pl

Electron band structure and magnetostriction of the $Tb_{0.27}Dy_{0.73}(Fe_{1-x}Co_x)_2$ series

B. Winiarska[1,2], M. Szklarska-Łukasik[1], P. Stoch[3], W. Bodnar[1], W. Dorowski[1], J. Pszczoła[1]
[1] *AGH University of Science and Technology, Faculty of Physics and Applied Computer Science, Al. Mickiewicza 30, 30-059 Kraków, Poland*
[2] *The Henryk Niewodniczański Institute of Nuclear Physics, Polish Academy of Sciences, ul. Radzikowskiego 152, 31-342 Kraków, Poland*
[3] *AGH University of Science and Technology, Faculty of Materials Science and Ceramics, Al. Mickiewicza 30, 30-059 Kraków, Poland*

The crystal structure, electron band calculations and magnetostriction measurements of Fe/Co substituted $Tb_{0.27}Dy_{0.73}(Fe_{1-x}Co_x)_2$ intermetallics (x=0, 0.1, 0.2) were studied by powder X-ray diffraction, FLAPW (Full – potential Linear Augmented Plane Waves) calculation method and by standard strain gauge method.

A cubic Laves phase, Fd3m, $MgCu_2$-type for all compounds was observed. The unit cell parameter a(x) decreases linearly with the composition parameter.

Transition metal magnetic moments per atom m_{Fe}, m_{Co} and average m_M were obtained as FLAPW calculation results.

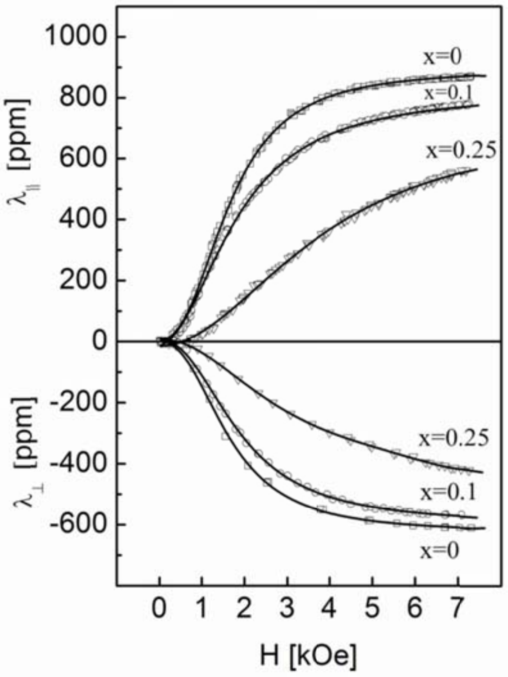

Figure 1. The magnetostriction parameters $\lambda_{||}$ and $\lambda_{\perp}$ vs. the magnetic field intensity H and the composition parameter x.

The huge magnetostriction parameters $\lambda_{||}$ (longitudinal) and $\lambda_{\perp}$ (transversal) were measured against the magnetic field intensity and the composition parameter. The magnetostriction parameters and magnetic moments are related and discussed each other.

Email of the presenting author: Barbara.Winiarska@ifj.edu.pl

Effects of Eu substitution on the physical properties of $BaTiO_3$ ceramics

D. Sitko[1], B. Garbarz-Glos[2], A. Kalvane[3] and W. Śmiga[1]
[1] *Institute of Physics, Pedagogical University, Kraków, Poland*
[2] *Institute of Technology, Pedagogical University, Kraków, Poland*
[3] *Institute of Solid State Physics, University of Latvia, Riga, Latvia*

Barium-based perovskite ferroelectrics are widely used as capacitors, actuators, sensors and electro-optical applications. Recently, special interest has been focused on the development of compounds exhibiting a perovskite crystal structure with a general formula ABO_3, which have been intentionally doped with trivalent rare-earth ions ($4f^n$ shell), such as Eu, Ce and La, Interactions between the rare-earth ion states and the electronic states of the based material can enhance or inhibit the material properties important in many of the most applications to form multifunctional. In this study the influence of Eu_2O_3 addition on the physical properties of $BaTiO_3$ was investigated. The addition of Eu is responsible for the changes of the electric permittivity and mechanical properties. The small amount of this element contributes to the slightly reduction in the temperature of a phase transition between tetragonal and cubic phases. Eu^{3+} ions substituting the A and/or B sites exhibit a donor character. The donor incorporation into the grain boundary shifts compensation from electronic to vacancy one, resulting in the formation of highly resistive layers and also, the decrease in grain size due to a significant dopant drag to the boundary mobility. The aim of this study was to measure and discuss the influence of 0,1 wt.% Eu_2O_3 addition on the physical properties of BT. The results of the research obtained with the use of the following techniques: X-ray Diffraction (XRD), Scanning Electron Microscopy (SEM), Energy-Dispersive X-ray Spectroscopy (EDS), elastic, and dielectric measurements for BTE ceramics were presented

Email of the presenting author: sitko.dorota@gmail.com

Effects of $PbTiO_3$ doping on dielectric, thermal and ferroelectric properties of $Na_{0.5}Bi_{0.5}TiO_3$ ceramics

Monika Karpierz[1], Jan Suchanicz[2], Dorota Sitko[1], Krzysztof Konieczny[2]
[1] Institute of Physics, Pedagogical University, ul. Podchorazych 2, 30-084 Krakow, Poland
[2] Institute of Technology, Pedagogical University, ul. Podchorazych 2,
30-084 Krakow, Poland

Lead titanate ($PbTiO_3$) and lead titanate - based ceramics are one of the most investigated ferroelectric materials because of their use for example for transducers, actuators and sensors [1]. $(1-x)Na_{0.5}Bi_{0.5}TiO_3-xPbTiO_3$ ($x = 0.05$ and 0.6) ceramics were fabricated by conventional solid phase sintering process. X-ray diffraction analysis show that obtained specimens possesses the perovskite structure. The microstructure study showed a dense structure in good agreement with that of above 95% relative density determined by the Archimedes method. Electric permittivity broad anomaly is shifted to low temperature after $PbTiO_3$ doping of $Na_{0.5}Bi_{0.5}TiO_3$. The crystal structure, phase transitions behaviour, thermal and dielectric properties of these ceramics were investigated. The maximum of electric permittivity was observed at about $T_m \approx 292$ and 513°C for $x = 0.05$ and 0.6, respectively (on cooling, at 100 kHz). The transitions temperatures observed by means of DSC measurements are in good agreement with those obtained from dielectric study.

Reference
[1] Ferroelectric devices, Uchino K. New York (NY): Marcel Dekker; 2000.

Email of the presenting author: mkarpierz@up.krakow.pl

Krakow and Prague
– *the formal and informal cooperation*

Nhu-Tarnawska Hoa Kim Ngan[1],*, Ladislav Havela[2], Zbigniew Tarnawski[3]
[1] *Institute of Physics, Pedagogical University, 30-084 Kraków, Poland*
[2] *Department of Condensed Matter Physics, Faculty of Mathematics and Physics, Charles University, Ke Karlovu 5, 12116 Prague, Czech Republic*
[3] *AGH University of Science and Technology, Faculty of Physics and Applied Computer Science, 30-059 Kraków, Poland*

We present a brief summary of our cooperation, in the framework of formal Polish-Czech cooperation projects as well as informal cooperation between Krakow and Prague group. Despite the difference between our main research topics and interests, for more than 20 years we have performed many investigations together which led to common publications, e.g. our first publications in 1993-1994 [1,2] and/or our fresh publication in Physical Review B in 2015 [3]. The outcome of our scientific cooperation is not only common publications, but also the Ph.D. education. Four Ph.D. students have finished their Ph.D. study for which their research work has been a part of Polish-Czech cooperation [4-7]. Three more Ph.D. students are now involved in the Polish-Czech bilateral project for 2014-2015.

Cracow Colloquium on f-electron systems (CCFES2015) is also a result of Polish-Czech fruitful cooperation, both in the framework of the bilateral project as well as of the informal cooperation and personal contact.

We would like to express our deep thanks to Prof. Vladimir Sechovsky. He has not always been a co-author of our publications nor involved formally in the Polish-Czech projects. But without his great support, mentally and financially, our cooperation would not gain such a momentum and results.

We would like to thank all people in the Department of Condensed Matter Physics and Magnetism and Low Temperature Laboratories for their great help in the experiments and during our stays in Prague.

References:
[1] N.C. Tuan et al., J. Appl.Phys. 73 (1993) 5677.
[2] E. Bruck et al., Phys. Rev. B 49 (1994) 8852.
[3] I. Tkach et al., Phys. Rev. B 91 (2015) 115116.
[4] Bilateral Polish-Czech project (2004-2006): *Electronic structure and thermodynamic properties of Rare Earth-3d intermetalic compounds and their hydrides*. Coordinators: Z. Tarnawski, L. Havela. Ph.D. defense in 2008 (L. Kolwicz-Chodak).
[5] The joint Polish-Czech Ph.D. study program (2007-2011): *Structure and electronic properties of metal hydrides*. Coordinators: N.-T.H. Kim-Ngan, L. Havela. Ph.D. defense in 2011 (A.M. Adamska, simultaneously doctoral Czech and Polish diplomas).
[6] Krakow Interdisciplinary PhD-Project in Nanoscience and Advanced Nanostructures (2009-2013). Polish coordinator: Z. Tarnawski. Ph.D. defense in 2013 (K. Drogowska).
[7] Bilateral Polish-Czech project (2014-2015): *Structure, electronic and magnetic properties of f-metal hydrides* (ID(CZ) 7AMB14PL036. ID(PL) 9004/R14/R15). Coordinators: N.-T.H. Kim-Ngan, L. Havela. Ph.D. defense in 2015 (I. Tkach).

*Abbreviation in the scientific publications: N.-T.H. Kim-Ngan

Email of the presenting author: tarnawsk@up.krakow.pl

CCFES2015 - List of registered participants

	Family name and name	Institution countr	y	e-mail	Ph.D. student	Session/ Talk
1	Abdelghani Benahmed	University of Saida, 23.Rue Belhachmi badre el dinne Balloul saida, Algeria	Algeria	benahmed_phys@yahoo.fr		
2	Abram Marcin	Marian Smoluchowski Institute of Physics, Jagiellonian University, Łojasiewicza 11, 30-348 Krakow, Poland	Poland	marcin.abram@uj.edu.pl	S	S4/ O-05
3	Andreev Alexander	Institute of Physics, Academy of Sciences, Na Slovance 2, 18221 Prague, Czech Republic	Czech	a.andreev@seznam.cz		P-01
4	Apinyan Vardan	Institute of Low Temperature and Structure Research, Polish Academy of Sciences, ul. Okólna 2, 50-422 Wrocław, Poland	Poland	v.apinyan@int.pan.wroc.pl		S6/ O-12
5	Bartha Attila	Charles University in Prague, Faculty of Mathematics and Physics, Department of Condensed Matter Physics, Ke Karlovu 5, 121 16 Praha 2, Czech Republic	Czech	bartha@mag.mff.cuni.cz		
6	Bauer Ernst	Vienna University of Technology, Institute of Solid State Physics, Wiedner Hauptstrasse 8-10, 1040 Wien, Austria	Austria	bauer@ifp.tuwien.ac.at		S1/ I-02
7	Beridze George	Forschungszentrum Juelich, Wilhelm-Johnen-Strasse, 52428 Juelich, Germany	Germany	g.beridze@fz-juelich.de	S	S8/ O-y2
8	Blachowski Artur	Institute of Physics, Pedagogical University. Podchorazych 2, Krakow 30084, Poland	Poland	ablachow@up.krakow.pl		P-06; P-13
9	Bopete Bomele Betty	Mohammed V University,4 Rue al ganzra, Morocco	Morocco	betty.bopete@um5s.net.ma	S	
10	Budziak Andrzej	Institute of Nuclear Physics PAN, ul. Radzikowskiego 152, 31-342 Kraków, Poland	Poland	andrzej.budziak@ifj.edu.pl		I-05
11	Bujakiewicz-Korońska Renata	Institute of Physics, Pedagogical University. Podchorazych 2, Krakow 30084, Poland	Poland	rbk@up.krakow.pl		S8/ O-y6
12	Drozdenko Daria	Charles University in Prague, Faculty of Mathematics and Physics, Department of Condensed Matter Physics, Ke Karlovu 5, 121 16 Praha 2, Czech Republic	Czech	drozdenko@karlov.mff.cuni.cz	S	S9/ O-16
13	El Miloudi El Moussafir	Laboratory Materials and Ingineering, Hassan II University Mohammedia. Faculty Science Ben Msik. BP 7955, Casablanca, Morocco.	Morocco	elmoussafir@hotmail.fr	S	P-22

14	Falkowski Michał	Institute of Molecular Physics, Polish Academy of Sciences, Smoluchowskiego 17, 60–179 Poznań, Poland	Poland	falkowski@ifmpan.poznan.pl		S3/ O-03
15	Fereira José-Luiz	Institut Néel CNRS-Grenoble, 42 av. des Martyrs, Grenoble, France	France	jose-luiz.ferreira@neel.cnrs.fr	S	S4/ O-06; P-04
16	Figiel Henryk	AGH University of Science and Technology, al. Mickiewicza 30, 30-059 Kraków	Poland	figiel@agh.edu.pl		S3/ I-05
17	Ganiyu bamidele	yejide girls gram school, qarter 4, yejide girls gram school, molete , ibadan , Nigeria	Nigeria	ganibamidele123@gmail.com		
18	Gofryk Krzysztof	Idaho National Laboratory, P.O. Box 1625 MS 3840 Idaho Falls, ID 83415-384, USA	USA	krzysztof.gofryk@inl.gov		S7/ I-09
19	Gonçalves António Pereira	C2TN, Instituto Superior Técnico, Universidade de Lisboa, Campus Tecnológico e Nuclear, Estrada Nacional 10, 2695-066 Bobadela LRS, Portugal	Portugal	apg@ctn.ist.utl.pt		S2/ I-03
20	Guaaybess Youssef	Institution: faculty of sciences Ben Msik, av. Driss Harty Casablanca. Morocco	Morocco	guaaybess@hotmail.com	S	
21	Halevy Itzhak	Research Center - Negev, Physics Department, P.O. Box 9001, Beer-Sheva, Israel	Israel	halevy.itzhak.dr@gmail.com		S2/ O-01 S10/ I-11
22	Havela Ladislav	Charles University, Faculty of Mathematics and Physics, Ke Karlovu 5, Prague 2, Czech Republic	Czech	Havela@mag.mff.cuni.cz		S9/ I-10
23	Hendriques Magrgarida	Institute of Physics, ASCR, Na Slovance 2 - Prague 8	Czech	henriques@fzu.cz	S	P-17
24	Hernandez-Gomez Pablo	Univ. Valladolid, Paseo de Belen 7, 47011 Valladolid, Spain	Spain	pabloher@ee.uva.es		P-24
25	Hintze Cornelia	Karlsruhe Institute for Technology, Hermann-von-Helmholtz-Platz 1, 76344 Eggenstein-Leopoldshafen, Germany	Germany	Cornelia.Hintze@kit.edu	S	S5/ O-08
26	Jarosiński Łukasz	Faculty of Physics and Applied Computer Science, AGH University of Science and Technology, A. Mickiewicza 30, 30059 Krakow, Poland	Poland	lukasz.jarosinski@yahoo.pl	S	P-25
27	Jasek Aleksandra	Institute of Physics, Pedagogical University. Podchorazych 2, Krakow 30084, Poland	Poland	aleksjasek@gmail.com	S	P-06

28	Kaczorowski Dariusz	Institute of Low Temperature and Structure Research, Polish Academy of Sciences, P.O. Box 1410, 50-950 Wrocław, Poland	Poland	d.kaczorowski@int.pan.wroc.pl		S1/ I-01
29	Kąkol Zbigniew	AGH University of Science and Technology, Mickiewicza 30 Av. 30-059 Kraków	Poland	kakol@agh.edu.pl		P-14
30	Karpierz Monika	Institute of Physics, Pedagogical University. Podchorazych 2, Krakow 30084, Poland	Poland	mkarpierz@up.krakow.pl	S	P-31
31	Kazubowski Paweł	Institute of Physics, Pedagogical University. Podchorazych 2, Krakow 30084, Poland	Poland	pawel.kazubowski@gmail.com	S	P-26
32	Kim-Ngan N.-T. H	Institute of Physics, Pedagogical University. Podchorazych 2, Krakow 30084, Poland	Poland	nthkimngan@gmail.com		P-07
33	Klicpera Milan	Institut Laue-Langevin. Address: 71 avenue des Martyrs - CS 20156 - 38042 GRENOBLE CEDEX 9. France	France	mi.klicpera@seznam.cz	S	
34	Klimczuk Tomasz	Gdansk University of Technology, ul. Narutowicza 11/12, 80-232 Gdańsk	Poland	tomasz.klimczuk@pg.edu.pl		S10/ O-18
35	Kołodziejczyk Andrzej	AGH University of Science and Technology, Mickiewicza 30 Av. 30-059 Kraków	Poland	akolo@uci.agh.edu.pl		
36	Komędera Kamila	Institute of Physics, Pedagogical University. Podchorazych 2, Krakow 30084, Poland	Poland	kamilakom@op.pl	S	P-13
37	Kozlowski Andrzej	AGH University of Science and Technology, al. Mickiewicza 30, 30-059 Krakow	Poland	kozlow@agh.edu.pl		P-14
38	Kozub Agnieszka	Gdansk University of Technology,Gabriela Narutowicza 11/12, 80-233 Gdansk, Poland	Poland	akozub@mif.pg.gda.pl	S	P-03
39	Krop Karol	Politechnika Rzeszowska, Rzeszów, Poland	Poland	k.krop@upcpoczta.pl		
40	Kruk Andrzej	AGH University of Science and Technology, Faculty of Materials Science and Ceramics, 30-059 Krakow, Poland	Poland	a.kruk@poczta.fm		P-15
41	Krupska Magdalena	Institute of Physics, Pedagogical University. Podchorazych 2, Krakow 30084, Poland	Poland	krupska.magdalena@gmail.com	S	S8/ O-y3
42	Kurleto Rafał	Marian Smoluchowski Institute of Physics, Jagiellonian University, Łojasiewicza 11, 30-348 Krakow, Poland	Poland	rkurleto@gmail.com	S	P-05

43	Lewczuk Urszula	Institute of Physics, Pedagogical University. Podchorazych 2, Krakow 30084, Poland	Poland	urszula.lewczuk@gmail.com	S	S8/ O-y5
44	Maksymov Artur	Advanced Materials Research Institute, University of New Orleans, 2000 Lakeshore Drive, New Orleans, LA 70148, USA	USA	maxyartur@gmail.com		P-23
45	Mašková Silvie	Charles University in Prague, Faculty of Mathematics and Physics, Department of Condensed Matter Physics, Ke Karlovu 5, 121 16 Praha 2, Czech Republic	Czech	maskova@mag.mff.cuni.cz		S3/ O-04
46	Mędala Magdalena	Institute of Technology, Pedagogical University. Podchorazych 2, Krakow 30084, Poland	Poland	mmedala@up.krakow.pl	S	P-21
47	Miliyanchuk Khrystyna	Ivan Franko National University of Lviv, Kyryla i Mefodiya St. 6, Lviv, Ukraine	Ukraine	k_miliyanchuk@lnu.edu.ua		S7/ O-14
48	Nalęcz Dawid M.	Institute of Physics, Pedagogical University, Podchorazych 2, Krakow 30084, Poland	Poland	dnalecz@up.krakow.pl	S	P-19
49	Ozkendir Osman Murat	Mersin University, Faculty of Technology, Tarsus Kampusu, Tarsus, Mersin, Turkey	Turkey	ozkendir@gmail.com		P-02
50	Paś Monika	Institute of Physics, Pedagogical University. Podchorazych 2, Krakow 30084, Poland	Poland	monika.pas@poczta.fm	S	
51	Paukov Mykhaylo	Charles University, Faculty of Mathematics and Physics, Ke Karlovu 5, Praha 2, Czech Republic	Czech	Michael.Paukov@gmail.com	S	S10/ O-17
52	Piotrowska Zuzanna	Institute of Low Temperature and Structure Research, Polish Academy of Sciences, ul. Okólna 2, 50-422 Wrocław, Poland	Poland	z.piotrowska@int.pan.wroc.pl	S	P-10
53	Pszczoła Jarosław	AGH University of Science and Technology, Mickiewicza 30 Av. 30-059 Kraków	Poland	pszczola@agh.edu.pl		P-27 /28/29
54	Radwanski Ryszard J.	Institute of Physics, Pedagogical University. Podchorazych 2, Krakow 30084, Poland	Poland	rjradwanski@gmail.com		P-20
55	Riseborough Peter	Physicss Department, Temple University, Philadelphia, PA 19122, USA	USA	prisebor@temple.edu		S6/ I-08
56	Ruebenbauer Krzysztof	Institute of Physics, Pedagogical University. Podchorazych 2, Krakow 30084, Poland	Poland	Ruebenbauer		P-06;P-13

57	Sahakyan Mane	Institute of Low Temperature and Structure Research, Polish Academy of Sciences, ul. Okólna 2, 50-422 Wrocław, Poland	Poland	m.sahakyan@int.pan.wroc.pl	S	P-12
58	Salakhitdinova Maysara	Samarkand state university, University blvd., 15, 140000, Samarkand, Uzbekistan	Uzbekistan	smaysara@yandex.ru		
59	Šebesta Jakub	Charles University in Prague, Faculty of Mathematics and Physics, Department of Condensed Matter Physics, Ke Karlovu 5, 121 16 Praha 2, Czech Republic	Czech	sebesta.j@email.cz	S	P-09
60	Sechovský Štěpán	Charles University in Prague, Faculty of Mathematics and Physics, Department of Condensed Matter Physics, Ke Karlovu 5, 121 16 Praha 2, Czech Republic	Czech	stepan@kfkl.cz		
61	Sechovský Vladimír	Charles University in Prague, Faculty of Mathematics and Physics, Department of Condensed Matter Physics, Ke Karlovu 5, 121 16 Praha 2, Czech Republic	Czech	sech@mag.mff.cuni.cz		I-07 P-09; P-11
62	Shick Alexander	Institute of Physics, Academy of Sciences, Na Slovance 2, 18221 Prague, Czech Republic	Czech	shick@fzu.cz		S6/ O-10
63	Sitko Dorota	Institute of Physics, Pedagogical University. Podchorazych 2, Krakow 30084, Poland	Poland	sitko.dorota@gmail.com		P-30
64	Ślebarski Andrzej	University of Silesia, Bankowa 14, Katowice, Poland	Poland	andrzej.slebarski@us.edu.pl		S3/ I-04
65	Sowa Sylwia	Institute of Physics, Pedagogical University, Podchorazych 2, Krakow 30084, Poland	Poland	sowas.agh@gmail.com	S	S8/ O-y1
66	Spałek Józef	Marian Smoluchowski Institute of Physics, Jagiellonian University, Łojasiewicza 11, 30-348 Kraków, Poland	Poland	ufspalek@if.uj.edu.pl		S4/ I-06
67	Starowicz Paweł	Jagiellonian University, Łojasiewicza 11, Kraków, Poland	Poland	pawel.starowicz@uj.edu.pl		S7/ O-13
68	Strychalska Judyta	Gdansk University of Technology, ul. Narutowicza 11/12, 80-232 Gdańsk	Poland	jstrychalska@mif.pg.gda.pl	S	S8/ O-y4
69	Suchanicz Jan	Institute of Technology, Pedagogical University. Podchorazych 2, Kraków 30084, Poland	Poland	sfsuchan@up.krakow.pl		S8/ O-y5 P-31
70	Synoradzki Karol	Institute of Molecular Physics Polish Academy of Sciences, Smoluchowskiego 17, 60-179 Poznań, Poland	Poland	karol.synoradzki@ifmpan.poznan.pl		P-16
71	Szklarska-Łukasik Monika	AGH University of Science and Technology, Mickiewicza 30 Av. 30-059 Kraków	Poland	monikaszklarska@gmail.com	S	P-28

72	Tarnawski Zbigniew	Faculty of Physics and Computer Science, AGH University of Sience and Technology, al. Mickiewicza 30, 30059 Krakow, Poland,	Poland	tarnawsk@agh.edu.pl		P-18
73	Taydakov Ilya V.	P.N. Lebedev Institute of Physics, Russian Academy of Scienses, S.I. Vavilov Department of Luminescence, Leninskiy pr-t. 53, 119991 Moscow, Russian Federation	Russia	taidakov@mail.ru		S5/ O-09
74	Tkach Ilya	Charles University in Prague, Faculty of Mathematics and Physics, Department of Condensed Matter Physics, Ke Karlovu 5, 121 16 Prague 2, Czech Republic	Czech	ilimp@yandex.ru		I-10, O-16, O-17, O-y1, P-07
75	Toliński Tomasz	Institute of Molecular Physics Polish Academy of Sciences, Smoluchowskiego 17, 60-179 Poznań, Poland	Poland	tomtol@ifmpan.poznan.pl		P-08
76	Tran Lan Maria	Institute of Low Temperature and Structure Research, PAN, ul. Okólna 2, 50-422 Wrocław, Poland	Poland	l.m.tran@int.pan.wroc.pl	S	S4/ O-07
77	Uhlířová Klára	Charles University in Prague, Faculty of Mathematics and Physics, Department of Condensed Matter Physics, Ke Karlovu 5, 121 16 Prague 2, Czech Republic	Czech	klara@mag.mff.cuni.cz		S5/ I-07
78	Valenta Jaroslav	Charles University in Prague, Faculty of Mathematics and Physics, Department of Condensed Matter Physics, Ke Karlovu 5, 121 16 Praha 2, Czech Republic	Czech	valeja@mag.mff.cuni.cz	S	P-11
79	Wdowik Urszula D.	Institute of Technology, Pedagogical University. Podchorazych 2, Krakow 30084, Poland	Poland	udw@up.krakow.pl		S6/ O-11
80	Wilhelm Fabrice	E.S.R.F., 71 avenue des martyrs 38000 Grenoble, France	France	wilhelm@esrf.fr		S10/ O-19
81	Winiarska Barbara	AGH University of Science and Technology, Mickiewicza 30 Av. 30-059 Kraków	Poland	barwin@gazeta.pl	S	P-27
82	Winiarski Michał J.	Gdansk University of Technology, ul. Narutowicza 11/12, 80-232 Gdańsk	Poland	mwiniarski@mif.pg.gda.pl	S	S7/ O-15
83	Wysokiński Marcin	Marian Smoluchowski Institute of Physics, Jagiellonian University, Łojasiewicza 11, 30-348 Krakow, Poland	Poland	marcin.wysokinski@uj.edu.pl	S	S2/ O02

Statistics:
83 registered participants including 35 Ph.D. students,
from 16 countries:
Poland (48 participants), Czech Republic (14), France (3), USA (3), Morocco (3), Germany (2), Austria (1), Portugal (1), Spain (1), Israel (1), Ukraine (1), Uzbekistan (1), Russia (1), Turkey (1), Nigeria (1), Algeria (1).
11 invited talks, 25 oral talks, 31 posters.

To get to the Pedagogical University (PUC) from the main Railway station and/or from Rynek (Centrum) you can take any tram to the direction “Bronowice” or “Bronowice Małe” (e.g. tram 4, 8, 13. 14, 24) and get out at the tram stop “Uniwersytet Pedagogiczny”.

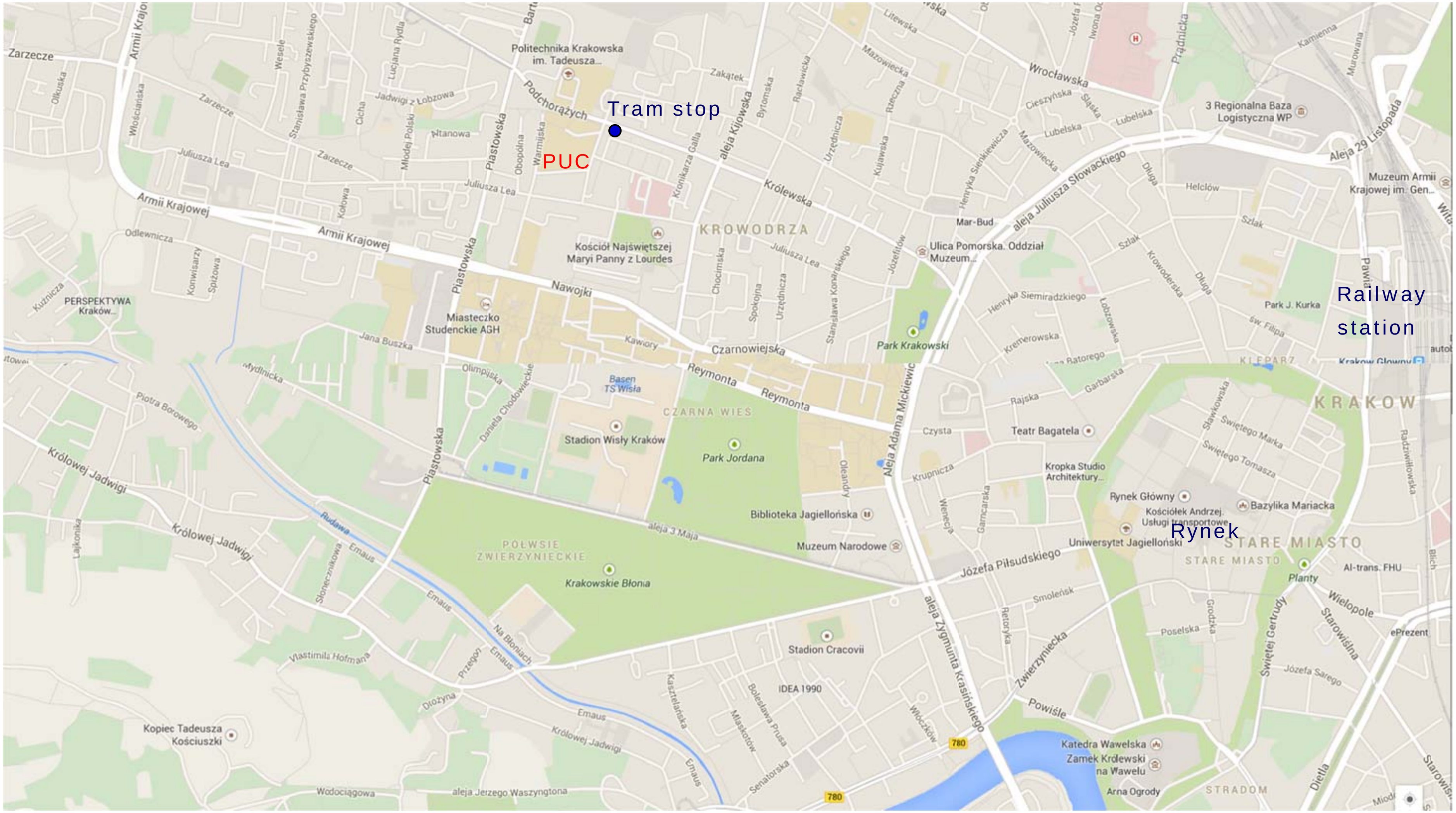

One can also walk from Rynek to PUC, via Kamelicka and Królewska street (blue path), or to the direction to AGH University of Science and Technology, then along Czarnowiejska –Kijowska street, through the park, then along Lea–Smoluchowskiego street (grey path). The distance is about 2.5 km.

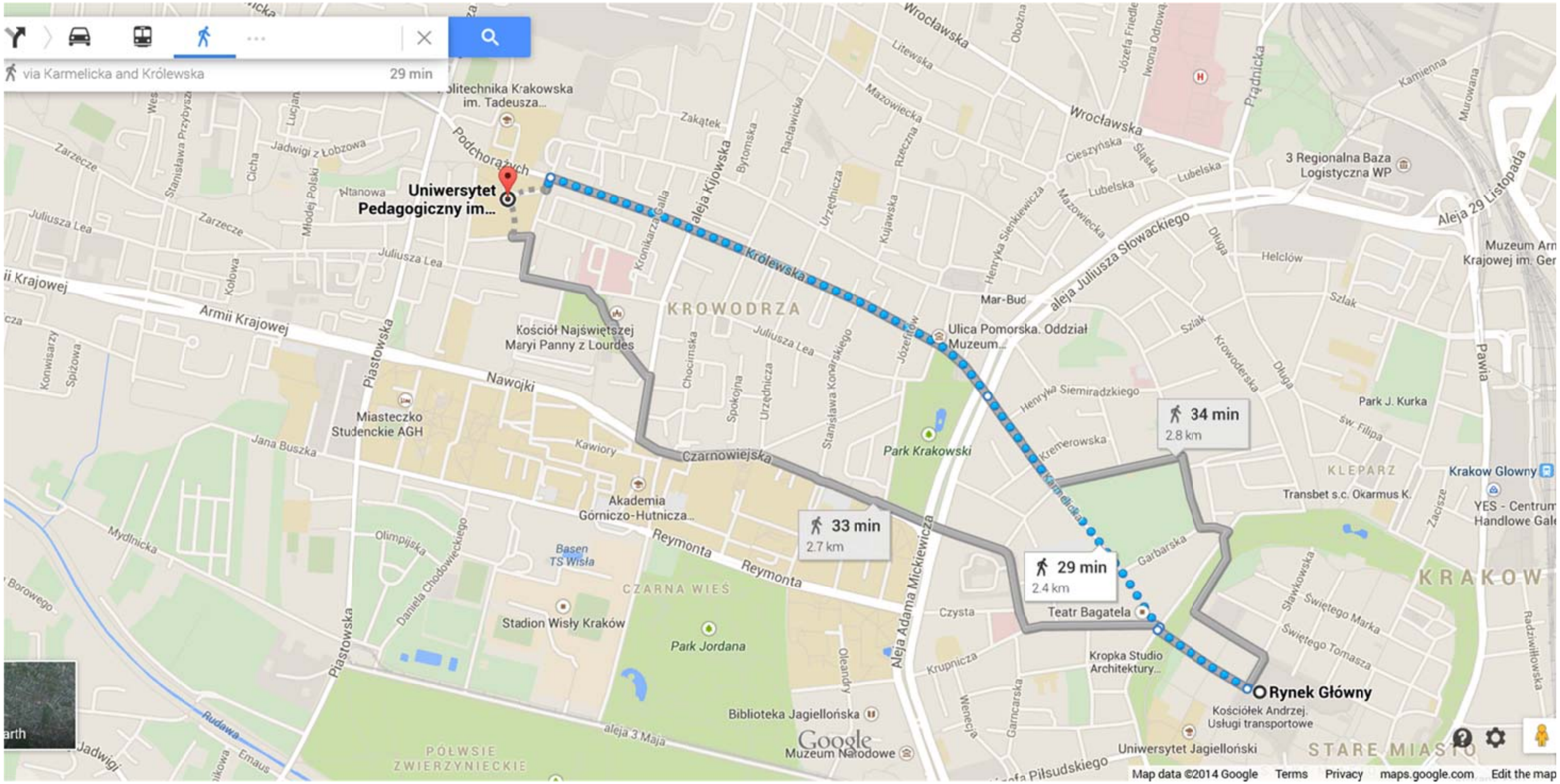

The colloquium venue: lecture hall 110 N on the first floor of the new building of PUC. The main entrance is at Chmiela street.

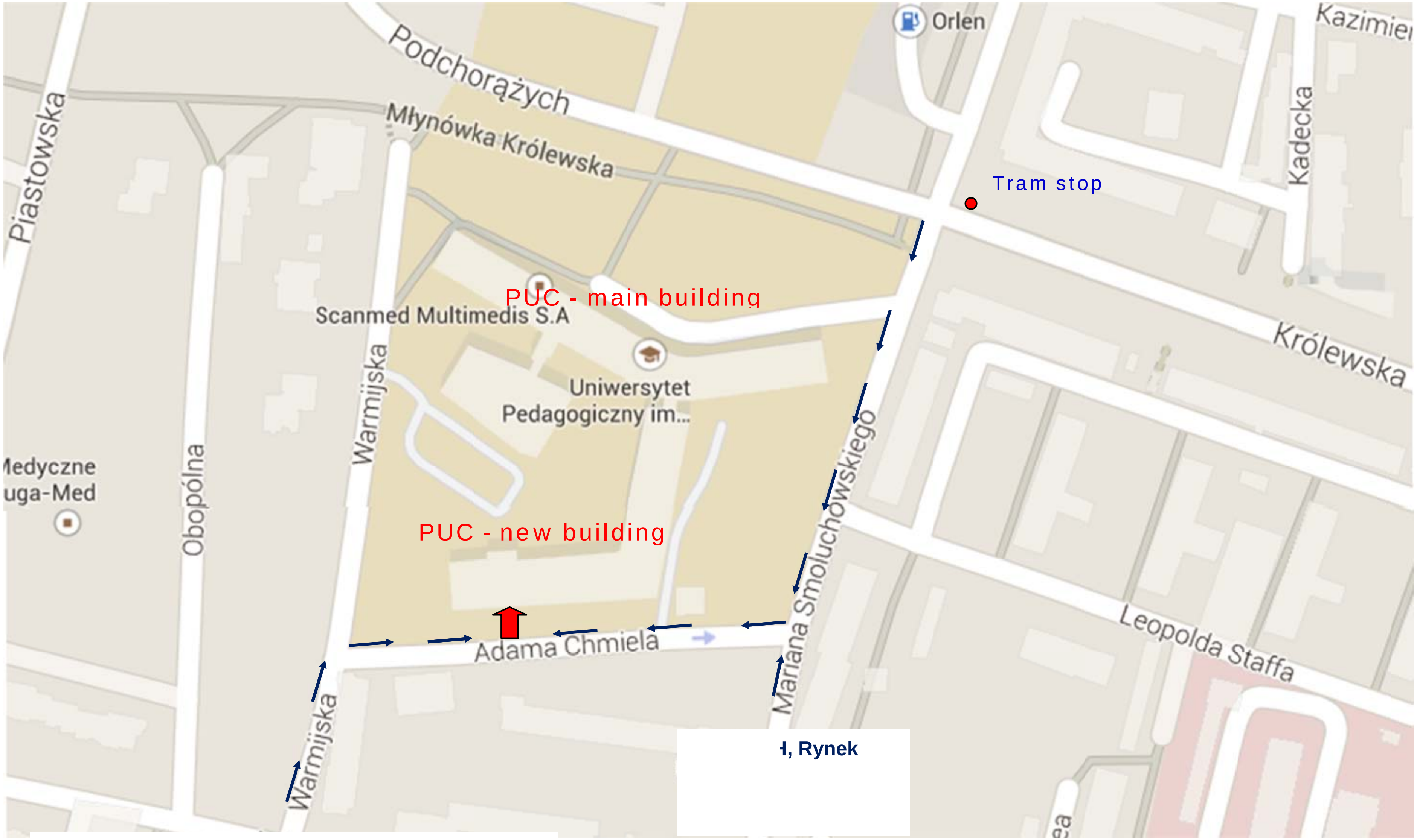

ɬ, Rynek

ɛowiak)

Lunches: Restaurant Eden, Bydgoska 19A, Kraków. 5 min. walk from PUC.

Conference dinner: Restaurant C.K. Browar, Podwale 6/7, 30-962 Kraków.
(walk downstairs, pass by several tables of the pub, turn left to the restaurant)